CENTRO INTERNACIONAL DE ESTUDOS
DE DOUTORAMENTO E AVANZADOS
DA USC (CIEDUS)

TESIS DOCTORAL

Enzyme-magnetic nanoparticle reactor for the advanced oxidation of micropollutants in wastewaters

Yolanda Moldes Diz

ESCUELA DE DOCTORADO INTERNACIONAL

PROGRAMA DE DOCTORADO EN INGENIERIA QUÍMICA Y AMBIENTAL

SANTIAGO DE COMPOSTELA

2019

USC
UNIVERSIDADE
DE SANTIAGO
DE COMPOSTELA

DECLARACIÓN DEL AUTOR DE LA TESIS

Enzyme-Magnetic Nanoparticle Reactor for the advanced oxidation of micropollutants in wastewaters

D./Dña. Yolanda Moldes Diz

Presento mi tesis, siguiendo el procedimiento adecuado al Reglamento, y declaro que:

1) *La tesis abarca los resultados de la elaboración de mi trabajo.*
2) *En su caso, en la tesis se hace referencia a las colaboraciones que tuvo este trabajo.*
3) *La tesis es la versión definitiva presentada para su defensa y coincide con la versión enviada en formato electrónico.*
4) *Confirmo que la tesis no incurre en ningún tipo de plagio de otros autores ni de trabajos presentados por mí para la obtención de otros títulos.*

En Santiago de Compostela, 11 de Octubre de 2019

Fdo. Yolanda Moldes Diz

USC
UNIVERSIDADE
DE SANTIAGO
DE COMPOSTELA

AUTORIZACIÓN DEL DIRECTOR / TUTOR DE LA TESIS

Enzyme-Magnetic Nanoparticle Reactor for the advanced oxidation of micropollutants in wastewaters

Prof. María Teresa Moreira Vilar

Prof. Gumersindo Feijoo Costa

INFORMA/N:

Que la presente tesis, corresponde con el trabajo realizado por **D/Dña. Yolanda Moldes Diz**, bajo nuestra dirección, y autorizamos su presentación, considerando que reúne los requisitos exigidos en el Reglamento de Estudios de Doctorado de la USC, y que como directores de ésta no incurre en las causas de abstención establecidas en Ley 40/2015.

En Santiago de Compostela, 11 de Octubre de 2019

Fdo. María Teresa Moreira Vilar *Fdo. Gumersindo Feijoo Costa*

USC
UNIVERSIDADE
DE SANTIAGO
DE COMPOSTELA

Resumen

USC
UNIVERSIDADE
DE SANTIAGO
DE COMPOSTELA

El continuo aumento de la población humana y el crecimiento económico están llevando a una demanda continua de agua. La contaminación química de las aguas naturales se ha convertido ya en una preocupación pública de primer orden en todo el mundo, ya que sus efectos a largo plazo sobre la vida acuática y la salud humana son en gran medida desconocidos. Por lo tanto, la protección de los recursos hídricos contra la explotación del agua y la contaminación antropogénica con productos químicos y patógenos es indispensable para preservar la salud ecológica y humana.

La sociedad moderna se beneficia del elevado número de productos químicos disponibles para diversas aplicaciones en la industria, la agricultura, la atención sanitaria y el saneamiento, así como para fines domésticos. En la Unión Europea hay más de 100.000 sustancias químicas registradas, de las cuales entre 30.000 y 70.000 son de uso diario. La mayoría de estos productos químicos llegan a las aguas naturales principalmente a través de las corrientes de aguas residuales municipales e industriales, los derrames de productos químicos y las emisiones difusas de las actividades agrícolas.

En la actualidad, la aparición nuevos métodos analíticos con límites de detección más bajos han permitido prevenir de la presencia de contaminantes emergentes en efluentes de aguas potables, superficiales y residuales de todo el mundo. Este tipo de compuestos y su eliminación suponen un desafío científico-tecnológico, sobre todo si se tiene en cuenta el hecho de que las plantas de tratamiento y depuración de aguas se diseñaron sin considerar la presencia de estos contaminantes. Por ello, el desarrollo de procesos que permitan eliminar este tipo de compuestos se sitúa entre las líneas de investigación prioritarias de los principales organismos dedicados a la protección de la salud pública y medioambiental, tales como la Organización Mundial de la Salud (OMS), la Agencia de Estados Unidos para la Protección del Medio Ambiente (US EPA) o la Agencia Europea de Medio Ambiente (EEA).

La creciente demanda de aguas más limpias por parte de los ciudadanos y las organizaciones medioambientales ha impulsado a la Comisión Europea a definir una lista de sustancias prioritarias con un riesgo significativo para el medio acuático. La lista actualizada incluye microcontaminantes de diferentes categorías: disruptores endocrinos, como el bisfenol, y productos farmacéuticos, en particular

el diclofenaco. Se ha alertado sobre la presencia de este tipo de compuestos en diferentes trabajos científicos, donde se han detectado concentraciones máximas de hasta 100 µg·L-1. Al tratarse de productos que resisten los tratamientos convencionales implementados en las estaciones depuradoras clásicas, estos se acumulan en las aguas superficiales, detectándose concentraciones de hasta 15000 ng·L-1 en algunos casos. Esto podría suponer un grave problema para la salud pública, ya que este tipo de compuestos pueden producir distintas alteraciones en los seres vivos y el medio ambiente.

La degradación de los contaminantes orgánicos implica un importante reto ecológico, ya que pueden tener una estructura compleja y/o una baja biodisponibilidad. Se han sugerido tecnologías de tratamiento avanzadas como la ozonización, la irradiación UV y el tratamiento con carbón activado para aumentar la eliminación de estos compuestos, pero una implementación a gran escala requeriría una inversión significativa y mayores costos de operación. Por lo tanto, es necesario sopesar los costes frente a los posibles beneficios de la introducción de nuevas tecnologías. Como resultado, todavía hay necesidad de desarrollar y examinar nuevas alternativas para eliminar eficientemente estos compuestos de las aguas residuales.

Conocedores de este hecho, esta tesis establece el interés de desarrollar sistemas de oxidación avanzada capaces de degradar este tipo de compuestos recalcitrantes, pero desde una perspectiva biotecnológica, de forma que se plantea como sistema de tratamiento innovador para aguas residuales contaminadas con este tipo de compuestos de difícil biodegradación.

Entre las diferentes opciones de biocatalizadores, las enzimas oxidativas, fundamentalmente oxidasas, son ampliamente reconocidas como sistemas capaces de catalizar la oxidación de fenoles, polifenoles y anilinas mediante la extracción de un solo electrón, con la reducción concomitante de oxígeno al agua en un proceso de transferencia de cuatro electrones. Este tipo de enzimas surge como biocatalizador de interés debido a algunas propiedades intrínsecas como su relativamente baja especificidad de sustrato, su alta estabilidad y también el hecho de utilizar oxígeno molecular como aceptador final de electrones. De hecho, las lacasas se han aplicado intensamente en la biorremediación de contaminantes ambientales como colorantes, pesticidas, hidrocarburos poliaromáticos y

diclorofenoles. Además, el uso de ciertos compuestos de bajo peso molecular llamados mediadores puede expandir la actividad catalítica de la lacasa hacia compuestos más recalcitrantes con mejores tasas de reacción.

Con el objetivo de mejorar la eficiencia y productividad de un sistema enzimático y contemplar su aplicación en plantas de tratamiento de aguas residuales, es importante diseñar un reactor para la eliminación de xenobióticos. En este sistema, la recuperación y reutilización de la enzima es obligatoria. Una alternativa se basa en el uso del reactor de membrana enzimática (EMR), que utiliza una membrana de ultrafiltración semipermeable para asegurar la retención del biocatalizador. Alternativamente al uso de enzimas libres, se puede considerar la inmovilización de enzimas, ya que permite la separación de la enzima del medio de reacción, de modo que el biocatalizador se puede aplicar en sistemas continuos y puede ser beneficioso para la estabilidad de la enzima y el almacenamiento prolongado.

Resulta especialmente interesante la posibilidad de inmovilizar las enzimas sobre nanopartículas magnéticas (mNP) ya que pueden proporcionar potencialmente una recuperación rápida y fácil del biocatalizador del medio de reacción bajo un campo magnético externo, lo que implicaría un estrés mecánico muy bajo en comparación con la centrifugación o filtración. En esta aproximación, es muy importante proporcionar un recubrimiento adecuado de la superficie y desarrollar algunas estrategias de protección eficaces para mantener la estabilidad de las NPs magnéticas. Las NPs de óxido de hierro magnético tienen una gran relación superficie/volumen y, por lo tanto, poseen altas energías superficiales. En consecuencia, tienden a agregarse para minimizar las energías de la superficie. Las estrategias más comunes para estabilizar el mNP incluyen el recubrimiento con moléculas orgánicas, incluyendo pequeñas moléculas orgánicas o surfactantes, polímeros y biomoléculas, o el recubrimiento con una capa inorgánica, como sílice, sustancia elemental metálica o no metálica, las cuales proporcionar la posibilidad de funcionalización de la superficie de las NPs de cara a llevar a cabo la inmovilización de la proteína. Estos aspectos se trataron en el Capítulo 2 en el que se evaluaron diferentes estrategias de inmovilización covalente y también mediante interacciones electrostáticas de las enzimas sobre la superficie de las nanopartículas magnéticas, e incluso a través del recubrimiento de NPs no magnéticas con una solución de ferrofluido (en colaboración con el Departamento de Nanotecnología de la Academica Checa de Ciencias.

Los mayores rendimientos de inmovilización de enzimas se lograron para los nanoconjugados de enzimas covalentes de nanopartículas magnéticas recubiertas de sílice, formadas por la unión covalente de la enzima entre los grupos de aldehídos de la nanopartícula funcionalizada con glutaraldehído y los grupos de aminoácidos residuales de las enzimas. Además, la estabilidad de los nanobiocatalizadores se demostró después de 4 meses con actividades residuales superiores al 90% en todos los casos.

Es esencial la caracterización del biocatalizador, determinando parámetros cinéticos, estabilidad a diferente pH y temperatura, presencia de agentes inactivantes, como variables de partida de cara a plantear la efectividad del mismo de cara a la degradación de compuestos objetivo, lo cual se desarrolla a lo largo del Capítulo 3. En esta sección se estudian las mejores condiciones de degradación de compuestos seleccionados como contaminantes orgánicos tales como el Bisfenol A, estradiol y verde de metilo, los primeros con potencial disruptor endocrino.

Uno de los puntos débiles en la formulación del biocatalizador se refiere al alto coste de la enzima, elemento esencial en la propuesta de investigación. Si no es posible producir cantidades elevadas de enzima lacasa a bajo coste, la viabilidad del proceso de degradación puede verse comprometido. Con esta premisa parte el capítulo 4, desarrollado en colaboración con el grupo de investigación Nanotechnology-Enabled Water Treeatment (NEWT) de Rice University (Houston, USA) en el cual se llevó a cabo la producción de una enzima a partir de residuos agrícolas como fuente de carbono para minimizar el coste de producción de la enzima. Esta enzima se inmovilizó sobre las nanopartículas magnéticas recubiertas de sílice, comprobando que tanto los rendimientos de inmovilización como el potencial oxidativo se mantenían en niveles comparables a la enzima comercial de cara a llevar a cabo la degradación de Bisfenol A y verde de metilo.

Más allá de la perspectiva de la degradación de contaminantes, los residuos agrícolas producidos por industrias o actividades agrícolas generan cada año 5 millones de toneladas métricas los cuales deben ser gestionados, o pueden ser recuperados y utilizados en otras cadenas de producción, de acuerdo con el concepto de biorefinería. En este contexto, en el Capítulo 5, se estudia la viabilidad de usar enzimas oxidativas en la producción de compuestos de valor añadido a partir de móleculas derivadas de la biomasa, más concretamente la conversión

bioquímica, mediante nanobiocatalizadores de enzima galactosa oxidasa y aril alcohol oxidasa sobre nanopartículas magnéticas recubiertas de sílice, con el objetivo de convertir 5-Hidroximetilfurfural (HMF) en químicos de alto valor añadido precursores de bioplásticos.

Gracias a la aplicación de un campo magnético, las nanopartículas magnéticas pueden separarse fácilmente y tienen un buen potencial para el tratamiento de aguas contaminadas. Hasta donde sabemos, no existen estudios sobre el uso de lacasa inmovilizada en el mNP para la descontaminación de aguas residuales, aunque se han llevado a cabo algunas actividades de investigación utilizando directamente el mNP como nanosorbentes o fotocatalizadores, la mayoría de los cuales se llevan a cabo en modo batch a escala de laboratorio utilizando agua sintética. El reactor secuencial por lotes (SBR) es una configuración de reactor comúnmente usada para el tratamiento microbiano de aguas residuales debido a su simplicidad y funcionalidad. En el capítulo 6 se plantea utilizar un SBR con mNPs de lacasa de forma que se aborda la oxidación de los contaminantes. El SBR desarrollado consistió en un reactor secuencial por lotes acoplado a un sistema de separación magnética interna formado por una serie de imanes toroidales magnetizados axialmente distribuidos con polaridad alternada en una barra de acero no magnética, generando un campo externo magnético capaz de conseguir la completa recuperación del nanobiocatalizador. La prueba de concepto del reactor se realizó evaluando la transformación de verde de metilo, como compuesto modelo presente en aguas residuales. Además, para estudiar la versatilidad del sistema se estudió la transformación de HMF, como compuesto modelo para la producción de compuestos de alto valor añadido. Para determinar la viabilidad del sistema se realizó un escalado del reactor a un volumen de 100-L para estimar los costes e impacto ambiental, los cuales fueron comparables a otros sistemas de oxidación avanzada como la ozonización.

Por último, no sólo la viabilidad del proceso es importante, sino que también la evaluación ambiental de los procesos de producción de los soportes empleados en los nanobiocatalizadores es importante. Por ello, en el Capítulo 7 se presenta un estudio comparativo de Análisis de Ciclo de Vida de las diferentes rutas de síntesis de las nanopartículas magnéticas empleadas como soportes para la inmovilización. Del estudio se concluye que las nanopartículas más adecuadas serían las nanopartículas magnéticas recubiertas de polietilenimina (PEI), aunque sin

embargo no presentaron los mayores rendimientos en la inmovilización, por lo que ha de adoptarse una solución de compromiso entre eficiencia e impacto ambiental asociado.

El presente trabajo de tesis aporta avances significativos en el ámbito científica y tecnológico para el desarrollo de nuevos procesos avanzados de oxidación para la eliminación de contaminantes orgánicos. El impacto esperado se basa en la innovación de esta propuesta, ya que la inmovilización de enzimas en nanopartículas magnéticas (mNPs) se encuentra en sus primeras etapas y, hasta donde sabemos, su aplicación para el tratamiento de aguas residuales está casi sin explotar. Además, se han planteado diferentes configuraciones de reactores mNPs enzimáticos, considerando no sólo la viabilidad tecnológica y operativa sino también los aspectos económicos y medioambientales de cara a la aplicación práctica de esta tecnología.

THESIS OUTLINE: OBJECTIVES AND STRUCTURE

This thesis aims to contribute in the development of new advanced oxidation processes for the elimination of organic pollutants. The innovation of this approach is related to the use of enzymes immobilized on magnetic nanoparticles (mNPs) as the biocatalyst for wastewater treatment and from this starting hypothesis, the evaluation of the potentiality of the process for other biotechnological applications. The idea behind the search of high-performance biocatalysts and the development of different configurations of enzymatic mNPs reactors should take into account not only the technological and operational feasibility but also the economic and environmental aspects for the practical application of this technology. With this in mind, the present document has been structured into the following chapters:

CHAPTER 1: General Introduction

In this first chapter a generic summary is presented about oxidoreductases and the main applications for which they will be used throughout this study. It also details the types of enzyme immobilization with their advantages and disadvantages. In addition, the idea of using magnetic nanoparticles as a support for immobilization is introduced. In addition, a bibliographic review and analysis is presented about the different enzymatic reactors that have been used for the biotransformation of compounds. Finally, the fundamental objective of the thesis is detailed.

CHAPTER 2: Immobilization of oxidoreductases to formulate robust and suitable biocatalysts

In this chapter different strategies of immobilization on magnetic and non-magnetic supports, as well as the formation of enzyme aggregates are presented. In particular, six different types of oxidoreductases are evaluated.

From the outcomes of this research, the target transformation reactions will be later developed on the basis of the selected nanobiocatalyst.

CHAPTER 3: Superparamagnetic nanobiocatalyst to biotransform micropollutants from wastewater

A nanobiocatalyst developed in the previous chapter will be evaluated in terms of stability against different pH, temperature and inhibiting compounds, and benchmarked with the values obtained for free laccase. In addition, its reusability will be demonstrated in consecutive oxidation cycles of Bisphenol A, estradiol and methyl green, which were selected as model compounds present in wastewater. It is also interesting to assess the toxicity associated to the degradation products from the enzymatic treatment that will be compared with the parent molecules.

CHAPTER 4: An eco-friendly nanobiocatalyst: *Pycnoporus sanguineus* laccase for environmental applications

This chapter focuses on the interest of using agro-industrial waste to produce laccase from *Pycnoporus sanguineus* as sources of natural carbon. The produced enzyme will be immobilized on the superparamagnetic silica-coated nanoparticles to evaluate the immobilization yields and stability. The nanobiocatalyst will be used in the biotransformation of Bisphenol A and methyl green in consecutive cycles. Finally, the potential toxicity of the nanobiocatalyst and the resulting medium will be checked.

CHAPTER 5: Superparamagnetic nanobiocatalyst in oxidation technologies for added value bio-based products

In this chapter two oxidoreductases, galactose oxidase and aryl alcohol oxidase, will be immobilized on the superparamagnetic silica-coated nanoparticles and used to perform cascade reactions to produce high value-added products from 5-Hydroxymethylfurfural (HMF). In addition, the

genotoxicity of the nanobiocatalyst will be studied to demonstrate the potential DNA damage, condition suggesting that the nanobiocatalyst is safe or not to be used in different biotechnological applications.

CHAPTER 6: Development of an enzymatic reactor with internal magnetic separation for biotechnological applications

A new sequential batch reactor will be designed, coupled to an internal magnetic separation system. The separator consists of a series of axially magnetized toroidal magnets, distributed along a non-magnetic steel bar and with alternate polarity, which generates an external magnetic field of up to 1.2 T. The proof of concept of the reactor will be conducted by evaluating the transformation of methyl green and HMF, with complete recovery of the nanobiocatalyst. Finally, the reactor will be scaled to a volume of 100-L to estimate costs and environmental impact.

CHAPTER 7: Comparative life cycle assessment of different synthesis routes of magnetic nanoparticles

In this chapter the environmental assessment of the different routes of synthesis of magnetic nanoparticles used as supports for immobilization will be carried out using the perspective of Life Cycle Analysis (LCA). The complexity of the production process for the nanoparticles suggests that a compromise must be adopted between efficiency and associated environmental impact.

USC
UNIVERSIDADE
DE SANTIAGO
DE COMPOSTELA

USC
UNIVERSIDADE
DE SANTIAGO
DE COMPOSTELA

Chapter 1

Introduction

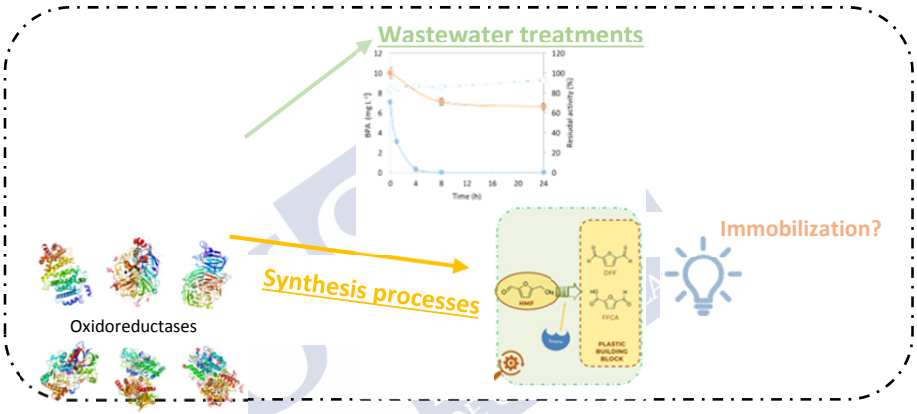

Oxidative biocatalysts by oxidoreductases arises as a promising alternative from the development of advanced oxidation processes for transformation of emerging contaminants to transformation of compounds into value added bio-based products. For technical and economic reasons, in most enzyme catalysed processes it is necessary to reuse the biocatalyst. In this context, enzyme immobilization can be defined as a technique that allows reuse or continued use of the biocatalyst. Envisaging the application of the different biocatalysts in wastewater treatment plants or other biotechnological applications it is important to design an enzymatic reactor in which the recovery and reuse of the enzyme is fulfilled.

USC
UNIVERSIDADE
DE SANTIAGO
DE COMPOSTELA

OUTLINE

CHAPTER 1

1.1. Oxidoreductases

Oxidoreductases are the enzymes using oxygen or peroxide and could be classified as oxidases (EC 1.X.3.X), peroxidases (EC 1.11.1.X), peroxygenases (EC 1.11.2.1), monooxygenases (EC.1.13.12.X, 1.14.13-18.X) and dioxygenases (EC 1.13.11.X, 1.14.12.X) (Gygj and van Berkel, 2015). These enzymes are capable of catalyze redox reactions due to their versatility using different electron acceptors and electron-donating substrates. Among the different oxidoreductases, fungal oxidoreductases have a great interest due to their robust and high redox-potential (Martinez *et al*. 2017). In biotechnological applications, the common fungal oxidoreductases included: heme-containing peroxidases and peroxygenases, flavin-containing oxidases and dehydrogenases and copper-containing oxidases and monooxygenases. Typical fungal oxidoreductases consisted on basiomycete ligninolytic peroxidases, and ascomycete and basidiomycete multicopper oxidases with variable redox potential and ability into react with lignin-derived products (Martinez *et al*. 2017). Glucose oxidase was the first oxidoreductase to attract industrial interest in order to improve flour and dough properties. Since then, many studies and reports have studied the use of different oxidoreductases for many industrial applications.

1.2. Copper-containing oxidases: Laccases

Laccases (EC 1.10.3.2) are enzymes with phenol oxidase activity that contain copper atoms in their active center and catalyze the oxidation of a wide variety of organic substances, in a process coupled with the reduction of molecular oxygen to water (Kunamneni *et al.,* 2008), as shown in Figure 1.1.

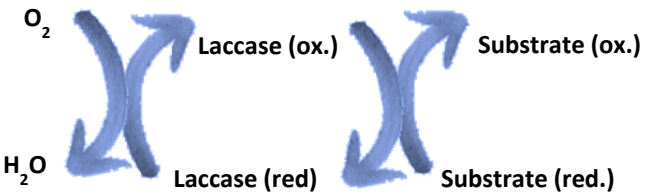

Figure 1.1. Oxidation mechanism of laccase

Due to the numerous biotechnological applications of laccase, its study has been increasing since its discovery in the 19th century (Cañas *et al.,* 2010). They

were first described in exudates of the Japanese tree *Rhus vernicifera* (Yoshida, 1883). However, it was not until 1986, when it was shown to be an enzyme present in fungi (Baldrian, 2006) and is now known to exist in insects (Dittmer *et al.,* 2009), bacteria (Claus, 2004) and archaea (Uthandi *et al.,* 2010). This demonstrates their wide distribution in nature, as well as their involvement in a multitude of different biological processes

The functions they perform are determined by the type of organism. For example, in the woody tissues of plants they would be part of the lignin synthesis (Ranocha *et al.,* 1999). In the case of soil saprophytic basidiomycetes, they play an important role in the degradation of soil organic matter, and thus in the formation of humus (Jonas *et al.,* 1998). Table 1.1 presents some laccase-producing fungi.

Table 1.1 Some laccase-producing fungi (Sánchez, 2006)

Fungi
Agaricus sp
Aspergillus nidulans
Batrytis cinérea
Ceriopsis subvermispara
Cerrena máxima
Trametes versicolor
Pyricularia oryzae
Neurospora crassa
Pycnoporus cinnabarinus

Other functions may be present in fungi. Thus, the ascomycete *Aspergillus nidulans* has at least two laccases, one of them involved in the green coloration of the conidia, and the other involved in the synthesis of the cell wall (Yaver *et al.,* 1996).

The wide specificity of the substrate, the use of oxygen as an electron acceptor, and the generation of water as the only bioproduct of the reaction (Bourbonnais *et al.,* 1990), confer to the enzyme high applicability in diverse biotechnological processes. However, they have a maximum redox potential of 0.8 eV, lower than peroxidases, limiting their range of action to aromatic compounds with low redox potential, such as phenolic units of lignin (Cañas *et al.,* 2010).

1.3. Flavin-containing oxidases

The flavin-containing oxidases catalyse the transfer of two electrons from alcohol substrates that reduced flavin passes the molecular oxygen to hydrogen peroxide as shown in Figure 1.2.

Figure 1.2. Oxidation mechanism of oxidases

1.4. Basidiomycete peroxygenase: Unspecific peroxigenase

Peroxygenases catalyse the incorporation of an oxygen atom from hydrogen peroxide into their substrate. A new class of peroxygenase has been recently discovered: Unspecific peroxygenase (UPO). UPO is the first discovered basidiomycete peroxygenase from *Agrocybe aegerita*, reported twelve years ago. UPO in contrast with ligninolytic peroxidases uses glutamate as acid-base catalyst for activation by peroxide. This behavior confers versatility for using in different oxygenation and oxidation reactions. However, UPO present oxidative instability with high amounts of peroxide.

1.5. Industrial applications

Oxidoreductases enzymes have great technological potential in the pulp and paper industries, food treatment, bioremediation of environmental pollutants and in the treatment of industrial effluents, among others (Zucca *et al.,* 2011, Martinez *et al*. 2017).

In the pulp and paper industry, the separation and degradation of lignin is conventionally obtained using oxidants based on chlorine or oxygen and it has been proven that the use of the enzyme laccase allows the preferential elimination of the lignin without transforming the cellulose (Barreca *et al.,* 2003).

In the food industry, they have been used for the treatment of polyphenols in the wastewater of breweries (Yagüe *et al.,* 2000) and in the decolorization of some beverages (González *et al.,* 2000). They have also been used to promote better food packaging, as they prevent oxidation (Kunamneni *et al*., 2008).

Laccase can also be applied in detoxification treatments of soils containing phenolic contaminants such as polycyclic hydrocarbons (Siripong *et al.,* 2009). As for the use for the elimination of recalcitrant compounds, numerous studies have been carried out. For this reason, research into the elimination of this type of compound is booming and the use of laccase is considered a promising technology for the elimination of contaminants

1.5.1. Concern on the effect of emerging contaminants

The ongoing increase of the human population and economic growth is leading to a continuous demand for clean water resources. More than one-third of the Earth´s accessible renewable freshwater is already used for agricultural, industrial and domestic purposes and water withdrawals are predicted to increase by 50% in developing countries, and 18% in developed countries by 2020 (UNEP 2007). According to this tendency, as many as 7 billion people in 60 countries could face water scarcity by 2050 if any action is taken. The revolutionized development of resources and technologies in the last century has produced a large amount of new chemicals and compounds which consequently increased the number of compounds that were identified threatening the environment and human health. These compounds such as pharmaceuticals and personal care products (PPCPs), surfactants, various industrial additives are endocrine disrupters and they are not metabolized and discharged into sewers and wastewater treatment plants (WWTPs).

The EU water framework directive 2000/06/CE announced in Annex X a list of priority substances with significant risk to the aquatic environment. The updated list includes metals, pesticides, phthalates, polycyclic aromatic hydrocarbons, and endocrine disruptors. These substances must be removed within an objective of quality and preservation of good ecological status of water. In addition, the REACH regulation, which aims to identify dangerous chemicals and less dangerous replacements, was established in 2007 in Europe (Deblonde *et al*. 2011). Therefore, the removal of emerging contaminants of concern is now an ever important in the

production of safe drinking water and the environmentally responsible release of wastewater (Bolong *et al*. 2009).

The presence of metals, bacteria, hydrocarbons or other ions like nitrates, ammonia in water are described for several decades and their impact on human health and the environment are known; these contaminants are subject to regulation and control. But the occurrence and effects of phthalates, pharmaceuticals compounds and endocrine disrupting compounds (such as bisphenol A) is often not available. They are originated from industry or from the discharge in wastewaters. The problem of emerging pollutants is the lack of knowledge of their impact in the middle or long-term effect on human health, the environment and aquatic environments. The degradation of organic pollutants implies an important challenge as they may have complex structure and/or low bioavailability. Moreover, conventional WWTPs are not primarily designed to remove them (Deblonde *et al*. 2011).

Treatment options which are typically considered for the removal of emerging contaminants from drinking water as well as wastewater include adsorption, advanced oxidation processes (AOPs), nanofiltration (NF), and reverse osmosis (RO) membranes (Grassi *et al*. 2012). Advanced treatment technologies such as ozonization, UV irradiation and activated carbon adsorption have been suggested to increase the removal of such compounds (Liu *et al*. 2009) but a full-scale implementation would require significant investment and increased operation costs. In this sense, the costs need to be weighed against the possible benefits of introducing new technologies. As a result, there are still need to develop and further examines new alternatives to efficiently remove these compounds from wastewater.

1.6. Enzymatic immobilization

For technical and economic reasons, in most enzyme catalysed processes it is necessary to reuse or continuously use the biocatalyst for a prolonged period of time (Katchalski-Katzir *et al*., 2000). In this context, enzyme immobilization can be defined as a technique that allows reuse or continued use of the biocatalyst. In addition, immobilization allows for greater stability and longer enzyme storage time (Lloret *et al.,* 2011).

1.6.1. Methods of immobilization

There are a large number of immobilization methods and since the method used greatly influences the properties of the resulting biocatalyst, the selection of the immobilization strategy determines the process specifications for the catalyst (Durán *et al*., 2002). A classification of the main methods may be the following (Illanes *et al*., 2008):

- Enzyme entrapment by physical retention in the inner cavities of a solid matrix such as polyacrylamide, collagen or alginate
- Encapsulation of the enzyme by physical retention in synthetic membranes
- Immobilization of the enzyme by cross-linking with bifunctional reagents
- Immobilization in supports by physical, ionic or covalent bonds

Entrapment

Entrapment is defined as the physical retention of enzymes in a solid porous matrix, such as polyacrylamide, collagen, alginate, or gelatin. The enzyme is suspended in a monomer solution and a subsequent polymerization process keeps the enzyme trapped, avoiding direct contact with the environment. It is the simplest method of immobilization and there are no alterations in the enzymatic structure. However, this methodology has limitations in terms of mass transfer and also has a low enzyme load (Fernández-Fernandez *et al*., 2013).

Encapsulation

The enzyme is retained by a membrane that allows the passage of substrates and reaction products (Illanes *et al*., 2008). Retention can be achieved by microencapsulation in semi-permeable membranes or by adsorption of the enzyme onto a membrane that will form the reactor. As in the previous case, the enzyme is protected from the environment and the mass transfer represents an important limitation (Fernández-Fernández *et al.,* 2013).

Cross-linking

The use of solid supports for enzymatic immobilization can reduce the activity of the biocatalyst. Cross-linking is an alternative in which immobilization is carried out without support, achieved through the use of a bifunctional cross-linker agent.

Cross-linkers include dialdehydes, diiminosteres, diisocyanates and diamines activated by carbodiimide (Fernández-Fernández *et al*., 2013). Despite achieving greater activity and remaining stable in extreme conditions, they present deficiencies in mechanical properties and a high cost in protein purification (Illanes *et al.,* 2008).

Immobilization on supports

Different types of materials have been used as supports for the immobilization of enzymes, both organic and inorganic compounds. The main properties of the substrates are: large surface area, high bonding capacity with the enzyme, compatibility and insolubility in the reaction medium, mechanical and chemical stability, recovery after use and conformational flexibility. There is not a support that fulfills all the characteristics reason why this one is chosen depending on the requirements of the process (Illanes *et al*., 2008). In the present work, immobilization will be considered according to two methods of immobilization: adsorption and covalent bond (Fernández-Fernández *et al*., 2013). Both methods will be explained in more detail below.

Adsorption

The adsorption of enzymes on a substrate is based on ionic bonds and other weak attraction forces. Adsorption is a relatively simple and low-cost method of immobilization, making it potentially more competitive than other methodologies. Variables such as pH, ionic strength of the medium and hydrophobicity of the support must be taken into account in the immobilization process (Fernández-Fernández *et al.*, 2013). In spite of obtaining a high immobilization yield, in this method the enzyme is easily desorbed, especially in aqueous solutions (Illanes *et al*., 2008).

Covalent bond

Immobilization by covalent bond is the most interesting method in industrial applications. Therefore, covalent bonding has become the most widely used method of immobilization. In this technique, the chemical groups on the surface of the support are activated and react with the nucleophilic groups of the protein. Different supports have been studied for the immobilization of laccase by covalent bond, from silica supports, epoxy resins, gold, silver and magnetic supports, among others (Fernández-Fernández *et al*., 2013). In the present work, magnetic

nanoparticles will be used as supports both in the case of covalent bonding and in adsorption.

1.7. Nanoparticles as a support for immobilization

The rapid development of nanotechnology has provided a basis for innovation in a wide range of fields, such as health, agriculture, food, transport, environment, electronics and communications, resulting in a significant increase in research into new nanomaterials (Figura 1.3) (Grillo *et al*., 2015).

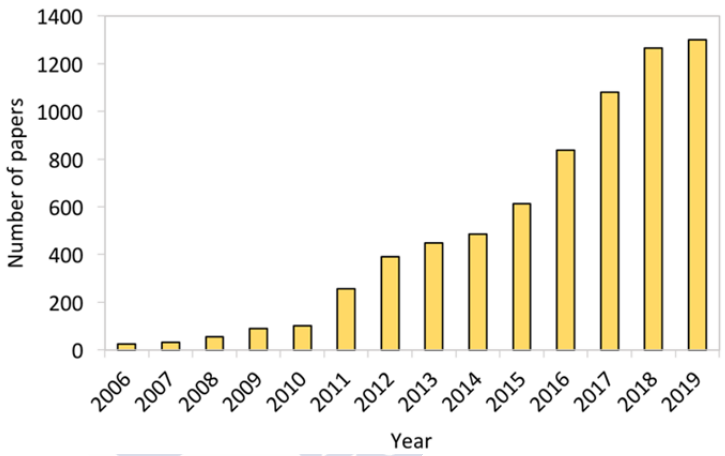

Figure 1.3. Number of publications on nanoparticles over time (ISI Web of Knowledge)

According to the European Committee for Standardisation (CEN), nanomaterials are defined as materials with any external dimension at the nanoscale, or having internal or surface nanoscale structures. The nanoscale size range is between 1 and 100 nm (ISO/TS 27687:2008) (JRC, 2010).

Nanoparticles (NPs), the most studied field within nanomaterials, have external dimensions of the order of 100 nm or less (JRC, 2010). NPs may be spherical, tubular, or irregularly shaped, and may exist as aggregates, fused or agglomerated (Nowack *et al*., 2007). There are two main types: engineered nanoparticles (ENP) and non-engineered nanoparticles. Non-engineered NPs are present in the environment in natural phenomena such as dust storms, erosion, volcanic eruptions and forest fires (Nowack *et al*., 2007; Cupaioli *et al*., 2014). ENPs are intentionally produced by humans as metals (including Ag, Zn, Au, Ni, Fe, and

Cu) (Kaegi *et al*., 2013), metal oxides (TiO_2, Fe_3O_4, SiO_2, CeO_2 and Al_2O_3) (Bozon-Verduraz *et al*., 2009), non-metallic (silica and quantum dots) (Probst *et al.,* 2013), carbon nanotubes and fullerene) (Isaacson *et al*., 2009; Ma *et al*., 2010), polymers (alginate, chitosan and polyhydroxyalkanoates) (Rao *et al*., 2011), and lipids (Faraji *et al*., 2009).

Nanomaterials can be used as support in enzymatic immobilization thanks to their properties such as surface area, resistance to mass transfer and others (Feng *et al*., 2011). Table 1.2 summarizes the advantages and disadvantages of the use of nanomaterials for enzymatic immobilization.

Table 1.2. Advantages and disadvantages of nanoinmobilisation (Cipolatti *et al.*, 2014)

Advantages	**Disadvantages**
Mass transfer resistance	Cost of the process
High enzyme load	Large scale application
High surface area	
High mechanical resistance	
Minimization of diffusion problems	
Separation of the reaction medium	

In recent decades, superparamagnetic particles of nanometric size (maghemite, γ-Fe_3O_4 or magnetite, Fe_3O_4) have been widely studied both in biology and medicine in areas such as magnetic resonance, DNA and RNA purification and immobilization of proteins and enzymes (Cipolatti *et al*., 2014).

Immobilization in nanomaterials offers numerous advantages in terms of separation as it is possible to separate them by physical methods, such as filtration or sedimentation (centrifugation) and they can be reused. Magnetic nanoparticles as media provide a simple and fast recovery of the biocatalyst by applying an external magnetic field and, compared to centrifugation or sedimentation, are subjected to much less mechanical stress. In addition, the use of magnetic nanoparticles as media has the following advantages: greater specific surface area to achieve greater enzyme load, lower resistance to mass transfer, less fouling, less diffusion problems and reduced operational cost (Kalkan *et al.,* 2011).

Based on the above, it is interesting to evaluate the immobilization of oxidorreductases in magnetic nanoparticles for the elimination of endocrine

disrupting compounds and the production of high value-added compounds in order to gain experience for the development of a possible future process on an industrial scale.

1.8. Opening the scope: Biotechnological applications of enzymes

Beyond the perspective of degradation of target contaminants, the use of an enzyme emerges as a biocatalyst in conversion/transformation processes. Accordingly, the oxidation process based on the use of oxidases and peroxidases may be of special interest in the case that the objective pursued is the transformation of substrates based on synthesis reactions.

Several industries and research/academic groups have demonstrated the feasibility of using new or improved (i.e. genetically modified) oxidative enzymes in the production of value-added compounds from molecules derived from biomass (such as sugars and lipids) to replace others of petrochemical origin and/or to develop more ecological and specific transformations. Of special interest in this field are several biochemical reactions of oxidation and oxyfunctionalization by fungal oxidases (Dijkman *et al*., 2013; Hernández-Ortega *et al*., 2012) and peroxidases, including new hemetiolate biocatalysts with monooxygenase activity (peroxygenases) (Bormann *et al*., 2015; Hofrichter and Ullrich, 2014). These peroxygenases are excellent biocatalysts for the regal and stereoscopic oxyfunctionalization of a variety of organic compounds. These enzymes also have the advantage of being stable (due to their secreted nature) and self-sufficient (Hofrichter and Ullrich, 2006), in the sense that they do not require the activation of a reducing power source and/or an auxiliary flavoenzyme/domain as in the case of other monooxygenases, such as cytochromes P450 (P450s) and flavinoxygenases (Kim and Oh, 2013).

In this context, this thesis evaluates the exploratory biochemical conversion of 5-hydroxymethylfurfural (HMF) into diformylfurane, a platform chemical, and 2,5-furandicarboxylic acid (FDCA), a basic plastic component. Oxidases and peroxygenases will be used to perform three-stage oxidation of HMF to FDCA in a single pot conversion without substrate and without by-products. FDCA (and HMF) occupied one of the first positions in the ranking of most interesting bio-based chemical building blocks published by the US Department of Energy in 2004 (Werpy

and Petersen, 2004), that they still maintain in similar studies published several years after (Bozell and Petersen, 2010; IAR, 2015a; 2015b).

Concerning FDCA production, the possibility to contribute to substitution of non-renewable PET by biomass-based PEF by using an enzymatic technology is a desirable goal, making the process more efficient and competitive. PEF itself has several advantages with respect to PET, including 50% better CO_2 footprint, several folds better O_2 and CO_2 permeability, higher density, and higher field strength, among others. The main advantage of the bio-chemical technology (using oxidases and/or peroxygenases) for PEF production is, in addition to the cost reduction due to milder operation conditions (high pressure and temperature is required when using Co/Mn/Br catalysts), the absence of the undesirable by-products formed due to the low selectivity of the current chemical technology for FDCA production (de Diego *et al.,* 2011). Such by-products include monocarboxylic acids that cause chain termination reactions in the intended polymer applications, and require greater energy and capital expenditure for product purification (van Putten *et al.,* 2013). Once optimized, the enzymatic conversion will circumvent the above problem due to its high selectivity. Biotechnological production of FDCA by selected *Pseudomonas* strains has been proposed as an alternative to the chemical conversion in several studies of Corbion (a leader company in the lactic acid sector, which is also interested in PEF production) (Wierckx *et al.,* 2015). However, due to different issues -including the need of a carbon and nitrogen source in the microbial transformation and the toxicity of furfural products for microorganisms - the biochemical process based on oxidative enzymes would be undoubtedly superior once optimized.

This thesis aims to provide innovative answers to develop a new generation of biochemical technologies for future biorefineries, allowing the transformation of molecules of plant origin with exquisite regio-selectivity and stereoselectivity that cannot be achieved by classical chemical technologies. Due to the above characteristics, the biochemical technologies to be developed will represent a real advance in lignocellulose biorefineries, improving competitiveness and allowing the development of new production routes. These oxidation/oxyfunctionalization reactions by oxidases and peroxygenases will allow a more integral and efficient use of the different types of feedstocks.

1.9. Enzymatic reactors

Envisaging the application of the different magnetic nanobiocatalysts in wastewater treatment plants or other biotechnological applications it is important to design an enzymatic reactor in which the recovery and reuse of the enzyme is fulfilled. In previous works, different systems based on the use of free enzyme or immobilized systems were proposed.

The first approach relies on the use of an enzymatic membrane reactor (EMR), which comprises a CSTR coupled with a semipermeable ultrafiltration membrane to ensure the retention of free biocatalyst. This system has been successfully applied for the enzymatic decolorization of dyes (López *et al*.2011) and also for the removal of endocrine disrupting compounds from filtered-secondary wastewater effluent. Laccase was highly stable during 100 h of operation until the reactor was discontinued. Alternatively, to the use of free enzyme, the use of immobilized laccase to facilitate its retention allowing the separation of the enzyme from the reaction medium, so that the biocatalyst can be applied in continuous systems and it can be beneficial for enzyme stability and prolonged storage (Lloret *et al*. 2011). Although laccase showed high stability during the operation of the reactor and the pollutants were efficiently removed, the main constraints are related to the complexity of the operation and the difficulty to add fresh enzyme. Regarding magnetic reactors, the available literature on configurations is very limited. Some alternatives are provided below.

In recent investigations, magnetic enzyme reactors have been used, such as the case of Wang *et al*. (2012), which designed a magnetically stabilized fluidized bed reactor, or Duan *et al*. (2014) in which reactor had a system of electromagnets where the reaction took place, both for the transformation of phenol in wastewater. However, these two configurations need an external power supply which implies drawbacks as the cost of the electricity or the high temperatures that reaches, among others. Ardao *et al*. (2013), also presented a configuration of a continuous reactor for eliminating micropollutants in which the separation system was a magnet in the outlet stream that collects the nanoparticles by means of a system of valves that reversed the flow, bringing the nanoparticles back to the reactor.

1.10. Enzyme-aided processes as a way of reducing the environmental impacts

The application of oxidative enzymes combined with nanoparticles as a high-performance nanobiocatalysts for environmental and bio-chemical processes is directly linked to the concept of Green Chemistry as a carrier for effective environmental sustainability. It is widely accepted that biocatalytic processes offer extensive advantages over traditional chemistry in terms of environmental impact as a result of milder reactions conditions (physiological pH and temperature), biodegradable enzymatic catalysts that reduce waste disposal requirements, and substitution of organic/toxic solvents by water (Sheldon, 2007).

In addition, the combination of higher regio- and stereo-selectivities also enables shorter processes that generate less waste. It has been shown that enzyme-catalyzed oxidations result in: i) Reduction of toxic reagents, solvents and metal catalysts; ii) Reduced consumption of energy and water; and iii) Reduction of waste and GHG emissions.

Besides its intrinsic, underlying sustainable character, this thesis aims at quantifying these indicators, especially those related to the production of the nanoparticles and the operation of the enzymatic reactor. This work will specifically address the evaluation of environmental impact reductions through process scale-up of selected case studies, which will support life cycle assessment of the processes. The broader use of optimized oxidoreductase based biocatalysts will help to develop enzyme-aided processes for environmental and biotechnological processes in a sustainable process that helps in their successful implementation.

1.11. References

Ardao, I.D., P. Demarche, R. Nair, S.N. Agathos. 2013.Micropollutants clean-up by bioinspired entrapped laccases in a continuous reactor with magnetic retention, Proceedings of the 2nd European Symposium of Water Technology and Management. (2013) 141-146.

Barreca A, Fabrini, M., Galli, C., Gentili, P., Ljunggren, S. 2003. Laccase mediated oxidation of a lignin model for improved delignification procedures. Journal of Molecular Catalysis B: Enzymatic, 26: 105-110.

Bolong, N Ismail, A.F. Salim, M.R. M.R. Matsuura, M.R.2009. A review of the effects of emerging contaminants in wastewater and options for their removal, Desalination,229 (1-3). 229-246

Bormann,S, Baraibar,AG, Ni,Y, Holtmann,D, Hollmann,F. 2015. Specific oxyfunctionalisations catalysed by peroxygenases: opportunities, challenges and solutions. Catal. Sci. Technol. 5:2038-2052.

Bozell,JJ, Petersen,GR. 2010. Technology development for the production of biobased products from biorefinery carbohydrates-the US Department of Energy's "Top 10" revisited. Green Chem. 12:539-55

Bozon-Verduraz F, Fernand-Fivet, J., Piquemal, R., Brayer, K, El, K., Yaghoub, S. 2009. Nanoparticles of metal oxides: some peculiar synthesis methods, size and shape control, application to catalysts preparation. Journal of Physics, 39: 134-140

Cañas A, Camarero, S. 2010. Laccases and their natural mediators: Biotechnological tools for sustainable eco-friendly processes. Biotechnology Advances, 28: 694-705

Cupaioli F, Zucca, F.A., Boraschi, D., Zecca, L. 2014. Engineered nanoparticles. How brain friendly is this new guest?. Progress in Neurobiology, 119-120: 20-38

Deblonde, T., Cossu-Leguille, C., Hartemann,P. 2011. Emerging pollutants in wastewater: A review of the literature, International Journal of Hygiene and Environmental Health, 214 (6): 442-448,

Diego,CM, Schammel,WP, Dam,MA, Gruter,GJM. 2011. Method for the preparation of 2,5-furandicarboxylic acid and esters thereof. Patent (International) WO 2011043660 A2.

Dijkman,WP, de Gonzalo,G, Mattevi,A, Fraaije,MW. 2013. Flavoprotein oxidases: classification and applications. Appl. Microbiol. Biotechnol. 97:5177-5188.

Dijkman,WP, Fraaije,MW. 2014. Discovery and characterization of a 5-hydroxymethylfurfural oxidase from Methylovorus sp strain MP688. Appl. Environ. Microbiol. 80:1082-1090.

Dijkman,WP, Groothuis,DE, Fraaije,MW. 2014. Enzyme-catalyzed oxidation of 5-hydroxymethylfurfural to furan-2,5-dicarboxylic acid. Angewandte Chemie 126:6633-6636

Duan, X., S.C. Corgié, D.J. Aneshansley, P. Wang, L.P. Walker, E.P. Giannelis, 2014. Hierarchical hybrid peroxidase catalysts for remediation of phenol wastewater, Chemphyschem. 15: 974–980

Durán N, D´Annibale, A., Gianfreda, L. 2002.Applications of laccases and tyrosinases (phenoloxidases) immobilized on different supports: a review. Enzyme and Microbial Technology, 31: 907-931

Faraji A, Wipf P. 2009. Nanoparticles in cellular drug delivery. Bioorganic and Medicinal Chemistry, 17: 2950-2962

Fernández-Fernández M, Sanroman, MA, Moldes, D. 2013. Recent developments and applications of immobilized laccase. Biotechnology Advances, 31: 1808-1825

Grassi M., Kaykioglu G., Belgiorno V., Lofrano G. (2012) Removal of Emerging Contaminants from Water and Wastewater by Adsorption Process. In: Lofrano G. (eds) Emerging Compounds Removal from Wastewater. SpringerBriefs in Molecular Science. Springer, Dordrecht

Grillo R, Rosa, AH, Fraceto, LF. 2015. Engineered nanoparticles and organic matter: A review of the state-of-the-art. Chemosphere, 119: 608-619 (2015)

Gygli, G., van Berkel, W.J.H., 2015. Oxizymes for biotechnology. Curr. Biotechnol. 4, 100–110.

Hernández-Ortega,A, Ferreira,P, Martínez,AT. 2012. Fungal aryl-alcohol oxidase: A peroxide-producing flavoenzyme involved in lignin degradation. Appl. Microbiol. Biotechnol. 93:1395-1410.

Hofrichter,M, Ullrich,R. 2006. Heme-thiolate haloperoxidases: versatile biocatalysts with biotechnological and environmental significance. Appl. Microbiol. Biotechnol. 71:276-288.

Hofrichter,M, Ullrich,R. 2014. Oxidations catalyzed by fungal peroxygenases. Curr. Opin. Chem. Biol. 19:116-125.

IAR. 2015a. International overview of bio-based chemical intermediates. Vol 1. Analysis of the last 10 years.

IAR. 2015b. International overview of bio-based chemical intermediates. Vol 2. Fact sheets on studied molecules

Isaccson C, et al., Quantitative Analysis of Fullerene Nanomaterials in Environmental Systems: A critical review. Environmental Science and Tecnhology, 43: 6463-6474 (2009)

Joint Research Center (JRC) of the European Commision, 2010. https://ec.europa.eu/jrc/sites/default/files/jrc-refreport-definition-nanomaterial-eur24403en.pdf, (Accessed July, 2019)

Illanes A,. 2008. Heterogeneous Enzyme Kinetics. In: Illanes A. (ed.) Enzyme Biocatalysis. Chile: Springer,155-203.

Kaegi R, Voegelin A, Ort C, Sinnet B, Thalmann B, Krismer J, Hagendorfer H, Elumelu M, Mueller E. 2013. Fate and transformation of silver nanoparticles in urban wastewater systems. Water Res.; 47(12) 3866-3877.

Kalkan, N. A., Aksoy, S. , Aksoy, E. A. and Hasirci, N. (2012), Preparation of chitosan-coated magnetite nanoparticles and application for immobilization of laccase. J. Appl. Polym. Sci., 123: 707-716.

Katchalski-Katzir E, Kraemer, DM. 2000. C, a carrier for immmobilization of enzymes of industrial potential. Journal of Molecular Catalysis B: Enzymatic, 10: 157-176.

Kim,KR, Oh, DK. 2013. Production of hydroxy fatty acids by microbial fatty acid-hydroxylation enzymes. Biotechnol. Adv. 31:1473-148

Kunamneni, A., Ghazi, I., Camarero, S., Ballesteros, A., Plou, F.J., Alcalde, M., 2008. Decolorization of synthetic dyes by laccase immobilized on epoxy-activated carriers. Process Biochem. 43, 169-178.

López, C., Moreira, M.T. Feijoo, G. Lema, J.M. 2011. Economic comparison of enzymatic reactors and advanced oxidation processes applied to the degradation of phenol as a model compound. Biocatalysis and biotransformation. 29: 344-353.

Lloret, L., Eibes, G. , Feijoo, G. , Moreira, M. T., Lema, J. M. and Hollmann, F. (2011), Immobilization of laccase by encapsulation in a sol–gel matrix and its characterization and use for the removal of estrogens. Biotechnol Progress, 27: 1570-1579.

Ma P, Naveed, A., Siddiqui, G., Jan-Kyo, K. 2010. Dispersion and functionalization of carbon nanotubes for polymer-based nanocomposites: A review. Composites: Part A, 41: 1345-1367

Martínez, A.T., Ruiz-Dueñas, F.J., Camarero, S., Serrano, A., Linde, D., Lund, H., Vind, J., Tovborg, M., Herold-Majumdar, O.M., Hofrichter, M., Liers, C., Ullrich, R., Scheibner, K., Sannia, G., Piscitelli, A., Pezzella, C., Sener, M.E., Kılıç, S., van

Berkel, W.J.H., Guallar, V., Lucas, M.F., Zuhse, R., Ludwig, R., Hollmann, F., Fernández-Fueyo, E., Record, E., Faulds, C.B., Tortajada, M., Winckelmann, I., Rasmussen, J.-A., GeloPujic, M., Gutiérrez, A., del Río, J.C., Rencoret, J., Alcalde, M., 2017. Oxidoreductases on their way to industrial biotransformations. Biotechnol. Adv. 35 (6), 815–831.

Nowack B, Bucheli, T.D., 2007. Occurrence, behavior and effects of nanoparticles in the environment. Environmental Pollution, 150: 5-22

Probst C, Zrazhevskiy, P., Bagalkot, V., Gao, X. 2013. Quantum dots as a platform for nanoparticle drug delivery vehicle design. Advanced Drug Delivery Reviews, 65: 703-718

Rao J, Geckeler, K. 2011 Polymer nanoparticles: Preparation techniques and size-control parameters. Progress in Polymer Science, 36: 887-913

Sheldon,RA. 2007. The E factor: fifteen years on. Green Chem. 9:1273-1283.

Siripong, P., Oraphin, B., Sanro, T., Duanporn, P. 2009. Screening of fungi from Natural Sources in Thailand for Degradation of Plychlorinated Hydrocarbons. American-Eurasian Journal Agriculture and Environmental Sciences, 5: 466-472 (2009)

United Nations Environment Programme´s (UNEP). 2007. http://wedocs.unep.org/bitstream/handle/20.500.11822/7647/UNEP%202007%20Annual%20Report-2008806.pdf?sequence=5&isAllowed=y. (Accessed July, 2018)

van Putten,RJ, van der Waal,JC, de Jong,E, Rasrendra,CB, Heeres,HJ, de Vries,JG. 2013. Hydroxymethylfurfural, A versatile platform chemical made from renewable resources. Chemical Reviews 113:1499-1597.

Wang, F., Y. Hu, C. Guo, W. Huang, C.-Z. Liu,.2012.Enhanced phenol degradation in coking wastewater by immobilized laccase on magnetic mesoporous

silica nanoparticles in a magnetically stabilized fluidized bed, Bioresource Technology. 110: 120–124.

Werpy,T, Petersen G. 2004. Top value added chemicals from biomass. Vol. I: Results from screening for potential candidates from sugars and synthesis gas. DOE (http://www1.eere.energy.gov/biomass/pdfs/35523.pdf), Oak Ridge.

Wierckx,N, Elink Schuurman T, Blank L, Ruijssenaars H. 2015. Whole-cell biocatalytic production of 2,5-furandicarboxylic acid, p. 207-223. In B. Kamm (ed.), Microorganisms in Biorefineries. Springer Berlin Heidelberg

Yagüe S, et al., Biotreatment of tannin-rich beer-factory wastewater with white-rot basidiomycete Coriolopsis gallica monitored by pyrolysis/gas chromatography/mass spectrometry. Rapid Communications in Mass Spectrometry, 14: 905-910 (2000)

Zucca P, et al., Induction, purification, and characterization of laccase isozyme from Pleurotus sajor-caju and the potential in decolization of textile dyes. Journal of Molecular Catalysis B: Enzymatic, 68: 216-222 (2011)

Chapter 2

Immobilization of oxidoreductases to formulate robust and suitable biocatalysts

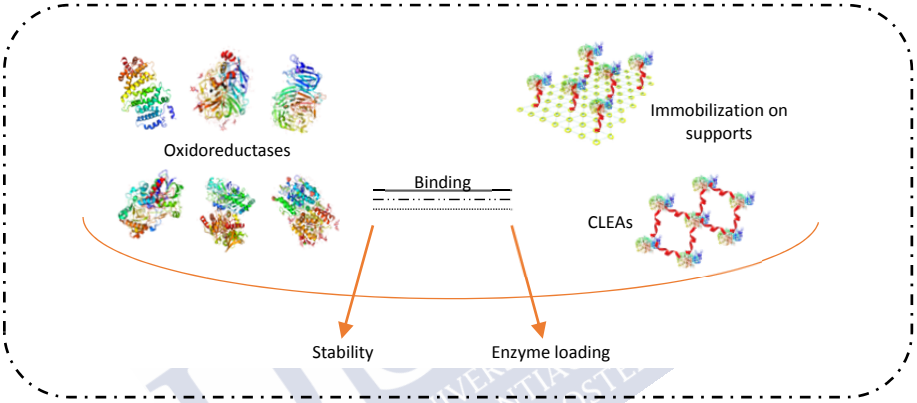

Oxidative biocatalysts based on oxidoreductases arise as a promising alternative in the development of advanced oxidation processes for the removal of emerging pollutants but also for the production of platform chemicals/building blocks such as those necessary for the manufacture of bioplastics. The aim of this work is to develop various types of immobilized biocatalysts based on self-immobilization as cross-linked aggregates (CLEAs) or on covalent binding on commercial supports and superparamagnetic nanoparticles. The highest yields of enzyme immobilization were achieved for the covalent enzyme nanoconjugates of silica-coated magnetic nanoparticles, formed by the covalent attachment of the enzyme between the aldehyde groups of the glutaraldehyde-functionalized nanoparticle and the residual amino groups of the enzymes. Moreover, the stability of the nanobiocatalysts was proven after 4 months with residual activities above 90% in all cases.

USC
UNIVERSIDADE
DE SANTIAGO
DE COMPOSTELA

OUTLINE

CHAPTER 2

2.1. Introduction

In this research, the use of enzymes is proposed as an alternative to perform the oxidation of pollutants of emerging concern and the production of building blocks. Although enzymes constitute promising biocatalysts, the use of enzymes for large-scale applications needs to bear in mid not only the catalytic activity and specificity but also its stability and reusability in a continuous operation. When free enzymes are used, their recovery can be only be performed by means of ultrafiltration membranes coupled to an enzymatic reactor. In contrast, the use of enzymes in an immobilized or insolubilized form favours their easy recovery and retention in the reaction system (Datta *et al*. 2013; DiCosimo *et al.* 2013). Conceptually, there are two basic methods for enzyme immobilization, as the immobilization can occur by physical or chemical interactions. Physical coupling methods include the entrapment of the enzyme within a tridimensional matrix, its encapsulation in an organic or inorganic polymer, and its absorption to the support surface by ionic exchange, whereas covalent bonding assures the irreversible binding of enzyme by self-immobilization using bifunctional cross-linkers or the binding to a support matrix (Fernández-Fernández *et al.* 2013). In this research, attention was paid to two different immobilization methods: self-immobilization using crosslinking agents and covalent immobilization of enzymes on commercial supports and superparamagnetic nanoparticles.

Self-immobilization of enzymes as cross-linked aggregates (CLEAs) is a simple technique to increase stability and reusability of biocatalyst (Torres *et al*. 2013). The procedure to prepare CLEAs usually involves an enzyme precipitation step and followed by protein cross-linking via the reaction of glutaraldehyde with reactive amine residues of the protein (Schoevaart *et al*. 2004). As aggregation and precipitation are commonly used for enzyme purification, the production of CLEAs combines purification and immobilization into a single operation (Sheldon *et al.* 2011). The method is extremely simple and amenable to swift optimization. However, CLEAs may suffer drawbacks as softness or poor mechanical stability, and often leaching of enzyme in the reaction medium during the biocatalysis may occur (Wilson *et al.* 2006).

On the other hand, enzyme immobilization by covalent binding onto a support has the advantage of multipoint covalent attachment which typically rigidifies the

enzyme structure, preventing it from undergoing inactivation deformations, which translates in an increased stability, activity and selectivity (Torres *et al.* 2013). The application of covalent immobilization techniques considers two different possibilities: either the use of inert supports which can be properly activated or the use of commercially available active supports. Among the latter, glyoxyl and epoxy-activated supports are considered very promising and have been reported to be effective supports for enzyme immobilization (Mateo *et al*. 2007; Lloret *et al*. 2012). However, to avoid enzyme leaching, it is convenient to disperse the enzyme on high specific surface areas, an intrinsic characteristic of nanomaterials. In the development of nanotechnology, a number of different materials may be used for this purpose, such as nanoparticles, nanosheets, nanotubes, nanofibers, and nanocomposites (Johnson *et al.* 2011; Tran *et al.* 2012; Ma *et al.* 2012; Plessis *et al.* 2013). Among the different nanomaterials, magnetic nanoparticles (mNP) offer an additional advantage over others because the retention of the biocatalyst is possible by means of a magnetic field, as an alternative to centrifugation or filtration stages (Kalkan *et al.* 2012).

The main goal of the work presented in this chapter was to investigate the immobilization of different oxidoreductases: *Trametes versicolor* and *Myceliophtora thermophile* laccases, Galactose oxidase, Aryl alcohol oxidase, 5-Hydroxymethyl furfural oxidase and Unspecific peroxygenase, to select the best biocatalysts for the different applications. With this aim, enzymes were immobilized as CLEAs as well as on different supports from commercial to superparamagnetic nanoparticles and both procedures were optimized.

2.2. **Materials and methods**

2.2.1. Chemicals for enzyme immobilization

3-(aminopropyl)triethoxysilane (APTES) (≥98%), 2-2´-azinobis(3-ethylbenzothiazoline-6-sulfonic acid) (ABTS) (≥98%), glutaraldehyde (25%), 3-(Ethyliminomethyleneamino)-N,N-dimethylpropan-1-amine (EDC) (≥98%), N-hydroxysuccinimide (NHS), vanillyl alcohol (≥98%) and polyethylene glycol (PEG) 6000 and 3350 were purchased from Sigma-Aldrich. Ammonium sulfate (98%) and *tert*-butyl alcohol (98%) were obtained from Panreac. Veratryl alcohol (97%) was

purchased in Fluka. Ethanol (≥96%) and acetone (≥99.6%) were purchased from Merck and Labkem, respectively.

2.2.2. Enzymes

Commercial laccase from *Myceliopthora thermophile (Mt)* (85 kDa) and galactose oxidase (GAO) (68 kDa) were provided by Novozymes. These enzymes were produced by submerged fermentation of genetically modified *Aspergillus oryzae*. *Trametes versicolor (Tv)* laccase (70 kDa) was purchased by Sigma-Aldrich. Recombinant aryl alcohol oxidase (AAO) (67 kDa) from *Pleurotus ostreatus* was obtained by expressing in *Escherichia coli* and was kindly provided by the Environmental Biotechnology Laboratory (IHI Zittau, Technical Dresden University, Germany). The recombinant unspecific peroxygenase (UPO) (45 kDa) from isolate S358 (ascomycete) was obtained by expressing in *Pichia pastoris* and provided by Jena Bios GmbH. 5-Hydroxymethyl furfural oxidase (HMFO) (70 kDa) from *Pseudomonas nitroreducens* was provided by the Biological Research Center (CIB, Spanish National Research Council, Spain). Three-dimensional structures of the enzymes can be found in literature and are shown in Figure 3.1.

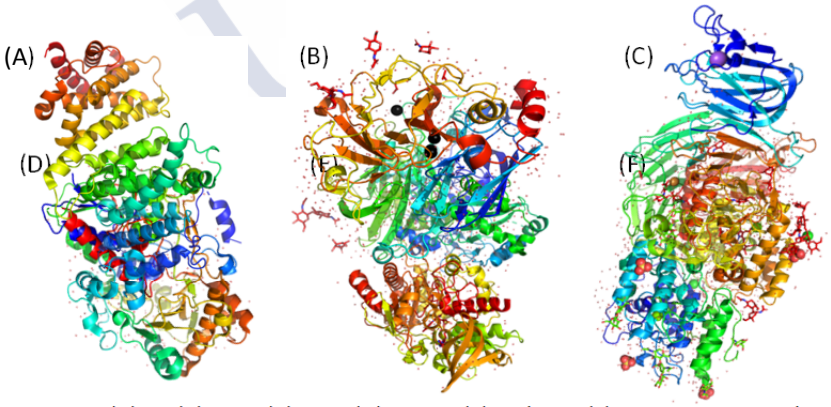

Figure 2.1. *Mt* (A), *Tv* (B), GAO (C), AAO (D), HMFO (E) and UPO (F). Figures generated using Pymol (pdb accession numbers 5LOI, 1GYC, 2EIB, 3FIM, 4UDP and 2YOR)

2.2.3. Supports for immobilization

2.2.3.1. *Epoxy and agarose-glioxyl based supports*

Epoxy-activated methacrylate polymers, Lifetech® ECR8204/F and ECR8215/F were purchased in Purolite and Relizyme® EP 403/M was purchased in Resindion. Agarose-glioxyl support was prepared from Agarose BCL-6 as described by other authors (Vieira *et al*. 2011) and was provided by the Institute of Catalysis and Petrochemistry (ICP, Spanish National Research Council, Spain). Detailed characteristics of these supports are presented in Table 2.1.

Table 2.1. Characteristics of the different supports

Support	**Size (μm)**	**Porosity (Å)**
Epoxy functional group		
Lifetech® ECR8204/F	150-300	300-600
Lifetech® ECR8215/F	150-300	1200-1800
Relizyme® EP 403/M	200-500	400-600
Agarose-glioxyl functional group		
Agarose-glioxyl	100	

2.2.3.2. *Superparamagnetic nanoparticles*

Non-coated magnetite nanoparticles (mNP), single-core silica-coated magnetic nanoparticles (smNP), polyacrylic acid magnetic nanoparticles (PAAmNP), polyethyleneimine-coated magnetic nanoparticles (PEImNP) were supplied by Nanomag (Universidade de Santiago de Compostela, Spain). Detailed characteristics of the nanoparticles evaluated are presented in Table 2.2.

Table 2.2. Characteristics of the different magnetic nanoparticles

Support	Size (nm)	Zeta potential (mV)
smNP	21.5±2.1	-24.2
PAAmNP	10.1±2.4	-40.1
PEImNP	10±1.2	4.7
mNP	9.9±1.4	-45.2

2.2.3.3. *Magnetized fumed silica nanoparticles*

Magnetized fumed silica nanoparticles (mfsNP) were prepared according with Safarik *et al*. (2012). Fumed silica nanoparticles (fsNP) (surface area: 390±40 m^2 g^{-1}; aggregates of particles with a size of 7 nm) were purchased from Sigma-Aldrich. The ferrofluid was provided by the Institute of Nanobiology and Structural Biology (GCRC, Czech Republic) and is composed of magnetic iron oxide nanoparticles (10-20 nm of diameter) and with a concentration of iron (Fe^{2+}, Fe^{3+}) oxide content of 48.11 mg mL^{-1}. The magnetized support from fumed silica nanoparticles is obtained after incubation with ferrofluid and methanol (1:7) under gentle agitation for 1 h. Afterwards, the nanoparticles were washed and re-suspended in phosphate buffer (pH 7) to remove residual methanol.

2.2.4. Determination of enzymatic activity

The enzyme activities of the free and immobilized enzymes were performed to assess the efficiency of the immobilization process. Below the analytical procedures that allow the determination of the activity of the different enzymes used in this study are described. The basis for the determination of enzyme activity is based on a common concept: the measurement of the oxidation of a model substrate, specific to each enzyme, which allows the indirect determination of activity by correlating the oxidation rate of the compounds with the reference enzyme units. All spectrophotometric measurements were carried out on a BioTeK PowerWave XS2 microplate spectrophotometer

2.2.4.1. *Myceliophthora thermophila (Mt) and Trametes versicolor (Tv)*

Laccase activity was determined by monitoring the oxidation rate of 0.267 mM ABTS to its cation radical ($ABTS^+$) at 420 nm (ε_{420} = 36,000 M^{-1} cm^{-1}) in McIlvaine buffer (80 mM citric acid and 40 mM Na_2HPO_4); pH 3) at 30˚C for 7 min (6-s intervals). One unit (U) of activity was defined as the amount of enzyme forming 1 µmol of $ABTS^+$ per min.

2.2.4.2. *Galactose oxidase (GAO)*

The activity of GAO was measured following the oxidation of 0.85 mM of ABTS into the radical cation $ABTS^+$ at 30˚C for 2 min (6-s intervals) under the catalysis of 2.55 U mL^{-1} of *Horseradish peroxidase* (HRP) and 85 mM of galactose in phosphate buffer (50 mM, pH 6) at 436 nm (ε_{436} = 29,300 M^{-1} cm^{-1}). One unit (U) of activity was defined as the amount of enzyme forming 1 µmol of $ABTS^+$ per min.

2.2.4.3. *Aryl alcohol oxidase (AAO) and Unspecific peroxygenase (UPO)*

AAO activity was measured following the oxidation of 10 mM of VE into veratraldehyde (as major compound) at 30˚C for 1 min (6-s intervals) in phosphate buffer (50 mM, pH7) at 310 (ε_{310} = 9,300 M^{-1} cm^{-1}). UPO activity was measured following the oxidation of 10 mM of VE into veratraldehyde (as major compound) at 30˚C for 1 min (6-s intervals) in presence of 0.5 mM of hydroxgen peroxide in phosphate buffer (50 mM, pH 7) at 310 nm (ε_{310} = 9,300 M^{-1} cm^{-1}). One unit (U) of activity was defined as the amount of enzyme forming 1 µmol of veratraldehyde per min.

2.2.4.4. *5-Hydroxymethyl furfural oxidase (HMFO)*

The activity of HMFO was measured following the oxidation of 35 mM of VA into vanillin at 30˚C for 1 min (6-s intervals) in TRIS buffer (50 mM, pH 7) at 309 nm (ε_{309} = 8,332 M^{-1} cm^{-1}). One unit (U) of activity was defined as the amount of enzyme forming 1 µmol of vanillin per min.

2.2.5. Self-immobilization of enzymes by cross-linking aggregates (CLEAs)

CLEAs are support-free covalently immobilized biocatalysts. First, a precipitant is used to form the enzyme agglomerates, and then a cross-linking agent binds these enzymes together, retaining them in the agglomerated form according to the scheme depicted in Figure 2.2.

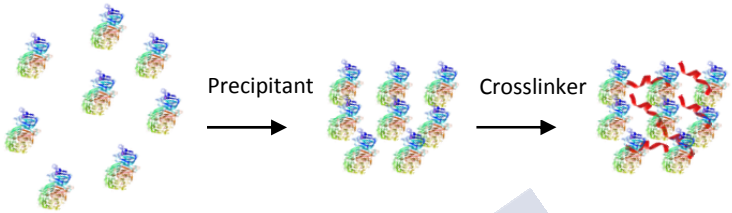

Figure 2.2. Scheme of CLEAs preparation.

As a first step, the enzyme (10,000 U L^{-1}) was incubated with the selected precipitants (PEG 3350 and 6000 (20 and 40 g L^{-1}), $(NH_4)_2SO_4$ (50% wt/v), EtOH (50% v/v), Acetone (36% v/v) and t-BuOH (90% v/v)) for 24 h at room temperature and at 100 rpm on a C24 Incubator shaker. The amount of aggregates formed is determined and re-dissolved in phosphate buffer (0.1 M, pH 7) and the activity was measured and compared to the initial activity. Thereafter, the aggregates of enzymes were incubated under agitation (100 rpm) at room temperature for 2, 8 and 24 h with the cross-linking agent glutaraldehyde 25% (v/v). Different concentrations of cross-linking agent (10, 50 and 100 mM) were considered. After each stage, the unreacted chemicals were removed after consecutive cycles of centrifugation/re-suspension in phosphate buffer (100 mN, pH 7). The immobilization efficiency was calculated as the ratio of the initial activity and the leached enzyme on the supernatants. All the experiments were performed in triplicate.

2.2.6. Immobilization of enzymes on epoxy and agarose-glioxyl based supports

Previous to immobilization process the supports (Lifetech® ECR8204/F, Lifetech® ECR8215/F, Relizyme® EP 403/M and agarose-glioxyl) were washed four times with carbonate buffer (100 mM, pH 10). The subsequent enzyme immobilization was carried out following the method described by Mateo *et al*. (2007). The schemes of the mechanisms of both immobilization processes are showed in Figure 2.3.

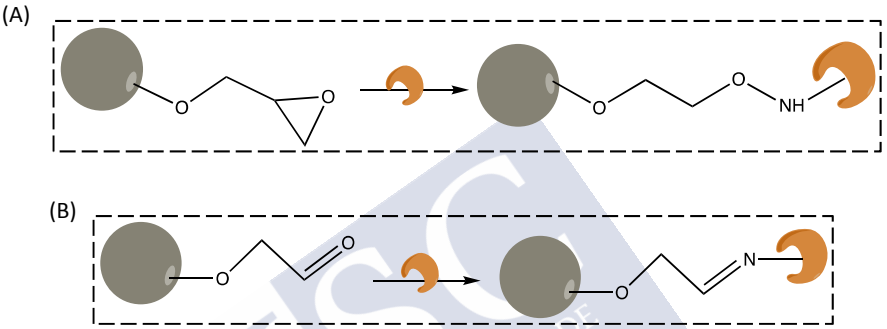

Figure 2.3. Mechanisms of enzyme immobilization onto epoxy (A) and agarose-glioxyl (B) based supports.

The washed support (100 g L^{-1}) was incubated with the enzymes (1.5 U mg^{-1} support) at 4°C for 24 h and 100 rpm on a C24 Incubator shaker. The non-covalently bound enzyme was washed with phosphate buffer (100 mM, pH 7) in five centrifugation/re-suspension steps for 5 min at 8000 g-force in a EBA-270 centrifuge. The immobilization yield was calculated as the ratio of the enzyme activity theoretically immobilized and the final enzyme loading.

2.2.7. Immobilization of enzymes on magnetic nanoparticles

2.2.7.1. *Immobilization of enzymes onto mNP*

Enzyme immobilization in magnetite nanoparticles (lacking any external coating) was carried out by ionic exchange of the enzyme with magnetite nanoparticles. Enzyme was added (0.55 U mg^{-1} mNP) to previously washed nanoparticles and incubated at 4°C and 25°C, 100 rpm, and pH 5, 6 and 7 for 4 h. After incubation, the nanobiocatalyst was washed five times in phosphate buffer (100 mM, pH 7) before storage.

2.2.7.2. Immobilization of enzymes onto smNP, PEImNP and mfsNP

The immobilization process for smNP and mfsNP requires their previous functionalization, in which reactive groups are added based on the modification of their surface by addition of APTES. The protocol starts with the incubation of the nanoparticles in phosphate buffer (100 mM, pH 7) and APTES (0.8 mmol mg^{-1} NP) for 12 h at room temperature. When the reaction was completed APTES excess was removed from amino-functionalized nanoparticles by 4 washed cycles with phosphate buffer (100 mM, pH 7).

Then, the nanoparticles were used to perform the immobilization of laccase according to the sorption-assisted immobilization (SAI) protocol (Zimmermann *et al*. 2011), where the nanoparticles and enzyme (2.82 U mg^{-1} NP) were incubated in phosphate buffer (100 mM, pH 7) at 4°C and 100 rpm for 2 h. Next, the glutaraldehyde (8 mmol g^{-1} NP) was added dropwise to the mixture of nanoparticles and enzyme, and the solution was incubated for an additional 18 h. The unreacted glutaraldehyde and the excess and unstable bound enzymes were washed away. The enzyme activity of the conjugates and supernatants of the NP enzyme was measured in these and the subsequent immobilization processes.

2.2.7.3. Immobilization of enzymes onto PAAmNP

The functionalization of the nanoparticles was conducted according to the method described by Nobs *et al*. (2003). The nanoparticles (5 mg mL^{-1}) were suspended in 2-(*N*-morpholino)ethanesulfonic acid (MES) buffer 0.1 M (pH 4.7), and EDC (12 mg mL^{-1}) and NHS (33 mg mL^{-1}) were added with gentle agitation (100 rpm) at room temperature to complete the reaction after 24 h. The unreacted NHS and EDC were removed by repeated washing and centrifugation (4000 rpm, 6 min), and were re-suspended in MES buffer. The amino-functionalized nanoparticles were then used to perform the immobilization of the enzymes by the aforementioned SAI method (Zimmermann *et al*. 2011) with 8 mmol glutaraldehyde g^{-1} NP and 1.88 U mg^{-1} NP.

2.3. **Results**

2.3.1. Immobilization of enzymes by CLEAs

Preparation of CLEAs was divided into two main steps consisting of precipitant choice followed by optimizing the cross-linker concentration and cross-linking time (Figure 2.2).

Precipitation, is a commonly method used for protein purification by the addition of salts, organic solvents or non-ionic compounds to aqueous solutions of proteins (Matijošytė *et al*. 2010). The supramolecular structures resulting after aggregation of enzymes are maintain together by non-covalent bonding and can be re-suspended in water (Schoevaart *et al*. 2004). Cross-linking produces the insolubilization of the enzymes as CLEAs maintaining the structural and catalytic activity of the proteins. The suitable optimization of the procedure (precipitant and cross-linker) may differ from one enzyme to another as they have different biochemical and structural properties (Matijošytė *et al*. 2010). The first goal was to optimize the conditions for the preparation of CLEAs with the different sources of enzymes selected.

2.3.1.1. *Selection of the optimum precipitant*

The precipitant selection is fundamental for the activity recovery as its depends on the nature of the precipitant (Sheldon *et al*.2011). Therefore, it was necessary to screen different water-miscible organic solvents, salts and polymers. The six enzymes were precipitated at room temperature for 24 h. Organic solvents such as ethanol, acetone and *tert*-butyl alcohol, ammonium sulfate solution, and water miscible polymer polyethylene glycol (PEG) with two different molecular weights were investigated as precipitants. Different concentrations of each precipitant were evaluated in excess of enzyme (10,000 U L^{-1}) with the aim of maximizing the precipitation of enzyme. In the screening, the activity recovery, which is defined as the activity after the precipitation step divided by the initial activity, was determined. Fig 2.4 shows eight different types of precipitants and their effect on residual activity after the precipitation process and before the cross-linking.

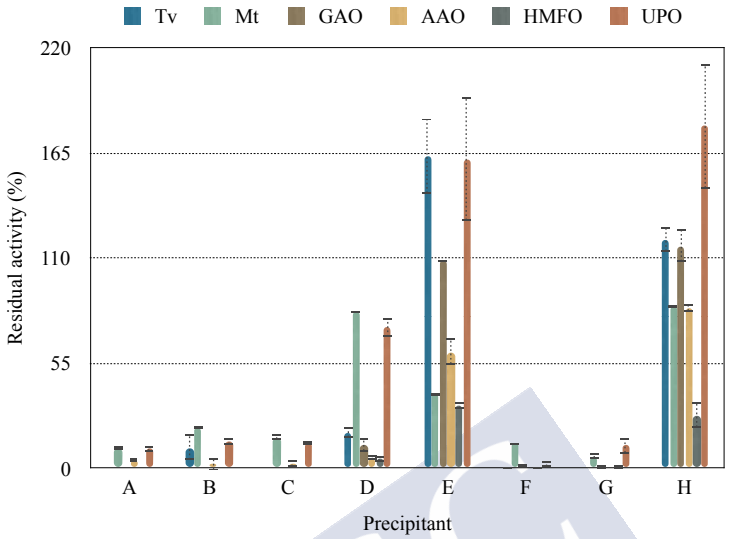

Figure 2.4. Residual activities of the enzymes for the different precipitants. (A, B: PEG 3350 (20 and 40 g L^{-1}), C, D: PEG 6000 (20 and 40 g L^{-1}), E: $(NH_4)_2SO_4$ (55% wt/v), F: Ethanol (50% v/v), G: Acetone (36% v/v) and H: *tert*-butyl alcohol (90% v/v))

Precipitating free laccases with *tert*-butyl alcohol (H) and ammonium sulfate (E) (Figure 2.4) yielded residual activities higher than 30% in all cases, but less than 20% residual activity was recovered with other precipitants such as ethanol (F) or PEG (A-D). Dennison and Lovrien (1997) suggested that ammonium sulfate and *tert*-butyl alcohol are the best precipitants for high enzyme recovery as the enzyme is in an excited state in their presence and hence, flexibility of the protein (B-value) is higher than for free enzymes. The optimum precipitant in *Mt*, GAO, AAO and UPO enzymes was the tert-butyl alcohol (Figure 2.4) and ammonium sulfate in the case of laccase from *Tv* and HMFO. Moreover, precipitating the enzyme with *tert*-butyl alcohol yielded high residual activities and even above 100% compared with equivalent free enzyme. Due to its size and branched structure, *tert*-butyl alcohol does not penetrate folded protein molecules and consequently does not induce denaturation (Kumar *et al*. 2012)

2.3.1.2. *Optimization of cross-linking concentration and time*

The second step of CLEA preparation is the cross-linking of the aggregate (Figure 2.2). Although various cross-linkers are known, glutaraldehyde remains as one of the most potent and cheap, even with clinical applications (Barbosa *et al*. 2013). Several cross-linking times and concentrations of glutaraldehyde were initially evaluated in order to determine the time and concentration required to obtain the highest enzyme immobilization as the amount and time is dependent on the type of enzyme (Talekar *et al*. 2013).

As observed in Table 2.3, hardly differences were noticed at 8 and 24 h in all the cases, so the lowest cross linking time was selected to design a short process for the CLEAs preparation. However, concentration of glutaraldehyde varies in each case as previously anticipated. In the case of laccases from *Tv* and *Mt* the optimal concentration of glutaraldehyde was 100 mM which leads to hyperactivation and highest immobilization yields (150 and 97%) whereas AAO was completely inactivated when glutaraldehyde exceeded 10 mM. In other studies, was found that other enzymes as nitralases low or no retention of activity was also detected when glutaraldehyde was used as cross-linker (Mateo *et al*. 2004; Nadar *et al*. 2016). Sheldon *et al*. (2007) suggested that glutaraldehyde with its high reactivity and small size could penetrate the protein and react with the amino acid residues crucial for the activity of the enzyme. For GAO and HMFO the optimal dose was 50 mM with immobilization yields of 62% and 129%. Slightly differences were observed in the case of UPO CLEAs at different concentrations of glutaraldehyde so the lowest one (10 mM) was selected leading in an immobilization yield of 87%.

Table 2.3. Immobilization yield (%) of CLEAs at different concentrations and cross-linking time

Enzyme	Glutaraldehyde (mM)	Immobilization yield (%) 2h	8h	24h
	10	24.2±3.1	56.3±5.8	52.4±1.9
Tv	50	52.0±0.9	67.0±0.6	74.0±0.5
	100	73.4±0.2	150.0±0.4	97.3±0.5
	10	-	41.6±10.4	11.8±34.5
Mt	50	-	55.1±17.6	27.1±1.6
	100	-	94.9±14.6	77.5±13.6
	10	21.1±5.8	26.0±1.4	59.3±2.3
GAO	50	11.2±0.1	62.2±20.2	41.3±25.1
	100	12.8±0.2	31.7±2.4	27.1±9.8
	10	-	-	-
AAO	50	-	-	-
	100	-	-	-
	10	11.6±0.2	20.7±1.2	35.6±2.3
HMFO	50	180.9±23.4	129.3±24.5	48.8±1.6
	100	134.0±25.6	156.7±26.7	107.0±17.5
	10	-	87.1±5.8	64.8±4.8
UPO	50	-	56.9±18.0	98.7±32.4
	100	-	106.2±22.6	86.1±7.5

2.3.2. Immobilization of enzymes on supports

Several strategies of enzyme immobilization were evaluated on magnetic and non-magnetic supports to obtain various types of biocatalysts. The enzymatic activity of both support-enzyme conjugates and supernatants were measured to determine activity yield and enzyme loading (Table 2.4). The tradeoff analysis of the different outcomes will be critical to identify the most suitable option for its further use.

Covalent bonding produces stronger bonds between the enzyme and the support, allowing its reuse more easily than with other available immobilization methods (Sheldon 2007; Ovsejevi *et al*. 2013). In this study, different functional

groups on the support surface were evaluated for enzyme immobilization (Table 2.4). The covalent bonding between the supports with carboxylic groups (polyacrylic acid) did not result in satisfactory immobilization (yields lower than 5%). This may be due to excessive crosslinking of the protein molecule (due to the presence of both NH_2 and COOH groups in the enzyme and also to the instability of carbodiimide, which led to very low activity yields, as was also observed in other studies with activity yields below 14%) (Majumder *et al*. 2008; Kumar *et al*. 2014).

However, enzymes were successfully immobilized in other supports such as PEI-mNPs, which showed an activity yield higher than 50% in all cases (Table 2.4). The stability of this biocatalyst was inferior to the enzyme immobilized on mfsNP and smNP. In the specific case of PEImNP, the enzyme activity after three months was lower than 50%, which was significantly lower than those for mfsNP and fsNP (93 and 99%, respectively). Similar results were observed for a previous report with silica nanoparticles, using remarkably higher dosages of APTES and glutaraldehyde than the values considered in this research (Arca-Ramos *et al*. 2016). The rationale behind the high activity yields attributed to the fact that immobilized enzymes on these supports would have high affinity for standard substrates such as ABTS. Arca-Ramos *et al*. (2016) reported the hyperactivation of laccase from *Tv* after the formation of covalent bonds with silica nanoparticles.

The process of immobilization by ionic exchange is based on the interaction of the charged groups of the enzyme with the groups of opposite charges in the support. It provides a weak bond between the enzyme and the support so that the native structure of the enzyme is unaltered. Moreover, the bonding is reversible and it is sensitive to changes in the pH and ionic strength, which can lead to the recovery of the support (Durán *et al*. 2002). When this approach was considered for the immobilization, not only limited yield was evidenced, but also the change of basic pH lead to enzyme desorption. When performing the immobilization of enzyme at different pH values, the best results were observed at pH 5 with an activity yield higher than 50% from *Tv* (Table 2.4), possibly because the point zero charge (PZC) of the magnetite is between pH 6.5-7.9 (Corgié *et al*. 2012), while the isoelectric point of the enzymes is around pH 3.0-4.2 (Claus *et al*. 2002). The main drawback is that laccase stability decrease with lower pH, which was evidenced by the reduction of the immobilized enzyme. Considering the best results of activity yield and enzyme loading, smNP were selected for the following experiments.

Table 2.4. Immobilization yield (IY) and enzyme loading (EL) for the different enzymes and supports

Supports	*Tv*		*Mt*		GAO	
	IY (%)	EL (U mg^{-1})	IY (%)	EL (U mg^{-1})	IY (%)	EL (U mg^{-1})
Agarose glyoxyl based supports						
Agarose-glyoxil (Ag)	0.22 ± 0.02	<0.01	0.51 ± 0.14	<0.01	1.53 ± 0.01	<0.01
Epoxy based supports						
ECR8204/F	0.07 ± 0.01	<0.01	0.13 ±0.01	<0.01	1.11 ± 0.01	<0.01
ECR8215/F	0.14 ± 0.02	<0.01	0.36 ± 0.17	<0.01	3.40 ± 3.90	<0.01
Relizyme	0.06 ± 0.01	<0.01	0.62 ± 0.60	<0.01	8.00 ± 5.00	<0.01
Nanoparticles						
mNP	58.50±0.22	0.69±0.01	31.60±0.57	0.45±0.05	-	-
smNP	103.50 ± 0.35	2.66 ± 0.65	102.84 ± 12.90	0.65 ± 0.01	51.21 ± 1.68	2.66 ± 0.65
PEI-mNP	80.50 ± 0.21	1.54 ± 0.03	70.32 ± 0.05	<0.01	55.19 ± 1.80	1.54 ± 0.03
mfsmNP	70.30 ± 0.10	1.48 ± 0.01	55.32 ± 0.12	<0.01	42.30 ± 1.99	1.48 ± 0.01

Table 2.5. Immobilization yield (IY) and enzyme loading (EL) for the different enzymes and supports (cont.)

Supports	AAO		HMFO		UPO	
	IY (%)	EL (U mg^{-1})	IY (%)	EL (U mg^{-1})	IY (%)	EL (U mg^{-1})
Agarose glioxyl based supports						
Agarose-glyoxil (Ag)	0.10 ± 0.02	<0.01	2 .00± 0.56	<0.01	15.60 ± 2.05	0.08±0.02
Epoxy based supports						
ECR8204/F	0.03 ± 0.01	<0.01	0.50 ±0.01	<0.01	0.50 ± 0.03	<0.01
ECR8215/F	0.03 ± 0.02	<0.01	2.00± 0.23	<0.01	1.20 ± 0.67	<0.01
Relizyme	0.04 ± 0.01	<0.01	2.30 ± 0.76	<0.01	3.00 ± 0.35	<0.01
Nanoparticles						
mNP	-	-	-	-	-	-
smNP	46.05 ± 7.71	0.95± 0.01	45.30 ± 11.80	0.21 ± 0.02	115.87 ± 5.95	1.04 ± 0.05
PEI-mNP	16.97 ± 5.58	0.55 ± 0.09	82.20 ± 11.3	0.37 ± 0.03	137.06 ± 0.92	0.92 ± 0.06
mfsmNP	16.68 ± 2.28	0.36 ± 0.01	68.30 ± 12.1	0.16 ± 0.02	128.32 ± 8.90	1.04 ± 0.02

2.4. Conclusions

Immobilization of two laccases (*Myceliophthora thermophila* and *Trametes versicolor*), three oxidases (Galactose oxidase, Aryl alcohol oxidase and Hydroxymethyl furfural oxidase) and one peroxygenase (Unspecific peroxygenase) was investigated aiming to facilitate its reuse and application in continuous operation such as water detoxification or for the production of building blocks. For this purpose, different methods were evaluated: first, the enzymes were immobilized by self-immobilization by precipitating the enzyme and further cross-linking with glutaraldehyde; also, enzyme immobilization was conducted by covalent and ionic exchange bonding to commercial epoxy- and glyloxyl-activated acrylic supports and superparamagnetic nanoparticles with different coatings (silica, polyethyleneimine and polyacrylic acid) by glutaraldehyde-activated and sulfo-NHS/EDC-activated. CLEAs were produced in all cases excepted for aryl alcohol oxidase which was completely inactivated when presence of glutaraldehyde. CLEAs of both laccases even leads to hyperactivation and high immobilization yields. However, the enzyme consumption and the difficulty of handling them are significantly higher compared with immobilization onto supports. Of all supports, superparamagnetic nanoparticles (functionalized with amino groups) showed the highest overall potential for enzyme immobilization with immobilization yields higher than 80%. Moreover, it was observed that the silica-coated superparamagnetic nanoparticles brought out a most stable biocatalyst after three months of storage. For those reasons silica-coated superparamagnetic nanoparticles arise as the most suitable form of immobilization of these enzymes.

2.5. References

Arca-Ramos, A. *et al*. (2016). Assessing the use of nanoimmobilized laccases to remove micropollutants from wastewater. *Environmental Science and Pollution Research International* 23 (4): 3217-28.

Barbosa, O, et al. (2013). Glutaraldehyde in Bio-Catalysts Design: A Useful Crosslinker and a Versatile Tool in Enzyme Immobilization. *RSC Advances* 4 (4): 1583-1600.

Claus, H.et al. (2002). Redox-Mediated Decolorization of Synthetic Dyes by Fungal Laccases. *Applied Microbiology and Biotechnology* 59 (6): 672-78.

Corgié, S.C. et al. (2012). Self-Assembled Complexes of Horseradish Peroxidase with Magnetic Nanoparticles Showing Enhanced Peroxidase Activity. *Advanced Functional Materials* 22 (9): 1940-51.

Datta, S. (2013). Enzyme immobilization: an overview on techniques and support materials. *3 Biotech* 3 (1): 1-9.

Dennison, C. et al. (1997). Three Phase Partitioning: Concentration and Purification of Proteins. *Protein Expression and Purification* 11 (2): 149-61.

DiCosimo, R. et al. (2013). Industrial Use of Immobilized Enzymes. *Chemical Society Reviews* 42 (15): 6437-74.

Durán, N. et al. (2002). Applications of laccases and tyrosinases (phenoloxidases) immobilized on different supports: a review. *Enzyme and Microbial Technology* 31 (7): 907-31.

Fernández-Fernández, M. et al. (2013). Recent developments and applications of immobilized laccase. *Biotechnology Advances* 31 (8): 1808-25.

Johnson, P. et al. (2011). Enzyme Nanoparticle Fabrication: Magnetic Nanoparticle Synthesis and Enzyme Immobilization BT- Enzyme Stabilization and Immobilization: Methods and Protocols. Edited by Shelley D Minteer, 183-91. Totowa, NJ: Humana Press.

Kalkan, N. et al. (2012). Preparation of Chitosan-Coated Magnetite Nanoparticles and Application for Immobilization of Laccase. *Journal of Applied Polymer Science* 123 (2): 707-16.

Klibanov, A. et al. (1979). Enzyme stabilization by immobilization. *Analytical Biochemistry* 93 (enero): 1-25.

Kumar, S. et al. (2014). Carbodiimide-Mediated Immobilization of Serratiopeptidase on Amino-, Carboxyl-Functionalized Magnetic Nanoparticles and Characterization for Target Delivery. *Journal of Nanoparticle Research* 16 (2): 2233. https://doi.org/10.1007/s11051-013-2233-x.

Lloret, L. et al. (2012). Immobilization of Laccase on Eupergit Supports and Its Application for the Removal of Endocrine Disrupting Chemicals in a Packed-Bed Reactor. *Biodegradation* 23 (3): 373-86.

López, C. et al. (2011). Economic comparison of enzymatic reactors and advanced oxidation processes applied to the degradation of phenol as a model compound. *Biocatalysis and Biotransformation* 29 (6): 344-53. https://doi.org/10.3109/10242422.2011.638056

Ma, Y-X. et al. (2012). Preparation and characterization of graphite nanosheets decorated with Fe_3O_4 nanoparticles used in the immobilization of glucoamylase. *Carbon* 50 (8): 2976-86. https://doi.org/10.1016/j.carbon.2012.02.080.

Majumder, A.B. et al. (2008). Designing cross-linked lipase aggregates for optimum performance as biocatalysts. *Biocatalysis and Biotransformation* 26 (3): 235-42.

Mateo, C. et al. (2007). Improvement of enzyme activity, stability and selectivity via immobilization techniques. *Enzyme and Microbial Technology* 40 (6): 1451-63. https://doi.org/10.1016/j.enzmictec.2007.01.018.

Mateo, C. et al. (2004). A New, Mild Cross-Linking Methodology to Prepare Cross-Linked Enzyme Aggregates. *Biotechnology and Bioengineering* 86 (3): 273-76. https://doi.org/10.1002/bit.20033.

Matijošytė, I. et al. (2010). Preparation and use of cross-linked enzyme aggregates (CLEAs) of laccases. *Journal of Molecular Catalysis B: Enzymatic* 62 (2): 142-48.

Nadar, S.S. et al. (2016). Macromolecular cross-linked enzyme aggregates (M-CLEAs) of α-amylase. *International Journal of Biological Macromolecules* 84: 69-78.

Nobs, L. et al. (2003). Surface modification of poly(lactic acid) nanoparticles by covalent attachment of thiol groups by means of three methods. *International Journal of Pharmaceutics* 250 (2): 327-37. https://doi.org/10.1016/S0378-5173(02)00542-2.

Ovsejevi, K. et al. (2013). Reversible Covalent Immobilization of Enzymes via Disulfide Bonds. *Methods in Molecular Biology (Clifton, N.J.)* 1051: 89-116.

Plessis, D.M. et al. (2013). Immobilization of Commercial Hydrolytic Enzymes on Poly (Acrylonitrile) Nanofibers for Anti-Biofilm Activity. *Journal of Chemical Technology & Biotechnology* 88 (4): 585-93.

Safarik, I. et al. (2012). One-step preparation of magnetically responsive materials from non-magnetic powders. *Powder Technology* 229: 285-89.

Schoevaart, R. et al. (2004). Preparation, Optimization, and Structures of Cross-Linked Enzyme Aggregates (CLEAs). *Biotechnology and Bioengineering* 87 (6): 754-62. https://doi.org/10.1002/bit.20184.

Sheldon, R. A. et al. (2007). Cross-Linked Enzyme Aggregates (CLEAs): Stable and Recyclable Biocatalysts. *Biochemical Society Transactions* 35 (Pt 6): 1583-87.

Sheldon, R. A. et al. (2011). Characteristic features and biotechnological applications of cross-linked enzyme aggregates (CLEAs). *Applied Microbiology and Biotechnology* 92 (3): 467-77.

Torres, M.P. et al. (2013). Cross-Linked Enzyme Aggregates (CLEAs) of Selected Lipases: A Procedure for the Proper Calculation of Their Recovered Activity. *AMB Express* 3: 25.

Tran, D-T. et al. (2012). Immobilization of Burkholderia sp. Lipase on a Ferric Silica Nanocomposite for Biodiesel Production. *Journal of Biotechnology* 158 (3): 112-19.

Vieira, M. et al. (2011). β-Glucosidase immobilized and stabilized on agarose matrix functionalized with distinct reactive groups. *Journal of Molecular Catalysis B: Enzymatic* 69 (1): 47-53.

Kumar, V. et al. (2012). Preparation and characterization of porous cross linked laccase aggregates for the decolorization of triphenyl methane and reactive dyes. *Bioresource Technology* 119: 28-34.

Wilson, L. et al. (2006). CLEAs of lipases and poly-ionic polymers: A simple way of preparing stable biocatalysts with improved properties. *Enzyme and Microbial Technology* 39 (4): 750-55. 1.

Zimmermann, Y-S. et al. (2011). Sorption-Assisted Surface Conjugation: A Way to Stabilize Laccase Enzyme. *Applied Microbiology and Biotechnology* 92 (1): 169-78.

Chapter 3

Superparamagnetic nanobiocatalyst to biotransform micropollutants from wastewater

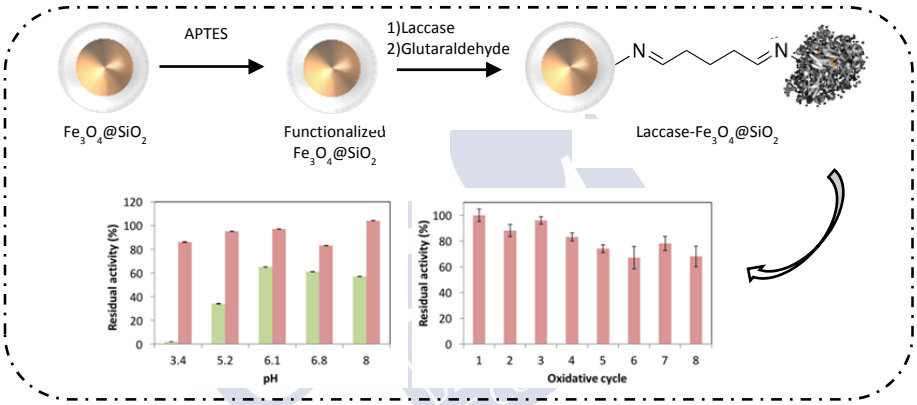

The development of nanotechnology has provided a range of diverse nanoscale carriers that can be potentially applied for enzyme immobilization. Among the different types of support, silica-coated magnetic nanoparticles (smNPs) have been selected and a high redox potential laccase from *Trametes versicolor* (*Tv)* was successfully immobilized. Enzyme loads of 2.66±0.07 U mg^{-1} smNPs were attained for the optimal doses of *Tv*. In general, the laccase-smNP conjugates showed higher resistance against acidic pH and higher storage stability, especially when incubated in the secondary effluent from a municipal wastewater treatment plant (WWTP). The ability of laccase-smNP to biotransform Bisphenol A (BPA), Phenol, Diclofenac (DCF), Estrone (E1), Estradiol (E2), 17ß-estradiol (EE2) and Methyl green (MG) was assessed in batch experiments. Compared to free laccase, immobilized enzyme led slower biotransformation rates but the superparamagnetic characteristic of the support allowed simple and fast recovery of the nanobiocatalyst.

USC
UNIVERSIDADE
DE SANTIAGO
DE COMPOSTELA

OUTLINE

CHAPTER 3

3.1. Introduction

Approximately 80% of all municipal and industrial wastewater are discharged to the environment without adequate treatment, resulting in harm on environment and human health. Among the main challenges defined in wastewater policy over the last years, emerging pollutants removal has arisen as key goal promoting the upgrade of conventional wastewater treatment plants (WWTPs) (WWAP, 2017). Conventional treatments in WWTP are not specifically designed to eliminate them so it becomes necessary the inclusion of tertiary treatments aimed at the removal of these compounds. One possible alternative is the enzymatic oxidation of these compounds by using fungal oxidorreductases such as laccases (Kunamneni et al. 2008). As mentioned in previous chapters, laccases are excellent biocatalysts for biotechnological and environmental applications because of their high oxidation potential as well as simple requirements for the catalysis (Majeau et al. 2010). Laccase was successfully applied to biotransform a wide range of pollutants, such as textile dyes, polycyclic aromatic hydrocarbons (PAHs), pesticides, and even pharmaceuticals and EDCs (Table 3.1).

Table 3.1. Biotransformation of different pollutants by laccases

Pollutants		References
Dyes	Remazol Brilliant Blue R, Lanaset Grey R	Daâssi et al. (2014)
	Acid Black 48, Reactive Black 5, Orange II	Blánquez et al. (2018)
	Reactive Blue 4	Afreen et al. (2017)
PAHs	Anthracene, naphathalene	Bautista et al.(2015)
	Benzo[a]pyrene, pyrene	Zeng et al. (2016)
Pharmaceuticals	Diclofenac, iodiquinol	Rodríguez-Delgado et al. (2016)
	Carbamazepine, acetominaphen	Hachi et al. (2017)
	Sulfadimethoxine	Liang et al. (2017)
EDCs	Bisphenol A	Lassouane et al. (2019)
	17-ß estradiol	Sun et al. (2016)
	Bisphenol A, nonylphenol, ethynilestradiol, triclosan	Garcia-Morales et al. (2015)

However, the use of enzymes for large-scale applications needs to bear in mind not only the catalytic activity and specificity of the biocatalyst but also its stability and reusability in a continuous operation. When free enzymes are used, their recovery can only be performed by means of ultrafiltration membranes coupled to an enzymatic reactor. In contrast, the use of enzymes in an immobilized or insolubilized for favours their easy recovery and retention in the reaction system (Datta et al. 2013; DiCosimo et al. 2013). Among the different immobilization methods, the most extensively used is covalent bonding of the enzyme to an insoluble polymer, such as epoxy-activated resins, silica-based supports, and several types of fibers and polymeric materiales, because this method will assure the irreversible binding of the enzyme to the support matrix (Fernández-Fernández et al. 2013). Moreover, it is of major interest to use enzyme carriers that not only provide the possibility of straightforward separation but also foster the catalytic action of the enzyme (Gasser et al. 2016).

Among a wide range of alternatives, the specific surface area of nanomaterials makes this type of support an ideal candidate for enzyme immobilization (Qu et al. 2013; Feng and Ji 2011). Nanobiocatalyst is an innovation that synergistically fuses nanotechnology and biotechnology breakthroughs. In its development, a number of different materials may have been used for this purpose, such as nanoparticles, nanosheets, nanotubes, nanofibers, and nanocomposites (Soozanipour et al. 2018; Kim et al. 2017; Huang et al. 2018; Dong et al. 2018), although few processes have been used for full-scale practical applications (DiCosimo et al. 2013). In the last decade, an increased attention is particularly focused on production of superparamagnetic iron oxide nanoparticles (SPIONs) as they show interesting characteristics such as superparamagnetism, high saturation field, high field irreversibility, extra anisotropy contributions or shifted loops after field cooling. Due to these characteristics, the nanoparticles only present magnetic interaction when an external magnetic field is present (Mahdavi et al. 2013). SPIONs are composed of iron core that can be coated with different functional coatings to stabilized them, such as silica. The superparamagnetic silica-coated nanoparticle is a novel class of magnetic material which present high biocompatibility and easy functionalization to bioconjugation with enzymes due to the surface reactive groups.

In this chapter, a novel nanobiocatalyst based on laccase immobilized on silica-coated superparamagnetic nanoparticles (Fe_3O_4@SiO_2) was developed applied for the oxidation of BPA, Phenol, E2, ABTS, MG and RB19. The influence of several factors (pH, T, cross-linker, enzyme activity, and additives) on the enzyme activity was evaluated. Moreover, other factors such as stability, reuse, regeneration of the support were also considered, especially when aiming the real application of the nanobiocatalyst to be environmental purposes.

3.2. Materials and methods

3.2.1. Chemicals for synthesis of nanoparticles and enzyme immobilization

All chemicals used were reagent-grade without further purification. Oleic acid (>99%) was provided by Merck; ammonium hydroxide solution (NH_4OH, 28 wt% in water) was supplied by Fluka. Iron(Fe^{3+}) chloride hexahydrate ($FeCl_3 \cdot 6H_2O$, 99%), iron(II) sulphate heptahydrate ($FeSO_4 \cdot 7H_2O$, 99%), Igepal CO-520 (polyoxyethylene (5) nonylphenylether, branched, Mn = 441), tetraethyl orthosilicate (TEOS, 99%), hydrochloric acid (HCl, 37%), cyclohexane (C_6H_{12}, 99.8%), 3-aminopropyl-triethoxy-silane (APTES) (≥98%), 2-2´-azinobis-3-ethylbenzothiazoline-6-sulfonate (ABTS) (≥98%), glutaraldehyde (25%), organic solvents (HPLC grade) and the commercial laccase from *Trametes versicolor* (activity≥ 10 U mg^{-1}) were purchased from Sigma-Aldrich. Buffer solutions were prepared with sodium hydrogen phosphate anhydrous (≥ 99%) from Panreac, sodium di-hydrogen phosphate anhydrous (≥ 99%) and acetic acid (≥ 98%) from J.T. Baker and citric acid from Vorquimia. The target pollutants BPA, E1, E2, EE2, DCF, Phenol and MG were purchased from Sigma-Aldrich.

3.2.2. Preparation and characterization of magnetic nanoparticles

Fe_3O_4@SiO_2 core-shell nanoparticles were prepared using a two-step procedure. In a first step, oleic-acid-coated Fe_3O_4 nanoparticles were prepared by the co-precipitation of Fe^{2+} and Fe^{3+} salts, following the Massart's method (Massart, 1981). In a typical synthesis, 2.43 g of $FeCl_3.6H_2O$ (9.0 mmol) and 1.67 g of $FeSO_4.7H_2O$ (6.0 mmol, molar ratio Fe^{3+}/Fe^{2+} ≈ 1.5) were placed in a 100-mL round-bottom flask and dissolved in 20 mL of 0.01 M HCl solution under mechanical stirring. Temperature was increased to 60ºC and 6 mL of 28% $NH_4(OH)$

solution was added to the mixture, with led to the immediate formation of black magnetite nanoparticles. After 30 s, 0.45 mL of oleic acid was added to the mixture and reaction was allowed to continue for 1 h. Then, the mixture was transferred to a beaker and heated on a hot plate until flocculation occurred. The nanoparticles were washed twice with deionized water and finally re-dispersed in cyclohexane.

In a second step, Fe_3O_4@SiO_2 core-shell nanoparticles were prepared through a water-in-cyclohexane reverse microemulsion starting from the oleic-acid-coated magnetite nanoparticles (Fang et al., 2011; Han et al., 2008). In a typical synthesis, Igepal CO-520 (15 g) and cyclohexane (180 mL) were placed in a 500-mL three-neck round-bottom flask and mechanically stirred for 15 min. Then, 20 mL of oleic-acid coated magnetite nanoparticles (0.5% wt in cyclohexane) was added and stirred for 30 min. Finally, $NH_4(OH)$ solution (2.1 mL, 28% wt) and TEOS (2.4 mL) were added to the mixture and left to complete the reaction for 16 h at room temperature. The core-shell nanoparticles were precipitated with isopropanol (IPA) and washed several times with IPA (four times) and deionized water (four times). Finally, they were subjected to several cycles of centrifugation (9000 rpm, 15 min) and washing with deionized water until no foam was observed. Then, the core-shell nanoparticles were re-dispersed in deionized water to a concentration ca. 0.5-1% wt (determined by thermogravimetric analysis).

3.2.3. **Characterization of magnetic nanoparticles**

The concentration of the magnetic nanoparticles dispersion was obtained by thermogravimetric analysis (TGA). The thermogravimetric curves were recorded with a Perkin Elmer TGA 7 thermobalance with increasing temperature up to 850ºC at a scanning rate of 10 °C min^{-1} under N_2 atmosphere.

The study of the crystalline phases was carried out by x-ray diffraction (XRD) on powder samples with a Philips PW1710 diffractometer (Cu Kα radiation source, λ=1.54186 Å). Measurements were collected between 10º<2θ<80º with steps of 0.020º and 5 s per step. TEM micrographs were taken with a JEOL JEM1011 transmission electron microscope operating at an accelerating voltage of 100 kV. A drop from a diluted sample solution was deposited onto an amorphous carbon film on 400 mesh copper grids and left to evaporate at room temperature.

Magnetization curves as a function of the applied magnetic field (up to 10 kOe) were performed with Quantum Design PPMS on dried samples.

3.2.4. Immobilization of laccase onto silica-coated magnetic nanoparticles

Laccase was immobilized onto smNP by following the procedure of sorption-assisted surface conjugation described in Chapter 2 (Section 2.2.7). Prior to immobilization, smNP (5 g L^{-1}) were amino-functionalized with APTES at concentrations of 0.4, 0.8, and 1 mmol APTES g^{-1} smNP and incubated at 150 rpm in an orbital shaker C24 Incubator shaker (New Brunswick Scientific, Edison, NY, USA) at room temperature for 15 h. Thereafter, the amino-functionalized nanoparticles and laccase were incubated under agitation (100 rpm) at 4°C for 2 h, just before the addition of cross-linking agent glutaraldehyde 25% (v/v). Different concentrations of cross-linking agent (1, 4, 8, 12 mmol glutaraldehyde mg^{-1} smNP) and laccase activity (1.88, 2.35, 2.82 U mg^{-1} smNP) were considered. After each stage the unreacted chemicals were removed after five consecutive cycles of magnetic separation and resuspension in phosphate buffer (100 mM, pH 7). The immobilization efficiency was calculated as the ratio of the laccase activity theoretically immobilized and the final enzyme loading. All the experiments were performed in triplicate. The determination of kinetic parameters was performed according to the Michaelis-Menten equation, as a function of ABTS concentration (1.17-750 µM). The data obtained were fitted by using a nonlinear least-square fit routine to provide K_M and V_{max} values.

3.2.5. Influence of pH, T, and inactivating compounds on the relative activity and stability of free and immobilized laccase

The influence of pH and temperature on the measurement of free and immobilized enzyme activity was investigated for variable ranges of pH between 2.4 and 8 and T between 22 and 60°C and compared with the maximum value (1000 U L^{-1}). The ratio between the activity at each condition and the maximum value (1000 U L^{-1}) was determined to calculate the relative activity. Enzyme stability was evaluated at different pH (from 3 to 8) and incubation periods of 1, 8 and 24 h and different temperature (10 to 50°C) for 24 h. Long-term stability of free and immobilized laccase at 4°C for 4 months was also evaluated. The enzyme stability against different inactivating compounds was determined by measuring residual

laccase activity after incubating free and immobilized laccase (1000 U L^{-1}) in different denaturing solutions: NaCl (90 mM), $CaCl_2$ (10 µM), methanol, acetone and ethanol (25%v/v) at pH 5 (200 mM acetate buffer). With the perspective of using the nanobiocatalyst for the removal of xenobiotics present in wastewater, the influence of the presence of secondary effluent on enzyme stability was evaluated for 24 days at 4°C. The composition of the wastewater effluent after filtration with a membrane of 0.45 µm is presented in Table 3.2. All the experiments were performed in triplicate.

Table 3.2. Characterization of the WWTP effluent

Parameter	**Value (mg L^{-1})**
Chemical oxygen demand (COD)	15.36
Total organic carbon (TOC)	6.97
Cations	
Na^+	20.25
K^+	2.03
Ca^{2+}	6.39
Anions	
Cl^-	26.10
NO_3^-	14.39
PO_4^{3-}	4.71
SO_4^{2-}	16.88

3.2.6. **Regeneration of the support**

The regeneration of the support after use for enzyme immobilization was performed in triplicate after the inactivation of the nanobiocatalyst, with acetone/ethanol (1/1, v/v), ultrasonication for 1 h (Transsonic 570/H, Auckland, New Zealand), and high temperature (85°C) for 30 min (Zhao et al. 2011). After repeated washing of the nanoparticles with phosphate buffer (100 mM, pH 7), the immobilization process was repeated following the procedure of sorption-assisted surface conjugation, but avoiding the previous stage of amino-functionalization.

3.2.7. **Biotransformation of the target pollutants**

To determine the capability of the enzymatic system the oxidation toward the target pollutants by free and immobilized enzyme (1000 U L^{-1}) was evaluated in batch reactors (30 mL flasks). The conditions of each experiment are detailed in Table 3.3.

Table 3.3. Summary of experiment conditions for the different target pollutant

Target pollutant	Concentration (mg L^{-1})	Reaction medium
BPA	10	Phosphate buffer (100 mM), pH 6
E1	2.5	
E2	2.5	
EE2	2.5	
Phenol	10	
MG	20	
DCF	5	Acetate buffer (100 mM), pH 5

BPA, DCF, E1, E2, EE2 and Phenol were quantified by High-Performance Liquid Chromatography (HPLC) at a detection wavelength of 270 nm on a Jasco XLC HPLC (Jasco Analítica, Madrid, Spain). This equipment was coupled with a diode detector 3110 MD, a 4.6 x 150 nm Gemini reversed-phase column (3 µm C 18 110 Å) from Phenomenex (supplied by Jasco Analítica, Madrid, Spain), and an HP ChromNav data processor. A 25-µL-sample volume was injected into the column. The mobile phase contained 50% acetonitrile and 50% water. The flow rate was fixed at 0.4 mL min^{-1} in isocratic conditions. MG was analyzed by following the decrease in absorbance at 630 nm.

3.2.8. **Biotransformation of the target pollutants in sequential batch reactors**

The biotransformation of Bisphenol A (100 µg L^{-1}), E2 (1 µg L^{-1}) and MG (20 mg L^{-1}) by immobilized laccase (1,000 U L^{-1}) incubated in the secondary effluent of a wastewater treatment plant (WWTP) was investigated in a sequential batch stirred reactor of 1 L for 10 cycles. In parallel, a control experiment with

functionalized mNP lacking laccase under the same conditions was also performed. After 6 h, the reaction medium was withdrawn, and the nanobiocatalyst and functionalized mNP (control) were magnetically separated for a new cycle biotransformation. The extent of the reaction was calculated as a ratio of the final and initial concentration of the compound. All experiments were performed in triplicate.

The percentage of BPA and E2 biotransformation was determined by Gas Chromatography-Mass Spectrometry (GC-MS) after a Solid Phase Extraction (SPE). The extraction procedure was carried out using 60 mg OASIS Hydrophilic-Lipophilic-Balanced (HLB) cartridges (Waters closet, Milford) previously conditioned with 3 mL ethyl acetate, 3 mL methanol, and 3 mL of distilled water acidified with HCl to pH 2. A nitrogen stream was used to dry the cartridges for 45 min and eluted with 200 mL ethyl acetate. The GC-MS analysis was conducted in a MS Saturn 2100T system with Zebron column (ZB-SemiVolatiles 30 m x 0.25 mm x 0.25 µm) (Phenomenex). The carrier gas was He with a flow rate of 1 mL min^{-1}. The injection was performed in splitless mode (2 min) at 280°C. The oven temperature was programmed to rise from 70 to 150°C at 25°C min^{-1}, at 3°C min^{-1} until 200°C and finally, at 8°C min^{-1} to reach 280°C, that was maintained for 5 min. Electron impact (EI) mass spectra were generated at 70 eV with a scan range of 50–500 amu. Each sample was analyzed in duplicate. MG decolorization was followed by spectrophotometry at 630 nm.

3.2.9. **Evaluation of toxicity**

To investigate the potential toxicity of the transformation products obtained from the enzymatic treatment, a Microtox® test based on the luminescent marine bacterium *Vibrium fischeri* was performed in triplicate using a Microtox® model 500 Analyzer. The results were expressed as $EC_{50\ (15\ min)}$, which corresponds to the concentration of the pollutant that causes a reduction in the light output by 50% after 15 min incubation. All the measurements were performed in triplicate.

3.3. Results and discussion

3.3.1. Characterization of silica-coated iron oxide nanoparticles

The X-ray diffraction patterns of both oleic acid and silica coated iron oxide nanoparticles are depicted in Figure 3.1. The crystalline phase was identified as magnetite (PDF-2 card number 19-0629) and the main reflections were labelled with the Miller indexes. In the silica-coated magnetite nanoparticles, a broad band between 20-30 º2Θ was observed due to the amorphous silica shell.

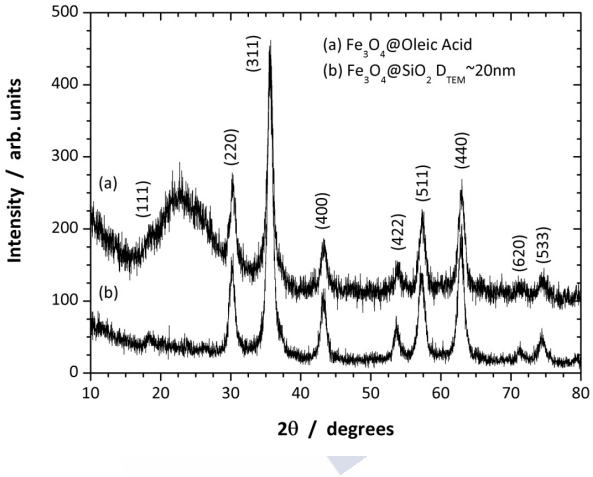

Figure 3.1. X-ray diffraction patterns of oleic-acid-coated magnetite and silica-coated magnetite nanoparticles

Transmission electron micrographs show the nearly spherical shape of both oleic-acid and silica-coated magnetite nanoparticles (Figure 3.2). The average particle size of the oleic-acid coated magnetite nanoparticles was 7.7±3.3 nm, and the silica-coated magnetite nanoparticles was 21.5±1.3 nm. From the TEM micrographs, it can be evidenced that the reverse microemulsion method allowed to develop an excellent silica coating on the magnetite nanoparticle. The samples were magnetically characterized by measuring the variation of the magnetization as a function of the applied magnetic field at 300 K (Figure 3.3). Both samples show superparamagnetic behaviour due to the small particle size (Lu et al., 2007). The oleic-acid-coated magnetite nanoparticles showed a high saturation magnetization

(measured as the magnetization at 10 kOe), M_s = 61.75 emu g^{-1}, and nearly zero values for both coercivity (H_c = 14Oe) and remanence (M_r = 1.35 emu g^{-1}). The decrease of saturation magnetization in the silica-coated magnetite nanoparticles was due to the non-magnetic silica shell, which did not affect the superparamagnetic behaviour negatively.

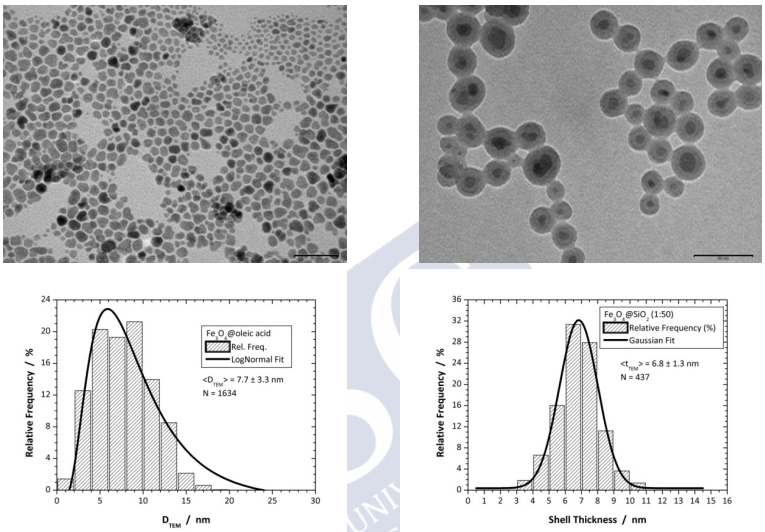

Figure 3.2. Transmission electron micrographs and corresponding size histograms of the oleic-acid-coated magnetite and silica-coated magnetite nanoparticles. Scale bar (50 nm).

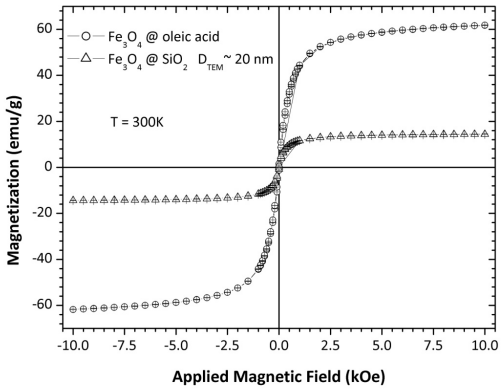

Figure 3.3. Magnetization study of the samples: plot of the variation of the magnetization with the applied magnetic field at 300 K

3.3.2. **Immobilization of laccase onto silica coated magnetic nanoparticles**

Silica allows the surface modification of the magnetite nanoparticles. The hydroxyl surface groups can be chemically modified to provide different bioconjugation groups, such as amine. To perform the aminofunctionalization of the nanoparticles, (3-aminopropyl) triethoxysilane (APTES) was added. In a further step, glutaraldehyde was used as cross-linker for the attachment of proteins via the amine groups of the lysine residues. Different concentrations of APTES and glutaraldehyde were evaluated in excess of laccase (3.29 U mg^{-1} mNP) with the aim of maximizing immobilization yield and enzyme loading while minimizing enzyme loss after washing.

As observed in Table 3.4, the optimal concentration of APTES was 0.8 mmol mg^{-1} mNP (run 2), which was the value selected for the following experiments. Regarding glutaraldehyde, the lowest concentration considered (run 4) was probably not sufficient to immobilize laccase, and almost 60% of the activity was lost after washing. As the concentration increased, the enzyme loading was also increased. However, washing losses markedly increased at the highest concentration (run 7), probably due to laccase inactivation caused by glutaraldehyde (Roy et al., 2006). Consequently, the optimal concentration of glutaraldehyde was found at 8 mmol mg^{-1} mNP, which led to the highest immobilization yield (83.7%). Finally, the maximum laccase immobilized on the mNP was similar (2.66-2.68 U mg^{-1} mNP for run 6 and 10, respectively) for the highest enzyme activities: 2.82 and 3.29 U mg^{-1} mNP, which is attributed to the likely saturation of the binding sites of the support by the enzyme. The enhancement of catalytic activity of the nanobiocatalyst was evidenced by the increase of ABTS oxidation, which rendered into values of immobilization yields above 100% (Table 3.4), revealing the superior affinity of immobilized laccase toward ABTS (Cabana et al., 2011; Arca-Ramos et al., 2016).

The immobilization of laccase into amino-modified silica nanoparticles using glutaraldehyde as cross-linker was shown to be dependent on laccase source, and reached values ranging from 0.77 to 4.77 U mg^{-1} mNP (Zimmermann et al., 2011; Hommes et al., 2012). When comparing the immobilization of laccase from *T. versicolor* onto fumed silica non-magnetic and magnetic nanoparticles, the maximum enzyme loading was significantly lower, between 2.5 and 1.7 times lower than the value reported here (Ammann et al., 2013; Deng et al., 2015).

Table 3.4. Immobilization of laccase in silica coated magnetic nanoparticles at different concentrations of APTES, glutaraldehyde and laccase activity

Run		Washing loss (%)	Immobilization yield (%)	Enzyme loading (U mg^{-1} mNPs)
APTES (mmol mg^{-1} mNPs)				
1	0.4	56.4±7.0	50.6±7.3	1.55±0.23
2	0.8	49.1±5.2	65.1±8.3	1.81±0.15
3	1.6	55.2±1.7	52.3±7.9	1.60±0.13
Glutaraldehyde (mmol mg^{-1} mNPs)				
4	1	59.8±2.3	36.0±3.8	0.89±0.07
5	4	22.5±17.8	82.8±11.6	2.07±0.25
6	8	21.1±1.8	83.3±1.1	2.66±0.07
7	12	35.7±12.3	77.0±11.0	2.72±0.45
Laccase (U mg^{-1} mNPs)				
8	1.88	16.4±2.81	103.5±1.3	2.11±0.18
9	2.35	28.4±6.9	103.7±16.0	2.31±0.43
10	2.82	30.7±6.4	64.2±4.6	2.68±0.08

3.3.3. Influence of pH, T and inactivating compounds on the relative activity and stability of free and immobilized laccase

While the optimal pH for the measurement of enzymatic activity was similar for both free and immobilized laccase: 3 (Figure 3.4), a significant effect was evident when evaluating the effect of pH on the enzyme stability at different incubation periods (Figure 3.5). It was observed that the immobilized enzyme showed higher activity, markedly enhanced under acidic conditions (pH 3-5), in agreement with other reports (Lloret et al., 2011; Rossi et al., 2004). On the contrary, free laccase was inactive after 24 h of incubation at pH 3.4, and remarkably low (18%) at pH 5.2. Comparatively, for the same incubation period, the activity of the immobilized laccase was similar: 41 and 43% at pH 3.4 and 5.2, respectively.

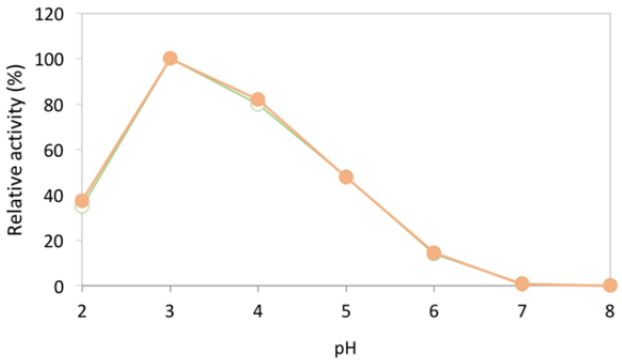

Figure 3.4. Effect of pH on the relative activity of free laccase (○) and laccase immobilized into mNP (●).

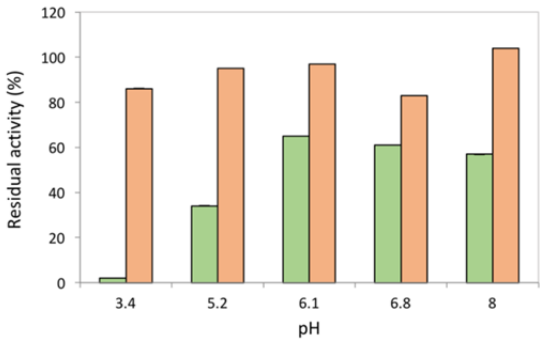

Figure 3.5. Residual activity (A/A_0) of free laccase (●) and immobilized on smNP (●) at different pH after 24 h incubation.

Regarding the effect of the temperature on the activity of free and immobilized laccase, the maximum activity was obtained at 60°C in both cases. However, immobilized laccase provided a remarkable broader profile and its relative activity was 4-13% higher than that of free laccase over the range tested (data not shown) (Lloret et al., 2011; D´Annibale et al., 1999; Kunamneni et al., 2008). Short-term stability of immobilized enzyme was also proved to be enhanced in comparison with free laccase, which is especially evident for the immobilized enzyme at 50°C (Figure 3.6). In contrast, the activity of free laccase dropped more rapidly than that of immobilized laccase, which is attributed to the conformational changes of the immobilized enzyme that increase enzyme rigidity, which protects the enzyme against denaturation at high temperature (Lloret et al., 2011; Osma et al., 2010).

Storage stability is one of the most important parameters to be considered in enzyme immobilization as it affects overall productivity. Free and immobilized laccases were stored at 4°C, with periodical sampling and monitoring. After 4 months, both biocatalysts maintain nearly 99% of its initial activity. When we compared the relative activity of the immobilized laccase by APTES/glutaradehyde with other immobilization methods, higher values of activity were obtained in this work (Lu et al., 2007; Deng et al., 2015; D´Annibale et al., 1999; Wang et al., 2012; Wang et al., 2014; Xu et al., 2013; Zhang et al., 2014).

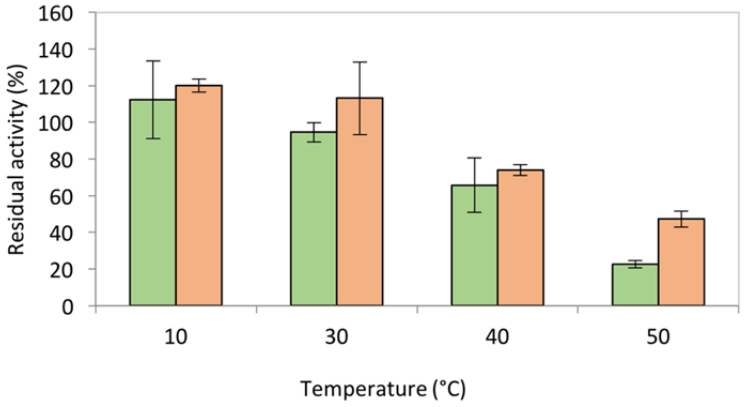

Figure 3.6. Residual activity (A/A_0) of free laccase (●) and immobilized on smNP (●) at different temperature after 24 h incubation.

Figure 3.7 presents the residual activity of immobilized and free laccase after the incubation of the enzyme in the presence of sodium acetate buffer (pH 5) and inactivating compounds (NaCl, $CaCl_2$, methanol, ethanol and acetone) at room temperature for 30 min. The immobilized laccase was observed to present higher stability in presence of the organic solvents and similar to free laccase when salts: NaCl and $CaCl_2$ are present.

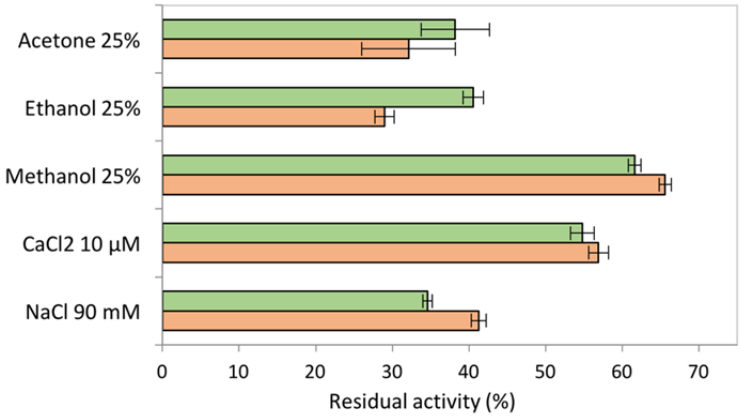

Figure 3.7. Residual activity (A/A_0) of free laccase (●) and immobilized on smNP (●) at different inactivating compounds after 24 h incubation.

The influence of the composition of a secondary effluent on enzyme stability was also evaluated (Figure 3.8). After an initial period, immobilized laccase was more stable than free laccase (about 36% higher activity from day 9 to 22). As a comparison with laccase immobilized on fumed silica nanoparticles, Hommes et al. (2011) observed a residual activity above 80% after 7 days of incubation in the secondary effluent of municipal wastewater, in contrast with free enzyme that retained only 2% of its initial activity.

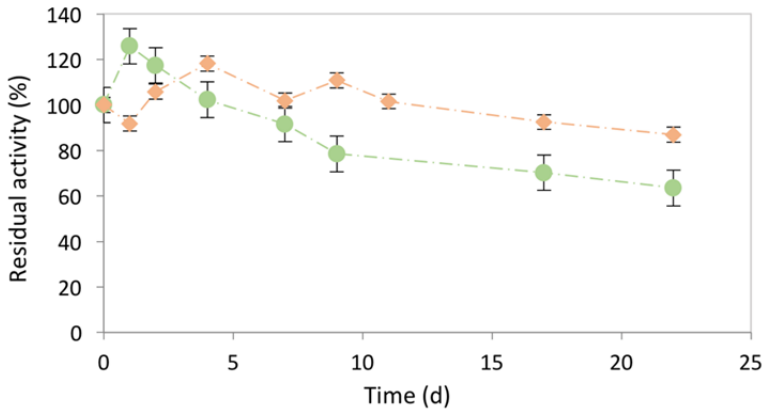

Figure 3.8. Residual activity of free (●) and immobilized laccase (●) during 22 days of incubation in a wastewater effluent collected from the WWTP of Calo (Milladoiro, Spain)

3.3.4. **Regeneration of the support**

The reusability of immobilized enzyme is fundamental for its practical application. However, since the loss of activity is a certainty over time, it would be interesting to regenerate the support for its further reuse with fresh enzyme. In this work, protein denaturation took place after ultrasonic incubation, heating and organic solvents addition. Thereafter, the three-dimensional network structure of protein would be broken and the protein chains would stretch up, thus the residual functional groups (e.g., $–NH_2$, –COOH, –SH) in protein chains could be used to react with other groups, as for instance, glutaraldehyde. After reactivation with glutaraldehyde (Zhao et al., 2011; Liu et al., 2012), immobilization of fresh enzyme was carried out following the optimal conditions previously described. Under these conditions, the enzyme loading obtained was 1.28±0.38 U mg^{-1} mNP, the immobilization yield was 61.8±0.5 % and the washing loss was 45.9±0.7%. Despite the reduction of enzyme loading, the immobilization yield was still high. Hence, it has been demonstrated that silica-coated mNP can be regenerated for enzyme repeated immobilization (Table 3.5). Similarly, a sharp drop in the immobilization capacity of the regenerated supports comparing to the original one was reported (Zhao et al., 2011). However, after three regeneration cycles, the immobilization capacity was not negatively affected and the enzyme activity was maintained.

Table 3.5 Potential of regeneration of the support in terms of washing loss, immobilization and enzyme loading with fresh enzyme with and without APTES functionalization**.**

Immobilization procedure	Washing loss (%)	Immobilization yield (%)	Enzyme loading (U mg^{-1} mNP)
Lacking functionalization	93.41±0.05	1.59±0.02	0.08±0.01
With functionalization	45.91±10.30	61.75±0.52	1.28±0.37

3.3.5. **Biotransformation of the target pollutants**

The capacity of free and immobilized enzymes on smNP to transform BPA, Phenol, DCF, E1, E2, EE2 and MG as model compounds was assessed in batch operation during 24 h, with an initial activity of 1000 U L^{-1}.

When the oxidation was considered for the biotransformation of BPA, results show that the BPA transformation rate was slightly higher with free enzyme (3.58 mg $L^{-1}h^{-1}$), whereas BPA transformation rate was around 1.38 mg $L^{-1}h^{-1}$ with immobilized enzyme. This behaviour was also reported by Pang *et al.* (2015) who observed that BPA transformation rate for free enzyme was 10 times higher than the one achieved by laccase immobilized onto carbon nanoparticles. Regarding the transformation of DCF, it was no attained appreciable transformation of the micropollutant with the nanobiocatalyst after 24 h (Figure 3.10). Arca-Ramos *et al.* (2016) observed that DCF transformation rate with laccase immobilized onto fumed silica nanoparticles was lower than 0.1 mg $L^{-1}h^{-1}$.

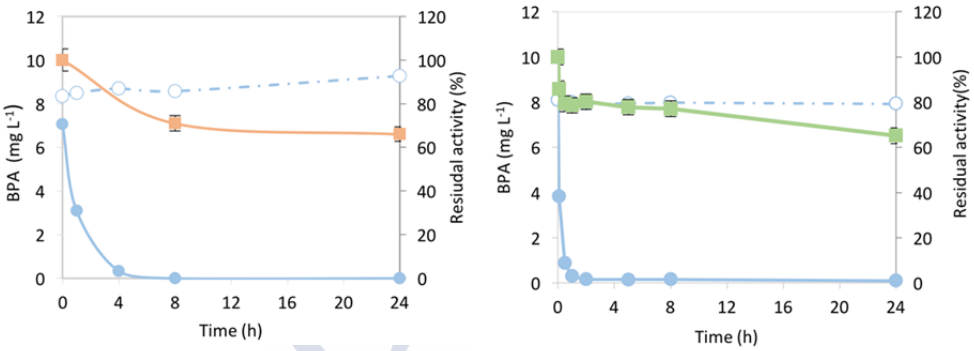

Figure 3.9. BPA concentration (●), BPA control lacking laccase (○) during the transformation by immobilized enzyme(■) and free enzyme (■) .

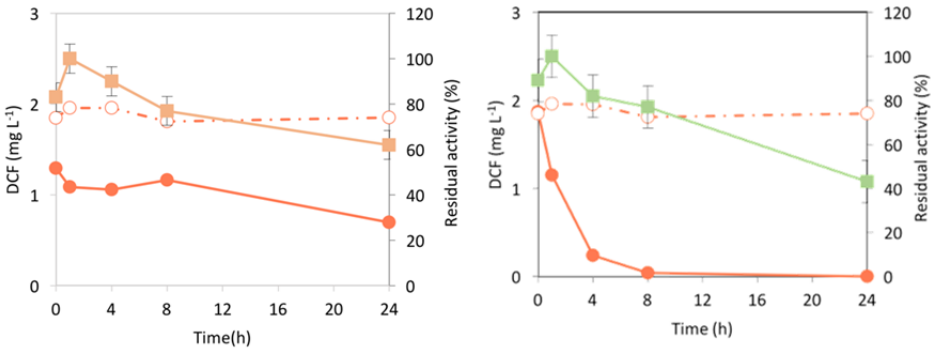

Figure 3.10. DCF concentration (●), DCF control lacking laccase (○) during the transformation by immobilized enzyme(■) and free enzyme (■) .

In the case of phenol transformation, the results showed that the higher phenol transformation was achieved by free laccase (2.39 mg $L^{-1}h^{-1}$), whereas phenol transformation rate was around 2.01 mg $L^{-1}h^{-1}$ for immobilized laccase (Figure 3.11). Lower activity of immobilized laccase towards phenolic substrates has been previously reported. This lower reaction rate was related to the potential aggregation of the nanoparticles which could reduce substrate accessibility. Wang *et al.* (2014) studied phenol transformation by immobilized laccase on magnetic silica nanoparticles, and similar results were observed at pH 7.

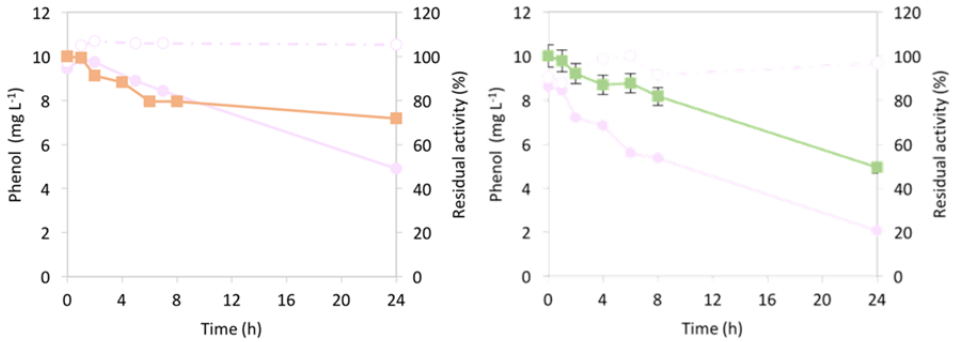

Figure 3.11. Phenol concentration ( ), Phenol control lacking laccase ( ) during the transformation by immobilized enzyme( ) and free enzyme ( ) .

The capacity of free and immobilized enzymes for E1, E2 and EE2 was evaluated and Figure 3.12-3.14 shows that in all cases the transformation with free enzyme was higher than with immobilized enzyme, close to 85%.

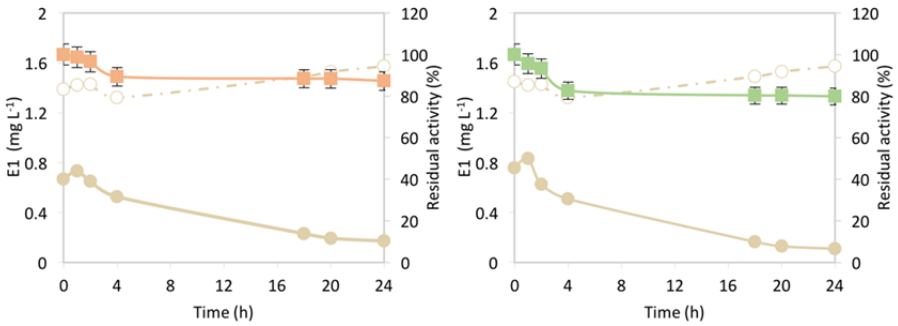

Figure 3.12. E1 concentration ( ), E1 control lacking laccase ( ) during the transformation by immobilized enzyme( ) and free enzyme ( ) .

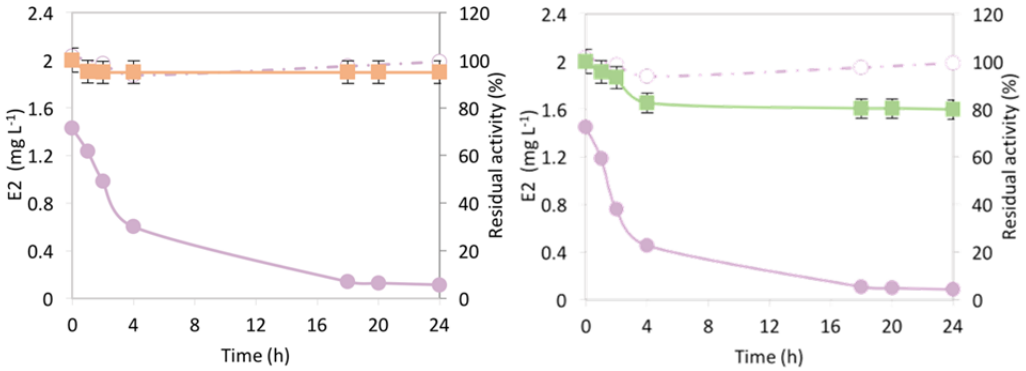

Figure 3.13. E2 concentration (●), E2 control lacking laccase (○) during the transformation by immobilized enzyme(■) and free enzyme (■) .

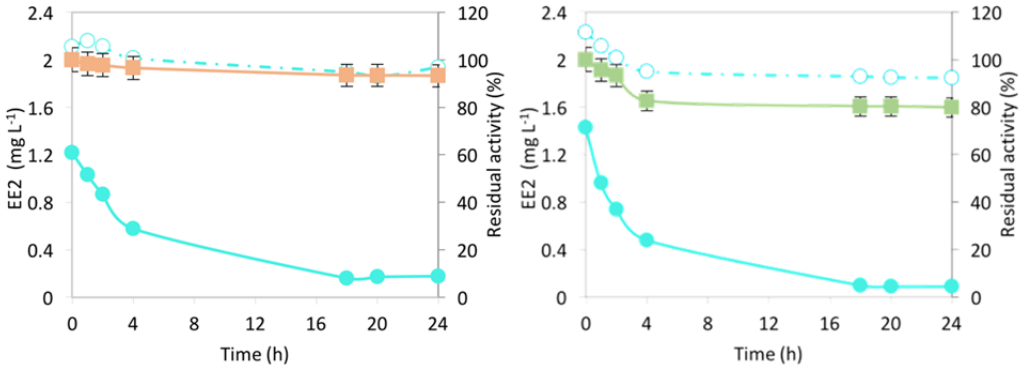

Figure 3.14. EE2 concentration (●), EE2 control lacking laccase (○) during the transformation by immobilized enzyme(■) and free enzyme (■) .

MG was chosen as model compound as textile wastewater dye and the decolorization was completely achieved for free and immobilized enzyme. Although slightly decolorization (40%) was also observed in control (lacking laccase) the complete transformation of MG by laccase is in less than 4 h (Figure 3.15).

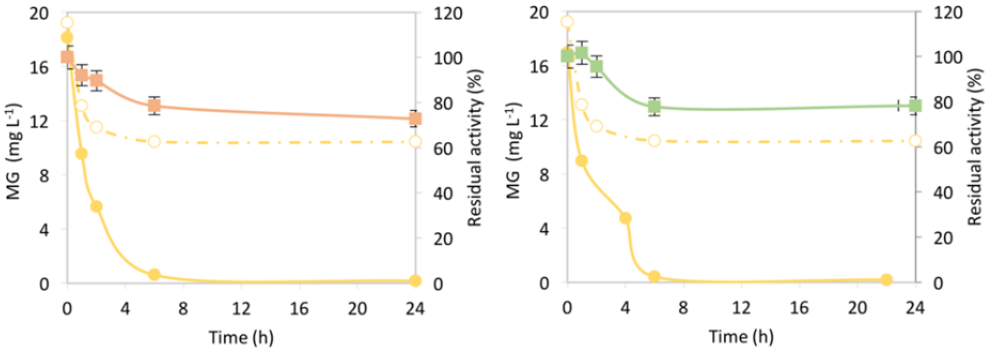

Figure 3.15. MG concentration (●), MG control lacking laccase (○) during the transformation by immobilized enzyme(■) and free enzyme (■) .

3.3.6. **Biotransformation of BPA, E2 and MG by laccase immobilized on magnetic nanosupport in sequential batch reaction**

The oxidative potential of the nanobiocatalyst was assessed in the oxidation of BPA, E2 and MG for several sequential cycles (Figure 3.15) of 6 h. The results showed that the transformation rates were slightly higher in the buffer medium (Fig 3.9-3.14) than in real wastewater, but in all cases the transformation percentage was maintained constant. It was also observed by other authors that the effect of wastewater matrices does not affect significantly to the degree of reactivity of the nanobiocatalyst (Auriol et al. 2007).

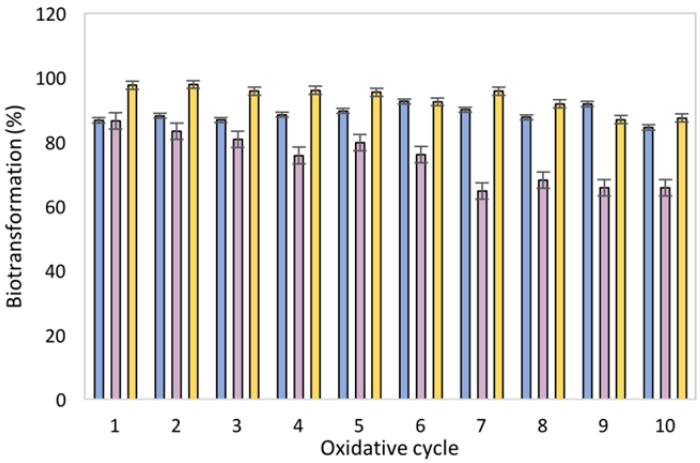

Figure 3.15. Biotransformation of BPA ( ), E2 ( ) and MG ( ) in consequtive cycles of oxidation by laccase immobilized on smNP.

3.3.7. **Evaluation of toxicity**

It is essential to evaluate the influence of the enzymatic treatment on the potential reduction of toxicity of the effluent. In the current study, Microtox® test was carried out to evaluate the toxicity of laccase catalyzed transformation products from BPA, MG and E2. After laccase treatment, no toxicity was detected using the Microtox® assay. Dudziak et al., (2015) observed that the decreased concentration of BPA in water was accompanied by the simultaneous decrease of the bioluminiscence inhibition and presented a linear correlation, confirming that toxicity in water depends on the concentration of micropollutant, with a detection limit of 500 μg L^{-1}. In the case of MG a higher value of $EC_{50\%,\ 15\ min}$ was observed which means that toxicity decreased, suggesting the generation of biotransformation products less toxic that the parent substrate.

3.4. Conclusions

In this chapter, it was developed a superparamagnetic laccase nanobiocatalyst for the enzymatic biotransformation of different micropollutants. The nanobiocatalyst showed broader pH and temperature ranges, satisfactory thermal and storage stability and higher stability against inactivating compounds than free enzyme. Additionally, its reusability was demonstrated in successive oxidation cycles, where the nanoparticle was easily recovered using a magnet. The immobilization of laccase on different types of nanoparticles such as silver and gold nanoparticles, chitosan-coated magnetic nanoparticles, and carbon nanotubes has been demonstrated in recent years, although few processes have been used for practical applications at full-scale, but the favorable properties of this nanobiocatalyst and its capability to perform the biotransformation of both compounds are the proof-of-concept towards nanobiocatalyst-driven applications. Ongoing work is focused on the reactor design to scale the process for environmental purposes.

3.5. References

Afreen, Sumbul, Tooba Naz Shamsi, Mohd Affan Baig, Nadeem Ahmad, Sadaf Fatima, M. Irfan Qureshi, Md Imtaiyaz Hassan, y Tasneem Fatma. 2017. A novel Multicopper Oxidase (Laccase) from cyanobacteria: Purification, characterization with potential in the decolorization of anthraquinonic dye. *PLOS ONE* 12 (4): e0175144.

Ammann EM, Gasser CA, Hommes G, Corvini PFX. 2013. Immobilization of defined laccase combinations for enhanced oxidation of phenolic contaminants. Appl Microbiol Biotechnol. 98, 1397-1406

Arca-Ramos A, Ammann EM, Gasser CA, Nastold P, Eibes G, Feijoo G, Lema JM, Moreira MT, Corvini PFX. 2016. Assessing the use of nanoimmobilized laccases to remove micropollutants from wastewater. Environ Sci Pollut R. 23, 3217-3228

Auriol M, Filali-Meknassi Y, Tyagi RD, Adams CD. 2007. Laccase-catalyzed conversion of natural and synthetic hormones from a municipal wastewater. Water Res 41:3281–3288.

Bautista, Luis Fernando, Gabriel Morales, y Raquel Sanz. 2015. Biodegradation of polycyclic aromatic hydrocarbons (PAHs) by laccase from *Trametes versicolor* covalently immobilized on amino-functionalized SBA-15. *Chemosphere* 136: 273-80.

Blánquez, Alba, Juana Rodríguez, Vânia Brissos, Sonia Mendes, Ligia O. Martins, Andrew S. Ball, María E. Arias, y Manuel Hernández. 2018. Decolorization and detoxification of textile dyes using a versatile *Streptomyces* laccase-natural mediator system. *Saudi Journal of Biological Sciences*, 26(5).

Cabana H, Ahamed A, Leduc R. 2011. Conjugation of laccase from the white rot fungus *Trametes versicolor* to chitosan and its utilization for the elimination of triclosan. Bioresorce Technol. 102, 1656-1662

Daâssi, Dalel, Susana Rodríguez-Couto, Moncef Nasri, y Tahar Mechichi. 2014. Biodegradation of textile dyes by immobilized laccase from *Coriolopsis gallica* into Ca-alginate beads. *International Biodeterioration & Biodegradation* 90: 71-78.

Datta, Sumitra, L. Rene Christena, y Yamuna Rani Sriramulu Rajaram. 2013. Enzyme immobilization: an overview on techniques and support material». *3 Biotech* 3 (1): 1-9.

Deng M, Zhao H, Zhang S, Tian C, Zhang D, Du P, Liu C, Cao H, Li H. 2015. High catalytic activity of immobilized laccase on core-shell magnetic nanoparticles by dopamine self-polymerization. J Mol Catal B-Enzym. 112, 15-24

DiCosimo, Robert, Joseph McAuliffe, Ayrookaran J. Poulose, y Gregory Bohlmann. 2013. Industrial Use of Immobilized Enzymes. *Chemical Society Reviews* 42 (15): 6437-74.

Dong, Sheying, Lei Peng, Wenbo Wei, y Tinglin Huang. 2018. Three MOF-Templated Carbon Nanocomposites for Potential Platforms of Enzyme Immobilization with Improved Electrochemical Performance. *ACS Applied Materials & Interfaces* 10 (17): 14665-72.

Dudziak M. 2015. Microtox as a tool to evaluate unfavourable phenomenon occurences during micropollutants decompositions in AOPs. Arch Civil Engin Environ. 8, 85-90

D'Annibale R, Stazi S, Vinciguerra V, Di Mattia E, Giovannozzi SG. 1999. Characterization of immobilized laccase from *Lentinula edodes* and its use in olive-mill wastewater treatment. Process Biochem. 34, 697-706

Fang, Yiping, Welley S. Loc, Weigang Lu, y Jiye Fang. 2011. Synthesis of In_2O_3@SiO_2 Core–Shell Nanoparticles with Enhanced Deeper Energy Level Emissions of In_2O_3. *Langmuir* 27 (23): 14091-95.

Feng, Wei, y Peijun Ji. 2011. Enzymes Immobilized on Carbon Nanotubes. *Biotechnology Advances* 29 (6): 889-95.

Fernández-Fernández, María, M. Ángeles Sanromán, y Diego Moldes. 2013. Recent developments and applications of immobilized laccase. *Biotechnology Advances* 31 (8): 1808-25.

Garcia-Morales, R., M. Rodríguez-Delgado, K. Gomez-Mariscal, C. Orona-Navar, C. Hernandez-Luna, E. Torres, R. Parra, D. Cárdenas-Chávez, J. Mahlknecht, y N. Ornelas-Soto. 2015. Biotransformation of Endocrine-Disrupting Compounds in Groundwater: Bisphenol A, Nonylphenol, Ethynylestradiol and Triclosan by a Laccase Cocktail from *Pycnoporus sanguineus* CS43. *Water, Air, and Soil Pollution* 226 (8).

Gasser, Christoph A., Erik M. Ammann, Andreas Schäffer, Patrick Shahgaldian, y Philippe F. -X. Corvini. 2016. Production of Superparamagnetic Nanobiocatalysts for Green Chemistry Applications. *Applied Microbiology and Biotechnology* 100 (16): 7281-96.

Hachi, Mohamed, Abdelmalek Chergui, Ahmed Reda Yeddou, Ammar Selatnia, y Hubert Cabana. 2017. Removal of acetaminophen and carbamazepine in single and binary systems with immobilized laccase from *Trametes hirsuta*. *Biocatalysis and Biotransformation* 35 (1): 51-62.

Han, Yu, Jiang Jiang, Su Seong Lee, y Jackie Y. Ying. 2008. Reverse microemulsion-mediated synthesis of silica-coated gold and silver nanoparticles. *Langmuir* 24 (11): 5842-48.

Hommes G, Gasser CA, Howald CBC, Goers R, Schlosser D, Shahgaldian P,Corvini PFX. 2012.Production of a robust nanobiocatalyst for municipal wastewater treatment. Bioresource Technol. 115, 8-15

Huang, Wen-Can, Wei Wang, Changhu Xue, y Xiangzhao Mao. 2018. Effective enzyme immobilization onto a magnetic chitin nanofiber composite. *ACS Sustainable Chemistry & Engineering* 6 (7): 8118-24.

Kim, Byoung Chan, Inseon Lee, Seok-Joon Kwon, Youngho Wee, Ki Young Kwon, Chulmin Jeon, Hyo Jin An, et al. 2017. Fabrication of enzyme-based coatings on intact multi-walled carbon nanotubes as highly effective electrodes in biofuel Cells. *Scientific Reports* 7 (1).

Kunamneni, Adinarayana, Iraj Ghazi, Susana Camarero, Antonio Ballesteros, Francisco J. Plou, y Miguel Alcalde. 2008. Decolorization of synthetic dyes by laccase immobilized on epoxy-activated carriers. *Process Biochemistry* 43 (2): 169-78.

Lassouane, Fatiha, Hamid Aït-Amar, Saïd Amrani, y Susana Rodriguez-Couto. 2019. A promising laccase immobilization approach for Bisphenol A removal from aqueous solutions. *Bioresource Technology* 271: 360-67.

Liang, Shangtao, Qi Luo, y Qingguo Huang. 2017. Degradation of sulfadimethoxine catalyzed by laccase with soybean meal extract as natural mediator: Mechanism and reaction pathway. *Chemosphere* 181: 320-27.

Liu X, Chen X, Li Y, Cui Y, Zhu H, Zhu W. 2012. Preparation of superparamagnetic sodium alginate nanoparticles for covalent immobilization of *Candida rugosa* lipase. J Nanop Res. 14, 1-7

Lloret L, Eibes G, Feijoo G, Moreira MT, Lema JM, Hollmann F. .2011.Immobilization of laccase by encapsulation in a sol-gel matrix and its characterization and use for the removal of estrogens. Biotechnol Progr. 27, 1570-1579

Lu A-H, Salabas EL, Schüth F. 2007. Magnetic nanoparticles: synthesis, protection, functionalization, and application. Angew Chem Int Ed. 46, 1222-1244

Mahdavi, Mahnaz, Mansor Bin Ahmad, Md Jelas Haron, Farideh Namvar, Behzad Nadi, Mohamad Zaki Ab Rahman, y Jamileh Amin. 2013. Synthesis, surface modification and characterisation of biocompatible magnetic iron oxide nanoparticles for biomedical applications. *Molecules* 18 (7): 7533-48.

Majeau, Josée-Anne, Satinder K. Brar, y Rajeshwar Dayal Tyagi. 2010. Laccases for removal of recalcitrant and emerging pollutants. *Bioresource Technology* 101 (7): 2331-50.

Massart, R. 1981. Preparation of aqueous magnetic liquids in alkaline and acidic media. *IEEE Transactions on Magnetics* 17 (2): 1247-48.

Osma JF, Toca-Herrera JL, Rodríguez-Couto S. 2010. Biodegradation of a simulated textile effluent by immobilised-coated laccase in laboratory-scale reactors. Appl Catal A- Gen. 373, 147-153

Pang R. 2015. Degradation of phenolic compounds by laccase immobilized on carbon nanomaterials: Diffusional limitation investigation. Talanta, 131: 38-45

Qu, Xiaolei, Pedro J.J. Alvarez, y Qilin Li. 2013. Applications of nanotechnology in water and wastewater treatment. *Water Research* 47 (12): 3931-46.

Rodríguez-Delgado, Melissa, Carolina Orona-Navar, Raúl García-Morales, Carlos Hernandez-Luna, Roberto Parra, Jürgen Mahlknecht, y Nancy Ornelas-Soto. 2016. Biotransformation kinetics of pharmaceutical and industrial micropollutants

in groundwaters by a laccase cocktail from *Pycnoporus sanguineus* CS43 fungi. *International Biodeterioration & Biodegradation* 108 (3): 34-41.

Rossi L, Quach A, Rosenzweig Z. 2004. Glucose oxidase–magnetite nanoparticle bioconjugate for glucose sensing. Anal Bioanal Chem. 380, 606-613

Roy JJ, Abraham TE. 2006.Preparation and characterization of cross-linked enzyme crystals of laccase. J Mol Catal B-Enzym. 38, 31-36

Soozanipour, Asieh, y Asghar Taheri-Kafrani. 2018. Enzyme immobilization on functionalized graphene oxide nanosheets: Efficient and robust biocatalysts. *Methods in Enzymology* 609: 371-403.

Sun, Kai, Qi Luo, Yanzheng Gao, y Qingguo Huang. 2016. Laccase-catalyzed reactions of 17β-Estradiol in the presence of humic acid: resolved by High-Resolution Mass Spectrometry in combination with (13) C Labeling. *Chemosphere* 145 (2): 394-401.

Wang Q, Gao DW, Gao CT, Wei Q, Cai Y, Xu J, Liu XY, Xu Y.. 2012. Activity of Laccase immobilized on TiO_2-Montmorillonite complexes. Int J Photoenergy. 6, 1001-1004

Wang Q, Cui J, Li G, Zhang J, Li D, Huang F, Wei Q. 2014. Laccase immobilized on a pan/adsorbents composite nanofibrous membrane for catechol treatment by a biocatalysis/adsorption process. Molecules. 19, 3376-3388

WWAP, 2017 - Wastewater, The Untapped Resource | United Nations Educational, Scientific and Cultural Organization». http://www.unesco.org/new/en/natural-sciences/environment/water/wwap/wwdr/2017-wastewater-the-untapped-resource/.

Xu R, Chi C, Li F, Zhang B, 2013. Laccase–Polyacrylonitrile nanofibrous membrane: Highly immobilized, stable, reusable, and efficacious for 2,4,6-Trichlorophenol removal. ACS Appl Mater Interfaces. 5, 12554-12560

Zeng, Jun, Qinghe Zhu, Yucheng Wu, y Xiangui Lin. 2016. Oxidation of Polycyclic Aromatic Hydrocarbons using *Bacillus Subtilis* CotA with High Laccase activity and Copper independence. *Chemosphere* 148 (4): 1-7.

Zhang P, Wang Q, Zhang J, Li G, Wei Q. 2014. Preparation of amidoxime-modified polyacrylonitrile nanofibers immobilized with laccase for dye degradation. Fibers Polym. 15, 30-34

Zhao, Guanghui, Jianzhi Wang, Yanfeng Li, Xia Chen, y Yaping Liu. 2011. Enzymes immobilized on superparamagnetic Fe_3O_4@clays nanocomposites: Preparation, characterization, and a new strategy for the regeneration of supports. *The Journal of Physical Chemistry C* 115 (14): 6350-59.

Zimmermann, Yannick-Serge, Patrick Shahgaldian, Philippe F. X. Corvini, y Gregor Hommes. 2011. Sorption-assisted surface conjugation: a way to stabilize laccase enzyme. *Applied Microbiology and Biotechnology* 92 (1): 169-78.

USC
UNIVERSIDADE
DE SANTIAGO
DE COMPOSTELA

Chapter 4

An eco-friendly nanobiocatalyst*: Pycnoporus sanguineus* laccase for environmental applications

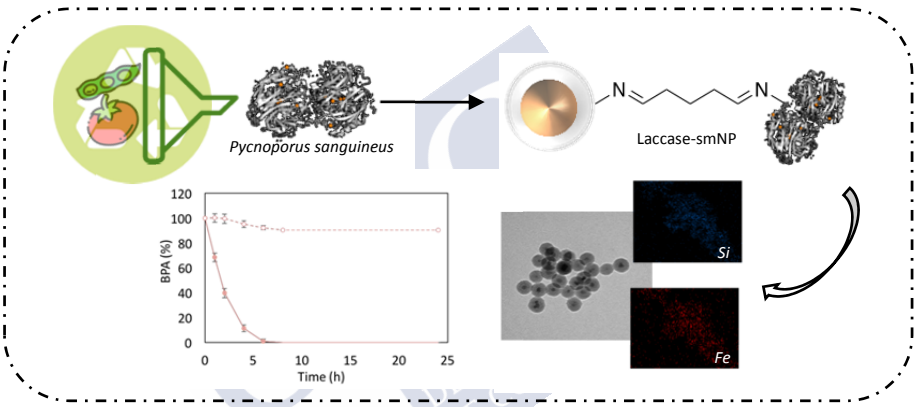

Agro-industrial wastes, such as sugar cane bagasse, coffee pulp, apple pomace, or tomato juice are abundantly available and it would be interesting to transform this waste into value-added products in order to create a circular economy. The present study was aimed to production of laccase *Pycnoporus sanguineus* using agro-industrial wastes (tomato juice and soybean oil) as the natural carbon sources. Furthermore, laccase was immobilized onto silica-coated magnetic nanoparticles (smNP) with high enzyme loadings (1.60 U mg^{-1} smNP) and characterized in terms of physical, chemical and morphological aspects. The nanobiocatalyst was applied for biotransformation of the emerging contaminant BPA and the triphenyl methane dye MG and the enzymatic action toward them was proven in 6 cycles with biotransformations rates higher than 85% in both cases. Finally, the potential toxicity of the nanobiocatalyst and the medium resulting from the enzymatic treatment were evaluated and not toxicity was detected.

USC
UNIVERSIDADE
DE SANTIAGO
DE COMPOSTELA

OUTLINE

CHAPTER 4

4.1. Introduction

In Chapter 3, *Trametes versicolor* laccase demonstrated high rates on transforming different compounds and immobilization onto silica-coated magnetic superparamagnetic nanoparticles (smNP). So far, the immobilization of laccase in magnetic nanoparticles for the removal of CECs present in wastewater has been reported (Arca-Ramos et al. 2016a, Gasser et al. 2016, Kumar et al. 2014, Moldes-Diz et al. 2018) and seems to be a promising technology. However, stability over a broad of industrially relevant pH and T values was not attained and enzyme used is relatively expensive.

Each year, five billion metric tons of agro-industrial waste, such as sugar cane bagasse, coffee pulp, apple pomace or tomato juice, are generated by industrial or agricultural activities (UNEP, 2018). In a circular economy perspective, it would be interesting to transform this waste into value-added products (Kappor et al. 2016). A possibility of recovery of this waste may be in the formulation of culture media in the biotechnological production of enzymes, such as laccases. Different microorganisms are capable of producing laccases, but they have mainly been reported for mesophilic macrofungi (*Basidiomycetes*, *Deuteromycetes*...) (González-Coronel et al. 2017). Due to the protein character of enzymes, enzyme production levels depend on the presence of inhibitors in the environment, such as high concentrations of salts, heavy metals and organic solvents, as well as optimal pH and T (Chandra et al. 2017). Therefore, it would be advisable to review the environmental conditions of production to select those that ensure not only an adequate C/N ratio for the microbial growth, but also those that minimize the deactivation of the enzyme produced. In the search for thermostable laccase, the production capacity of fungi belonging to the *Pycnoporus sanguineus* type has been investigated (Ramirez-Cavazos et al. 2014).

In the present work, a novel nanobiocatalyst based on *Pycnoporus sanguineus* laccase, produced using agro-industrial wastes (tomato juice and soybean oil) as substrates, covalently bonded onto silica-coated superparamagnetic nanoparticles (Fe_3O_4@SiO_2) (sMNP), was applied for the biotransformation of the CEC Bisphenol A (BPA) and the triphenyl methane dye Methyl green (MG). Unsolved issues as the morphology, structure, the enzymatic properties and the potential toxicity of the nanobiocatalyts were also investigated in detail.

4.2. Materials and methods

4.2.1. Chemicals and nanoparticles

3-aminopropyl-triethoxy-silane (APTES) (≥98%), 2-2′-azinobis-3-ethylbenzothiazoline-6-sulfonate (ABTS) (≥98%) and glutaraldehyde (25%) were purchased from Sigma-Aldrich (Saint Louis, MO, USA). Fluorescein isothiocyonate (FITC,>90%) was also obtained from Sigma-Aldrich. The CECs BPA and MG were purchased in Sigma-Aldrich (Saint Louis, MO, USA). Silica-coated superparamagnetic nanoparticles (sMNP) (21.5±2.1 nm) were supplied by Nanogap (Ames, Spain).

4.2.2. Microorganism and culture conditions

The microorganism used was a white-rot fungus isolated from northeastern Mexico, *P. sanguineus* CS43 (culture collection from Universidad Autónoma de Nuevo León, Mexico). Enzyme production was carried out according to the conditions reported by Ramirez-Cavazos et al. (2014) with some modifications. Laccase enzyme was produced in 14 L bioreactors (New Brunswick) with a nominal volume of 10 L. The fermentation was carried out at a temperature of 28°C for 11 days. The culture broth was collected, filtered and centrifuged (at 4000 x g for 10 min) to separate the crude enzyme extract.

4.2.3. Laccase purification

Pycnoporus sanguineus laccase was immobilized onto sMNP by following the procedure and optimal conditions described in a previous study (Moldes-Diz et al. 2017). The immobilization efficiency was calculated as the ratio of the theoretical activity of the immobilized laccase to the enzyme activity spectrophotometrically measured. Both free and immobilized laccase onto sMNP were biochemically characterized, evaluating their stability under different conditions. The influence of pH on the activity of the free and immobilized enzyme for a pH variable between 2.4 and 8 was investigated and compared with the maximum value as well as on the stability of both enzyme forms incubated in the same pH range for 24 h at room temperature (25°C). The residual activity was calculated as the quotient between the final and initial activity. The enzyme stability against different inactivating compounds was also studied by measuring the residual activity after 24

h incubation of free and immobilized enzyme (1000 U L^{-1}) in presence of NaCl (90 mM), $CaCl_2$ (10 μM), methanol, acetone, and ethanol (25% v/v) at pH 5 (100 mM acetate buffer).

4.2.4. **Nanobiocatalyst characterization**

The morphology and size of the magnetic material was determined through transmission electron microscopy (TEM, JEM1011, Japan). Thermogravimetric analysis (TGA) was conducted with a Perkin Elmer thermal analyser (Waltham, MA, USA) under the conditions of nitrogen pure gas 10˚C min^{-1} heating rate. Attenuated total reflection infrared spectroscopy (ATR-IR) (4000-400 cm^{-1}) were collected on a Nicolet™ iS™50 spectrometer (Thermo Fisher Scientific, Waltham, MA, USA) on a KBr tablet. The zeta potential measurements were carried out in phosphate buffer (pH 7) at 25˚C using a Zetasizer Nano ZS (Malvern Instruments Ltd., UK). Moreover, the enzyme conjugates immobilized on sMNP were confirmed by epliflourescence Axioskop 2 plus microscopy (Carl Zeiss Microscopy LCC, Thornwood, NY, USA).

4.2.5. **Biotransformation of Bisphenol A and Methyl green by free and immobilized enzyme**

The oxidation potentials of both free and immobilised *Pycnoporus sanguineus* laccase were evaluated following the 24 h-oxidation of BPA (10 mg L^{-1}) and MG (20 mg L^{-1}), dissolved in phosphate buffer (100 mM, pH 6) and acetate buffer (100 mM, pH 5), respectively. In parallel, control experiments with functionalized sMNPs in the absence of laccase were also carried out. Samples were withdrawn at specific time intervals to monitor biotransformation of the target compounds and residual enzyme activity.

4.2.6. **Reuse of the nanobiocatalyst in a sequential batch reactor**

The reuse of the laccase-sMNPs conjugates was demonstrated in 6 consecutive cycles of BPA (10 mg L^{-1}) and MG (20 mg L^{-1}), operating under optimum conditions. Between cycles, the immobilized enzyme was separated from the reaction medium by applying an external magnetic field for 2 min. Subsequently, a new oxidation cycle was initiated by adding fresh BPA or MG and buffer. Samples were taken at the beginning and end of each cycle to monitor biotransformation of compounds and residual enzyme activity.

4.2.7. **BPA and MG analysis**

The percentage of BPA biotransformation was determined by high-performance liquid chromatography (Shimadzu Prominence HPLC, Kyoto, Japan) at a detection wavelength of 278 nm. This equipment was coupled with a SPD-M20A diode detector and an Atlantis 3.9 x 150 mm (3 µm C18 110 Å) reversed-phase column from Waters (Milford, MA, USA). Gradient elution flow (0.8 mL min^{-1}) started with 20% acetonitrile in water, which was kept for 1 min, followed by an increase to 90% acetonitrile within 4 min. This concentration remained constant for 5 min, and decreased linearly to the initial concentration after 14 min. The biotransformation of MG was calculated by following the decrease of the characteristic MG absorbance (630 nm) in a SpectraMax® Plus 384 microplate spectrophotometer (Molecular Devices, San Jose, CA, USA).

4.2.8. **Toxicity evaluation**

Nanobiocatalyst

The toxicity of the nanobiocatalyst to Gram-negative bacteria was evaluated in *Escherichia coli* K-12 (ATCC 10798) cultures performed in spectrophotometer plates in the presence of the nanobiocatalyst in concentrations of 0.1 to 1 g L^{-1} and Lysogeny Broth (LB), formulated with 10 g L^{-1} peptone, 5 g L^{-1} yeast extract and 10 g L^{-1} of NaCl. The nanobiocatalyst-free LB was incubated under the same conditions and used as a control. The plates were incubated for 24 h at room temperature. Growth rates were calculated by optical density (OD) at 600 nm throughout the experiment on a SpectraMax® Plus 384 spectrophotometer (Molecular Devices, San Jose, CA, USA).

Biotransformation products

To determine the potential toxicity of the biotransformation products after the enzymatic treatment, a Microtox assay (Standard Methods, 1999), based on the luminescence *Vibrium fisheri* bacteria, was performed in triplicate using a Microtox Model 500 Analyzer (Modern Water, New Castle, Delaware). The results were expressed as $EC_{50(15\ min)}$, which corresponds to the concentration that caused 50% of bacteria mortality after 15 min of incubation.

4.3. **Results and discussion**

4.3.1. **High production rates of *Pycnoporus sanguineus* laccase**

Due to the use of laccase in numerous applications and its high production cost, different substrates have been studied in order to find an economic and eco-friendly culture medium for laccase production (Tisma et al. 2012). Agro-industrial residues are rich in soluble carbohydrates and also have laccase inducers, resulting in high laccase titers (Bharathiraja et al. 2017). Tomato juice and soybean oil were used in the culture medium for the production of *Pycnoporus sanguineus* laccase (Figure 4.1), and were found to allow very high laccase production (142,600 IU L^{-1} on day 11), in concordance with a previous study that reported an activity of 143,000 IU L-1.

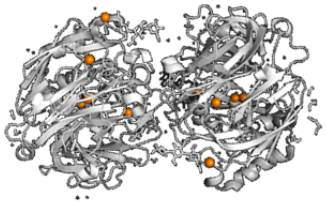

Figure 4.1. Three-dimensional representation of *Pynoporus sanguineus* (A), *Tv* (B), GAO (C), AAO (D), HMFO (E) and UPO (F). Figures generated from them crystal structures (pdb accession numbers 5NQ9) using Pymol.

These results were found to be the best production titers reported in the literature (Ramirez-Cavazos et al. 2014). Lomascolo et al. (2012) obtained an activity twice as low as that produced by the agro-industrial waste substrate using a monocaryotic strain grown in a maltose environment with inducers. In addition, the use of agro-industrial residues as substrates leads to a low cost and safe medium compared to conventional ones (Ramírez-Cavazos et al. 2014). The supernatant was collected, laccase was purified to obtain a crude extract, free of non-specific proteins and pigments, with an activity value of 279.6 U mg^{-1}.

4.3.2. **Stable and robust nanobiocatalyst by efficiently immobilizing of *Pycnoporus sanguineus* onto sMNP**

Laccase from *Pycnoporus sanguineus* was immobilized onto silica-coated magnetic nanoparticles (sMNP) under conditions optimized for *Trametes versicolor* (Moldes-Diz et al. 2017). Prior to immobilization, the nanoparticles were aminofunctionalized under the APTES reaction (0.8 mmol APTES g^{-1} sMNP). Then, the support (5 g L^{-1}) was incubated with the enzyme (1.88 U mg^{-1} support) and glutaraldehyde (8 mmol glutardehyde g^{-1} sMNP) was used as cross-linker for protein binding through the amine groups of lysine residues. This optimized immobilization process led to a high immobilization performance of 111.73% and an enzyme load of 1.60 U mg^{-1} sMNP, which is comparable to the values reported for *Trametes versicolor* laccase (Moldes-Diz et al. 2017). Previous studies with *Pycnoporus sanguineus* reported from 1.15 to 7 times lower of immobilization yields using Eupergit-C and multichannel ceramic membrane as supports, respectively (González-Coronel et al. 2017, Barrios-Estrada et al. 2018).

Due to the inverse proportionality of size versus specific surface area a higher rate of attachment points is present on sMNP and therefore, an increase on enzyme loading (Dai et al. 2016). Furthermore, immobilization yields above 100% is related to the superior affinity of the immobilized laccase for ABTS (Cabana et al., 2011).

The optimal pH for the measurement of enzyme activity was pH 3 for both free and immobilized laccase (data not shown), in agreement with previous studies for *Trametes versicolor* or *Miceliephthora thermophila* laccases (Arca-Ramos et al. 2016b, Lloret et al. 2012). However, the effect was remarkable when the effect of pH on enzyme stability after 24 h was evaluated (Figure 4.2). The immobilized enzyme showed higher activity, specially under acidic conditions (pH 2-5), in line with other reports (Gonzalez-Coronel et al. 2017, Rossi et al. 2004). Even so, both free and immobilized laccase presents higher stability than in previous studies when *Trametes versicolor* (Moldes-Diz et al. 2018) where partial inactivation of 98% and 14% was noticed for free and immobilized enzyme at pH 3, respectively.

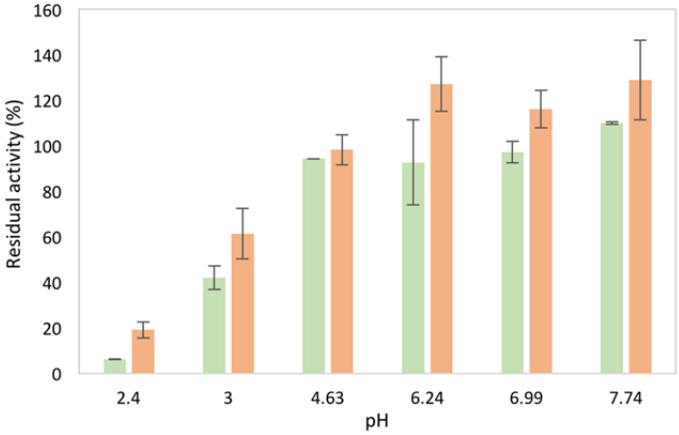

Figure 4.2. Residual activity (A/A_0) of free (green bars) and immobilized laccase (orange bars) at different pH after 24 h of incubation

As for the effect of the inactivating agents (methanol, ethanol, acetone, $CaCl_2$ and NaCl) on the free and immobilized laccase, the immobilized enzyme presented higher stability in the presence on organic solvents and $CaCl_2$ and similar to free laccase when NaCl was present (Table 4.1). The increase in organic solvents was also notable compared to previous studies, almost 58, 49 and 24 times higher in the presence of acetone, ethanol and methanol, respectively (Moldes-Diz et al. 2018). The stability of the nanobiocatalyst was also studied and after 3 months of storage at 4˚C, almost 99% of its initial activity was maintained.

Table 4.1. Residual activity (A/A_0) of free and immobilized laccase after 24 h of incubation under different deactivating agents

	Residual activity (%)	
Deactivating agent	**Free enzyme**	**Immobilized enzyme**
Methanol (25% v/v)	-	81.01±7.06
Ehtanol (25% v/v)	1.68±1.57	75.93±0.22
Acetone (25% v/v)	44.37±2.69	80.83±6.85
$CaCl_2$ (10 µM)	5.11±5.01	70.32±2.27
NaCl (2.5 mM)	56.11±5.11	74.96±13.04

4.3.3. **Multipoint covalent immobilization and enzyme shell distribution on sMNP were confirmed**

The morphology of the nanoparticles was characterized by TEM. The sMNP with core-shell architecture showed good dispersity, and the average size was 21.5±2.1 nm (Figure 4.3). The EDX elemental mapping showed that the elements Fe and Si existed in the sMNP (Figure 4.3).

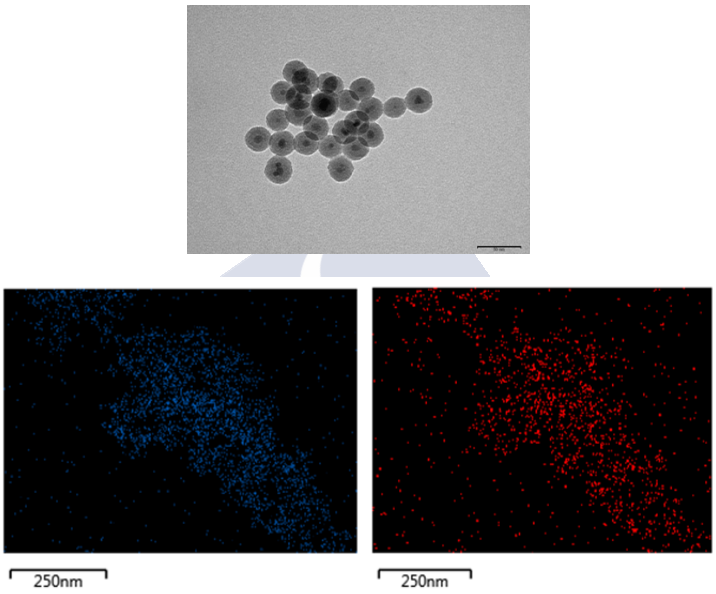

Figure 4.3. TEM image of Fe_3O_4@SiO_2; EDX elemental mapping images of Fe (red), and Si (blue) of sMNPs.

The functionalization of sMNP and the laccase conjugates was evaluated by ATR-FTIR analysis and compared with sMNP-free samples (Figure 4.4). The existence of SiO_2 layers in the sMNP spectrum can be seen by the Fe-O-Si and Si-O-Si stretching vibration at the characteristics absorption bands at 1103 and 1077 cm^{-1}, respectively. The sMNP spectrum should show an absorption at around 1390 cm^{-1} for the Fe-O stretching mode, but cannot be observed due to the existence of SiO_2 layers on the surface (Quy et al., 2013). ATR-FTIR spectra involve successful functionalization of sMNPS with APTES ($C_9H_{23}NO_3Si$) using a chemical bonded reaction via Si-O covalent bonds and modified with the amino group. Two peaks associated with the stretching and bending of the amino group (NH_2^-) can be found

at 3403 and 1652 cm^{-1} in the functionalized sMNP. Besides, the peak at 1077 cm^{-1} is associated with the asymmetric stretch vibration of Si-O bond. It can also be seen from the spectrum that the nanoparticles were successfully functionalized as the C-H stretching (3018 cm^{-1}) is increased because the hydrocarbon chain length is C_9 for APTES (Zhang et al. 2007). Similar to the confirmation of functionalization, the laccase conjugates obtained by reaction of functionalized sMNP amino groups and glutaraldehyde amino groups were confirmed by ATR-FTIR. The characteristic absorption of 1735 and 1421 cm^{-1} in laccase-smNP conjugates bands is associated with characteristic absorptions of C=O and C-O bonds resulting from the glutaraldehyde reaction. Moreover, the characteristic absorption of the amino group (3403 and 1652 cm^{-1}) and C-H stretching (3018 cm^{-1}) increased compared to functionalized sMNPs. The above observations imply that the enzyme is chemically conjugated on the surface of the functionalized sMNP via multipoint covalent immobilization mechanism.

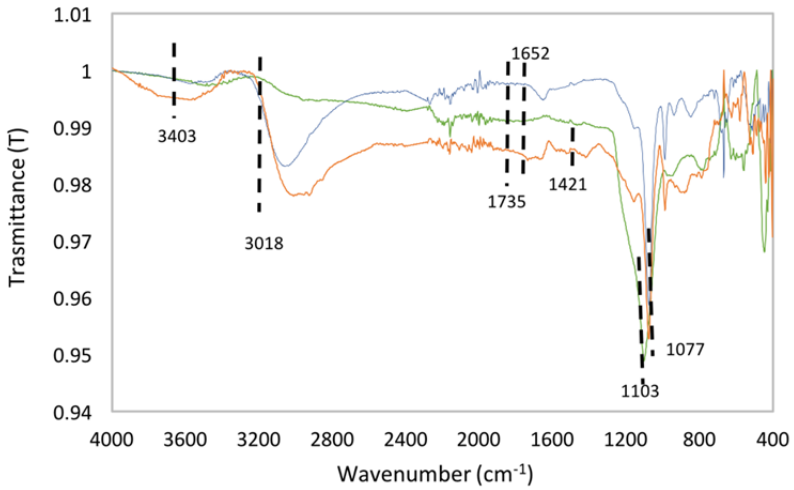

Figure 4.4. ATR-FTIR spectra of initial sMNP (green line) amino-functionalized sMNP (blue line) and laccase-sMNP conjugates (orange line)

Furthermore, the successful modification of APTES, and enzyme was also confirmed by the zeta-potential measurements with change of the surface charge from negative (-21.24±2.54 mV) to positive values (28.26±5.25 mV) and TGA analysis with a reduction in the masses of the magnetic materials. Elemental

analysis of the materials (Table 4.2) also indicated that the C, Si and O contents change after modification with APTES and enzyme. Although laccase was immobilized in the nanoparticles, it was unclear the distribution on it. The FM characterization of the laccase-sMNP conjugates verified that most of nanoparticles emitted green fluorescence under excitation and showed core-shell structures, indicating the FITC labeled laccase had been successfully immobilized into the shell of the nanoparticles (Figure 4.5).

Table 4.2. Results of elemental analysis for magnetic materials

Compound	sMNP	APTES-sMNP	Laccase-sMNP
C (%)	85.9	10.1	27.1
Si (%)	1.2	16.6	16.5
O (%)	2.2	20.1	26.9

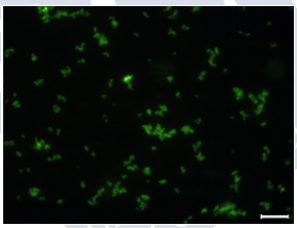

Figure 4.3. *Pycnoporus sanguineus* laccase-sMNP conjugates with laccase labelled by fluorescein isothiocyanate

4.3.4. The nanobiocatalyst was able to biotransform industrial wastewaters as resin intermediate BPA or textile dye MG

The oxidative potential of the free and immobilized enzyme for environmental purposes was evaluated for target pollutants such as BPA, an endocrine disrupting compound, and MG, as a triphenyl methane dye. When BPA was considered, higher BPA transformation was achieved using free laccase (>96%) after 2 h, whereas BPA conversion was around 88% for immobilized laccase (Figure 4.6). Other authors also observed slower BPA transformation rates for immobilized laccase (Arca-Ramos et al. 2016b). This lower reaction rate was related to the accessibility of the substrate to the enzyme active site (Sun et al. 2015). The activity remained constant in both free and immobilized enzymes. When considering the

biotransformation of MG by free and immobilized enzyme, the results showed that alike BPA, free enzyme has a high rate (Figure 4.7). However, the biotransformation rate of the nanobiocatalyst is 1.4 times higher than that observed by Kunamneni et al. (2008) when the MG was decolorized by *Myceliophtora thermophile* laccase immobilized on epoxy-activated carriers. The higher efficiency implies higher flow of pollutants treated and consequently to a reduction in the treatment cost. The immobilized enzyme maintained activity throughout the oxidation experiment, while for the free enzyme there is a slight decay of up to 25% of its initial activity. In both cases, controls with BPA and MG lacking laccase and with functionalized nanoparticles were performed, with no decrease in BPA or MG concentration (Figure 4.6 and 4.7).

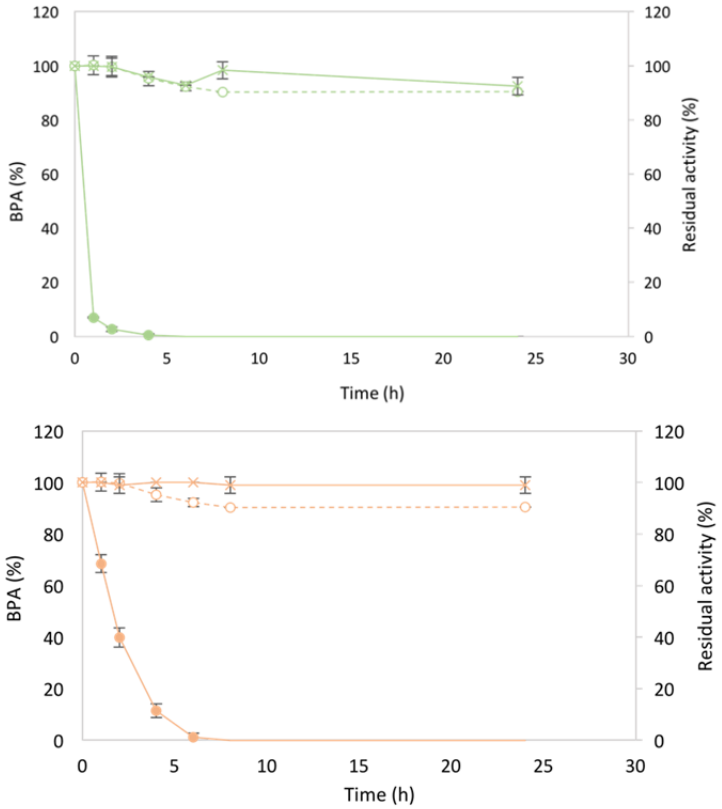

Figure 4.4. Biotransformation rate of 10 mg L^{-1} BPA (•), BPA control (o) and enzymatic residual activity (x) by free (green) and laccase-sMNP conjugates (orange)

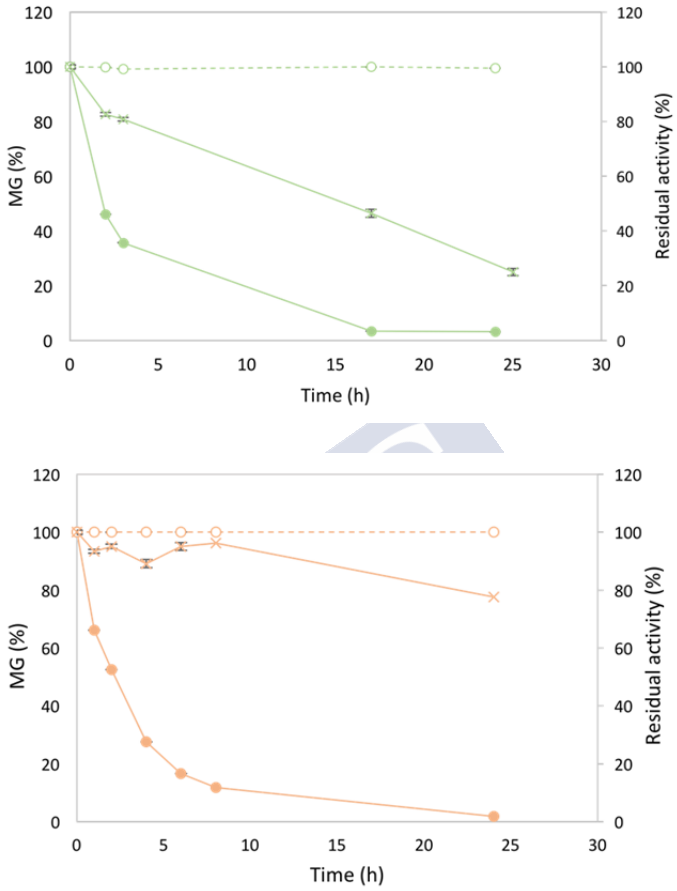

Figure 4.5. Biotransformation rate of 20 mg L^{-1} MG (•), BPA control (o) and enzymatic residual activity (x) by free (green) and laccase-sMNP conjugates (orange)

4.3.5. **Reusable and no toxic superparamagnetic nanobiocatalyst for industrial wastewater applications**

The reuse of the immobilized enzyme is essential for its practical application in real processes. The potential application was evaluated for 6 oxidation reaction cycles of BPA and MG. When the nanobiocatalayst was considered for the biotransformation of BPA in repeated batch operation of 6 h, above 95% of BPA biotransformation was attain in each cycle, 10% more than in previous studies with

Trametes versicolor laccase (Moldes-Diz et al. 2018) (Figure 4.8). MG biotransformation in 4 h-oxidation cycles (Figure 4.8) showed that the decolorization was maintained throughout the six cycles (>85%). Moreover, the nanobiocatalyst activity in both cases was maintained constant after 6 cycles. The above results imply that the nanobiocatalyst is expected to be meaningful in large-scale applications.

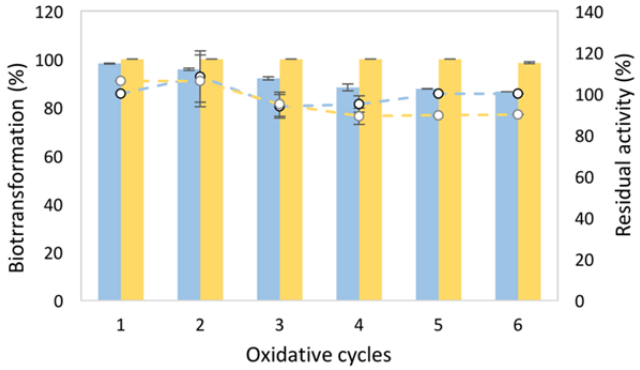

Figure 4.8. Biotransformation (%, solid bars) and residual activity (open circles) of BPA (blue) and MG (yellow) in subsequent cycles of enzymatic treatment with laccase-sMNP conjugates

The determination of the toxicity of nanobiocatalysts appears to be an important parameter, as unlike traditional catalysts, there has been no systematic risk characterization of nanomaterials (Jiang et al. 2014). The results obtained from the *E. coli* culture in the presence of the different samples and concentrations of nanoparticles showed that the current nanobiocatalyst is not toxic to gram-negative bacteria because no inhibitory effect on growth was detected in all scenarios (data not shown). Therefore, the nanobiocatalyst can be used for environmental applications without risk of damage.

4.3.6. **Successful detoxification of the treated wastewater**

The detoxification of model compounds by the nanobiocatalyst is an important parameter to consider, since, as previously reported, transformation products can lead to more toxic metabolites (Champagne et al. 2010, Donner et al.

2013). Microtox® was carried out to evaluate the toxicity of the laccase-catalyzed transformation products from BPA and MG. Control (untreated solution) and 24-h treated samples showed $EC_{50\%(15\ min)}$ values of 5 and 15% for MG, respectively. In the case of BPA, a $EC_{50\%\ (15\ min)}$ value of 28% was obtained for the untreated solution, but no toxicity was detected after enzymatic treatment. Similar results were observed by Dudziak et al. (2015). Therefore, these results suggest the generation of biotransformation products less toxic than the parent ones.

4.4. **Conclusions**

In the present work, an agricultural residue was used for the production of *Pycnoporus sanguineus* laccase and successfully immobilized onto silica-coated superparamagnetic nanoparticles. The behavior of the immobilized system was compared with that of free laccase. The results obtained showed that the stability of the laccase increased due to the immobilization in terms of pH, deactivating agents and storage. In addition, the immobilized laccase was successfully reused in 6 consecutive biotransformation cycles of BPA and MG and retained approximately 90% of the initial activity. The easy recovery of the nanobiocatalyst from the reaction media is a remarkable advantage from an operational prospecting. Regarding the toxicity impacts associated with the nanobiocatalyst and the biotransformation products, no-toxicity was observed for the nanobiocatalyst and the biotransformation products were less toxic that the parent ones. Therefore, *Pycnoporus sanguineus* laccase produced for agro-industrial wastes and immobilized onto sMNP could be a promising alternative for improving its stability, cost and large-scale reuse.

4.5. **References**

Arca-Ramos, A., Kumar, V.V., Eibes, G., Moreira, M.T., Cabana, H., 2016a. Recyclable cross-linked laccase aggregates coupled to magnetic silica microbeads for elimination of pharmaceuticals from municipal wastewater, Environ Sci Pollut Res. 23, 8929-8939

Arca-Ramos, A., Ammann, E.M., Gasser, C.A., Nastold, P., Eibes, G., Feijoo, G., Lema, J.M., Moreira, M.T., Corvini, P.F.-X., 2016b. Assessing the use of

nanoimmobilized laccases to remove micropollutants from wastewater, Environ Sci Pollut Res. 23, 3217-3228

Bharathiraja, S., Suriya, J., Krishnan, M., Manivasagan, P., Kim. S-K., 2017. Production of enzymes from agricultural wastes and their potential industrial applications, Adv Food Nutr Res. 80, 125-148

Bocchini, D., Ferreira, H., Ribeiro, R., Ferreira, H., Moretti, M., Gomes, E., 2011. Agroindustrial wastes as substrates for microbial enzymes production and source of sugar for bioethanol production, in: Kumar, S. (Ed.), Integrated waste management- Volume II. Intech, New York, pp. 319-360

Cabana, H., Ahamed, A., Leduc, R., 2011. Conjugation of laccase from the white rot fungus Trametes versicolor to chitosan and its utilization for the elimination of triclosan, Bioresorce Technol. 102, 1656-1662

Champagne, P.P., Ramsay, J.A., 2010. Dye decolorization and detoxification by laccase immobilized on porous glass beads, Bioresource Technol. 101, 2230-2235

Chandra, R., Kumar, V., Yadav, S., 2017. Extremophilic Ligninolytic Enzymes. In: Sani, R., Krishnaraj, R. (eds) Extremophilic Enzymatic Processing of Lignocellulosic Feedstocks to Bioenergy. Springer.

Dai, Y., Yao, J., Song, Y., Wang, S., Yuan, Y., 2016. Enhanced adsorption and degradation of phenolic pollutants in water by carbon nanotubes modified laccase-carrying electrospun fibrous membranes, Environ. Sci.: Nano. 3, 857-868

Donner, E., Kosjek, T., Qualmann, S., Kusk K.O., Heath, E., Revitt, D.M., Ledin, A., Andersen, H.R., 2013. Ecotoxicity of carbamazepine and its UV photolysis transformation products, Sci Total Environ. 443, 870-876

Dudziak, M., 2015. Microtox as a tool to evaluate unfavorable phenomenon occurrences during micropollutants decompositions in AOPs, ACEE Archit Civ Eng Environ. 8(2), 85-90

Gasser, C.A., Ammann, E.M., Schäffer, A., Shahgaldian, P., Corvini, P.F., 2016. Production of superparamagnetic nanobiocatalysts for green chemistry applications, Appl Microbiol Biotehcnol. 100 (16), 7281-7296

González-Coronel, L.A., Cobas, M., Rostro-Analis, M.J., Parra-Saldivar, R., Hernández-Luna, C., Pazos, M., Sanromán M.A., 2017. Immobilization of laccase of Pycnoporus sanguineus CS43, N Biotechnol. 39 A, 141-149

Jiang, C., Jia, J., Zhai, S., 2014. Mechanistic understanding of toxicity from nanocatalysts, Int J Mol Sci. 15, 13967-13992

Kappor, M., Panwar, D., Kaira, G.S., 2016. Bioprocesses for enzyme production using agro-industrial wastes: technical challenges and commercialization potential, in: Dhillon, G., Kaur, S. (Eds.), Agro-Industrial wastes as feedstock for enzyme production. Academic Press, San Diego, pp. 61-93

Kumar, V., Sivanesan, S., Cabana, H., 2014. Magnetic cross-linked laccase aggregates-Bioremediation tool for decolorization of distinct classes of recalcitrant dyes, Sci Total Environ. 487, 830-839

Kunamneni, A., Ghazi, I., Camarero, S., Ballesteros, A., Plou, F.J., Alcalde, M., 2008. Decolorization of synthetic dyes by laccase immobilized on epoxy-activated carriers. Process Biochem. 43, 169-178.

Lloret, L., Hollmann, F., Eibes, G., Moreira, MT., Lema, JM., 2012. Immobilisation of laccase on Eupergit supports and its application for the removal of endocrine disrupting chemicals in a packed-bed reactor. Biodegradation. 23(3), 373-386

Moldes-Diz, Y., Gamallo, M., Eibes, G., Vargas-Osorio, Z., Vázquez-Vázquez, C., Feijoo, G., Lema, J.M., Moreira, M.T., 2018. Development of a superparamagnetic laccase nanobiocatalyst for the enzymatic biotransformation of xenobiotics, J Enviro Eng. In press, DOI: 10.1061/(ASCE)EE.1943-7870.0001333

Quy, D.V., Hieu, N.M., Tra, P.T., Nam, N.H., Hai, N.H., Son, N.T., Nhhia, P.T., Anh, N.T.V., Hong, T.T., Luong, N.H., 2013. Synthesis of silica-coated magnetic nanoparticles and application in the detection of pathogenic viruses, J Nanomater. 2013, 1-6

Ramirez-Cavazos, L.I., Junghanns, C., Nair, R., Cárdenas-Chávez, D.L., Hernández-Luna, C., Agathos, S.N., Parra, R., 2014. Enhanced production of thermostable laccases from a native strain of Pycnoporus sanguineus using central composite design. J Zhejiang Univ-Sci B (Biomed & Biotechnol). 15 (4), 343-352

Rossi, L., Quach, A., Rosenzweig, Z., 2004. Glucose oxidase-magnetite nanoparticle bioconjugate for glucose sensing. Anal Bioanal Chem. 380(4), 606-613

Standard Methods For the Examination of Water and Wastewater, 1999. American Public Health Association, Washington, D.C.

Sun, H., Yang, H., Huang, W., Zhang, S., 2015. Immobilization of laccase in a sponge-like hydrogel for enhanced durability in enzymatic degradation of dye pollutants, J Colloid Interface Sci. 450, 353-360

Tisma, M., Znidarsic-Plazl, P., Vasic-Racki, D., Zelic, B., 2012. Optimization of laccase production by Trametes versicolor cultivated on industrial waste. Appl Biochem Biotechnol. 166, 36-46

United Nations Environment Programme (UNEP), 2018. http://web.unep.org/gpwm/what-we-do/waste-agricultural-biomass. Accessed April 2018.

WWAP (United Nations World Water Assessment Programme), 2017. The United Nations World Water Development Report 2017. Wastewater: The Untapped Resource. Paris, UNESCO.

Zhang, J., Misra, R.D.K., 2007. Magnetic drug-targeting carrier encapsulated with thermosensitive smart polymer: Core-shell nanoparticle carrier and drug release response, Acta Biomat. 3, 838-850.

Zimmermann, Y-S., Shahgaldian, P., Corvini, P.F-X., Hommes, G., 2011. Sorption-assisted surface conjugation: a way to stabilize laccase enzyme, App Microbiol Biotechnol. 92, 169-178.

USC
UNIVERSIDADE
DE SANTIAGO
DE COMPOSTELA

Chapter 5

Superparamagnetic nanobiocatalyst in oxidation technologies for added value bio-based products

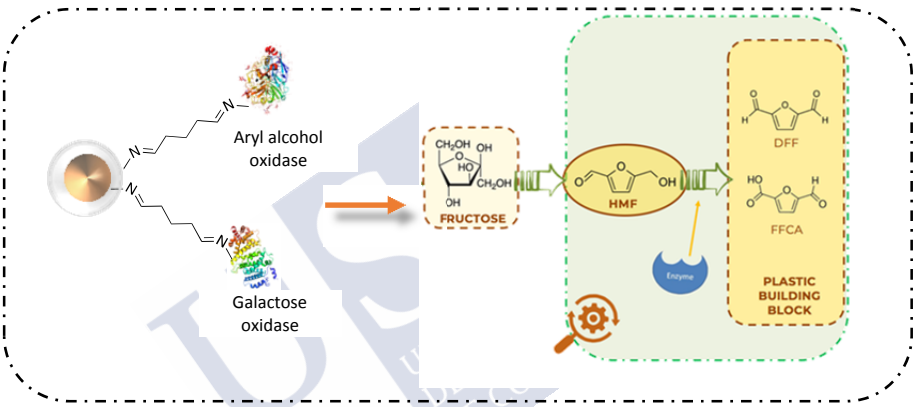

Galactose oxidase (GAO) and Aryl alcohol oxidase (AAO) has been shown to be promising biocatalysts for the oxidation of primary and secondary alcohols to their corresponding aldehydes and ketones, respectively. However, the possibility of applying these enzymes on an industrial scale depends on the stability of the biocatalyst and its potential reuse. Superparamagnetic silica coated nanoparticles seems to be a promising support with enzyme loadings of 1.19±0.02 U mg^{-1} smNP and 1.08±0.03 U mg^{-1} smNP for GAO and AAO, respectively. Envisaging the use of these nanobiocatalysts as first stage in enzyme cascade synthesis, the biotransformation of 5-HMF was performed and compared even better that of free enzyme, which needs an additional step in its future application as an industrial biocatalyst. Moreover, the genotoxicity of the nanobiocatalyst was studied, and no DNA damage was found when applying the nanobiocatalyst.

USC
UNIVERSIDADE
DE SANTIAGO
DE COMPOSTELA

OUTLINE

CHAPTER 5

5.1. Introduction

In Chapter 3 and 4, silica coated superparamagnetic nanoparticles demonstrated to be a good support for immobilization of two different laccases (*Trametes versicolor* and *Pycnoporus sanguineus*) and the nanobiocatalysts performed high transformation rates of different compounds present in wastewater treatment plants. However, the versatility and robustness of the nanobiocatalyst for different technologies was no clarified. For many years, fossil fuels have been the main source for plastic building blocks. However, due to the growing environmental concerns, there is an enormous interest to gradually move from traditional fossil fuel derived feedstocks towards a more sustainable and renewable biomass. In this context, 5-hydroxymethylfurfural (HMF) has emerged as one of the 14 top biomass platform molecules for the sustainable future (Wrigsted *et al.* 2017, Cherubini 2010). In fact, recently new catalytic routes have been developed to transform HMF into building blocks for plastics such as dimethylfuran (DFF) or 5-formyl-2-furancarboxylic acid (FFCA).

New unexploited enzymes as Galactose oxidase (GAO) and Aryl alcohol oxidase (AAO) reported to oxidize of primary alcohols to corresponding aldehydes while reducing molecular oxygen to hydrogen peroxide (Ito *et al.* 1994, Parikka *et al.* 2010) It presents a broad substrate tolerance for alcohols, but strict stereospecificity (Pickl et al. 2015). Oxidation of alcohols to carbonyl compounds is one of the most important reactions in synthetic chemistry; thus, enzymatic biocatalysts requiring only molecular oxygen as an oxidant is a valuable alternative to chemicals. It has recently been claimed that some variants of galactose oxidase and aryl alcohol oxidase transform 5-HMF in DFF and FFCA (Karich *et al.* 2018) (Figure 5.1).

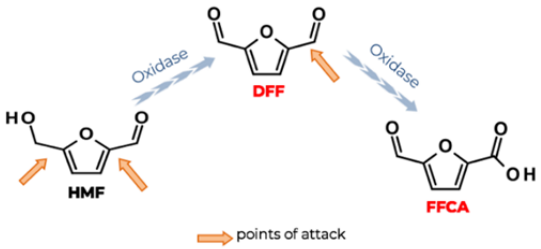

Figure 5.1. Pathway of 5-HMF oxidation by enzymatic treatment

Nevertheless, to scale-up the process, the reusability of the biocatalyst is a crucial point and therefore, an immobilization strategy should be selected. This study aims to produce a robust biocatalyst for the transformation of HMF to DFF and FFCA with GAO and AAO, respectively. For this purpose, enzymes were immobilized on silica-coated superparamagnetic nanoparticles that permits an easy recovery of the biocatalyst while maintaining an acceptable degree of enzymatic activity.

5.2. Materials and methods

5.2.1. Chemicals, nanoparticles and enzymes

3-(aminopropyl)triethoxysilane (APTES) (≥98%), glutaraldehyde (25%). Silica-coated magnetic nanoparticles (smNP) were supplied by Nanogap (Ames, Spain). Galactose oxidase (GAO) from *Aspergillus oryzae* and recombinant Aryl alcohol oxidase from *Pleurotus ostreatus* were provided by Novozymes and Environmental Biotechnology Laboratory (IHI Zittau, Technical Dresden University, Germany), respectively.

5.2.2. Immobilization of GAO and AAO on superparamagnetic silica coated nanoparticles

Prior to immobilization smNP were aminofunctionalized under the reaction of APTES (0.8 mmol APTES g^{-1} fsNP/smNP) for 24 h at room temperature. When the reaction was completed APTES excess was removed from aminofuctionalized nanoparticles by 4 washed cycles with phosphate buffer (100 mM, ph 7). The support (5 g L^{-1}) was incubated with GAO and AAO enzyme (1.88 U mg^{-1} smNP) at 4°C for 2h and 100 rpm in an orbital shaker (C24 Icubator shaker, New Brunswick Scientific, NJ). Thereafter, 8 mmol glutaradehyde per gram of nanoparticles was added and the reaction was completed at 4°C for at least 12 h. Once formed, the nanoparticles were washed 5 times with phosphate buffer (100 mM, pH 7). Immobilization efficiency was calculated as previously described in Chapter 2.

5.2.3. HMF biotransformation with GAO and AAO

A screening of the different enzymes (1000 U L^{-1}), at variable pH values (6-8), was investigated for the transformation of 5-HMF (2 mM), in order to evaluate the

selection of the enzyme to immobilized and use in different cycle, in 10-mL flasks for 24 h. Thereafter, the oxidation of 5-HMF was conducted by GAO and AAO immobilized on smNP at phosphate buffer (100 mM, pH 6) for 24 h and 1000 U L^{-1} of initial activity. In parallel, controls lacking enzyme but supports were also carried out to verify that oxidation took place only by enzymatic treatment.

5.2.4. Consecutive cycles of batch biotransformation of 5-HMF by AAO immobilized on smNP

The operation of the enzymatic system was conducted in a tank reactor (100 mL) under stirring at room temperature for several consecutive cycles. The reaction medium consisted of 5-HMF (2 mM), phosphate buffer (100 mM, pH 6), and a single initial pulse of AAO (1000 U L^{-1}) immobilized onto smNP. The effluent of the reactor was withdrawn at the end of the cycle and the nanobiocatalyst was recovered by an external magnetic field before a new cycle started. Samples were withdrawn at the beginning and at the end of each cycle to measure laccase activity and 5-HMF oxidation.

5.2.5. Analysis of 5-HMF transformation products

The oxidation products from HMF were determined by high-performance liquid chromatography (HPLC). The analysis was performed on a Jasco XLC HPLC (Jasco Analitica) equipped with a 3110 MD diode array detector (detection at 280 nm) and an Aminex HPX-87H column maintained at 60°C. Gradient elution (flow rate of 0.6 mL min^{-1}), with 5 mM of $H_2 SO_4$.

5.2.6. Genotoxicity of the nanobiocatalyst

The genotoxicity of the nanobiocatalyst was assessed. For this purpose, nine different concentrations of enzyme-sMNPs conjugates (12.5, 25, 50, 100, 200, 400, 600, 800 and 1000 mg L^{-1}) were dispersed in a final volume of 1 mL, containing 200 µg mL^{-1} of DNA in 100 mM of PBS. A control was run in parallel containing only DNA in PBS. The mixtures were incubated for 1 h at 37°C. After incubation, the testing solutions were subjected to electrophoresis in 0.75% (w/v) agarose gels, prepared with 40 mM Tris buffer (pH 7.6) containing 20 mM acetic acid and 1 mM EDTA. Gels were run in the above buffer, at 2.5 A for 1.25 h and the DNA bands were visualized using a molecular imager GELDOC XR+ (BioRad, Hercules, California, USA) and the

resulting image was processed using Image Lab Software v5.1 (BioRad, Hercules, California, USA). The band area for DNA positive control was manually defined (to measure the band intensity) and then copied into each sample lane, with the decrease in band intensity being considered as a result of a reduction of the amount of DNA present. The results were expressed as the percentage of DNA degradation calculated as the difference of the intensity of each sample and intensity of the background divided by the intensity of the intact DNA solution. All incubations were made in triplicate and loaded twice into the gel.

5.3. **Results and discussion**

5.3.1. HMF biotransformation transformation by GAO and AAO

Due to the remarkable effect of pH on 5-HMF conversion reported in previous works (Karich e*t al.* 2018), the biotransformation was assessed at different pH levels (6, 7 and 8) for free enzymes. The conversion efficiencies are shown in Table 5.1. An improvement of 5-HMF conversion was observed when pH decreased to 7 or 6, which lead to an increase of 10%. Furthermore, the enzymatic activity was maintained constant in all the experiments. Therefore, in subsequent experiments, pH 6 was selected as the optimal for 5-HMF transformation.

Table 5.1. 5-HMF transformation rates for GAO and AAO at different pH.

pH	Biotransformation rate (mmoles $L^{-1}h^{-1}$)	
	GAO	AAO
6	0.044±0.05	2.52±0.36
7	0.035±0.05	2.10±0.22
8	0.042±0.03	1.74±0.08

GAO and AAO was successfully immobilized, as related in Chapter 2, with enzyme loadings of 1.19±0.02 U mg^{-1} smNP and 1.08±0.03 U mg^{-1} smNP, respectively. In Figure 5.3 and 5.4 show the time-dependent formation of HMF oxidation products catalyzed by the nanobiocatalysts. The reaction was chosen based on the previous results presented above for free enzymes. Complete biotransformation of HMF on FFCA was observed by AAO in less than 4 hours

(Figure 5.2), whereas GAO biotransform up to 48% of HMF into DFF after 18 h (Figure 5.3). These results are in concordance with previous works where it was found that free GAO did not oxidize DFF into FFCA, but produced other unknown products (Karich *et al.* 2018). However, and enhance on biotransformation rates was observed in comparison with free enzyme.

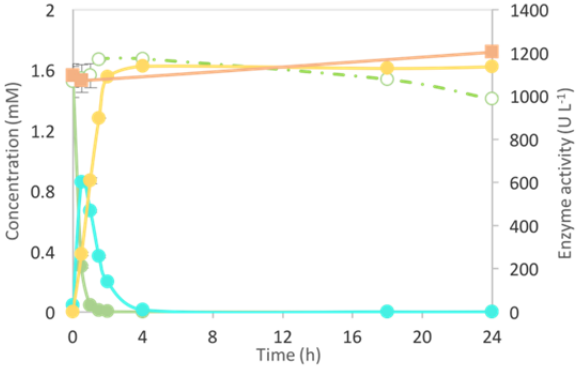

Figure 5.2. HMF concentration (●), HMF control lacking laccase (○), DFF concentration (●) and FFCA concentration (●) by AAO immobilized on smNP(■).

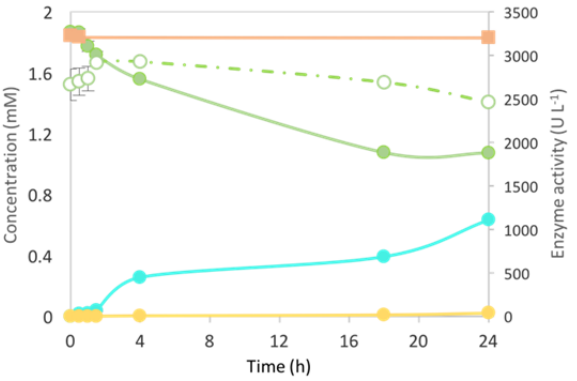

Figure 5.3. HMF concentration (●), HMF control lacking laccase (○), DFF concentration (●) and FFCA concentration (●) by GAO immobilized on smNP(■).

5.3.2. Biotransformation of 5-HMF by AAO immobilized on silica-coated superparamagnetic nanoparticles in sequential batch reaction

The reusability of the nanobiocatalyst was assessed in consecutive cycles of 4 h. It was observed that HMF transformation was higher than 90% and was maintained constant after 6 cycles (Figure 5.4). Moreover, the immobilized enzyme retained 97% of its initial activity after the consecutive batch treatments of 5-HMF with magnetic separation.

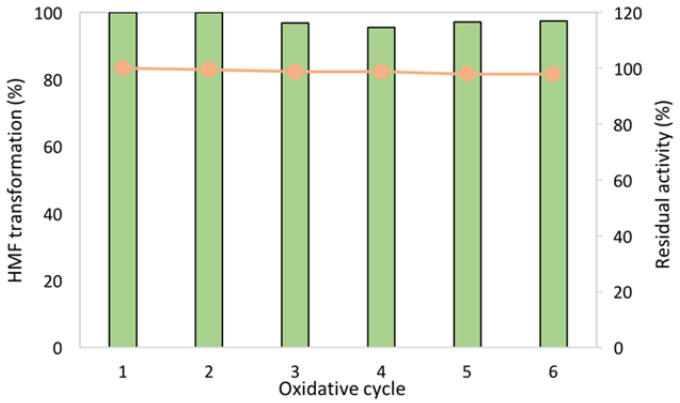

Figure 5.4. HMF transformation (■) in consecutive cycles by AAO immobilized on smNP (●).

5.3.3. Evaluation of genotoxicity

This study contributes to an understanding of the potential effects that the catalysis based on iron-based nanoparticles may have on the environment and human health. To guarantee its safety, nanobiocatalyst must not be toxic to the cells at concentrations suitable for the biotransformation of products. In previous studies was reported that silica-coated magnetic nanoparticles exhibit genotoxicity activity when the concentrations of the nanoparticles remaining below 100 µg L^{-1} (Fernández-Bertólez *et al.* 2018, Laurent *et al.* 2014). The genotoxicity results in this case indicate that no DNA damage was found when applying the smNP-based nanobiocatalyst (Figure 5.5) in the range of 12.5-1000 mg L^{-1}. This result is contradictory to findings stated in the study published by Královec *et al.* (2019) where silica-coated iron oxide nanoparticles strongly increased the levels of DNA damage. However, the DNA damage is directly related to iron release which is not

detected in our nanobiocatalyst, suggesting that surface engineering of the silica coated superparamagnetic nanoparticles created a safe nanosystem for diverse applications.

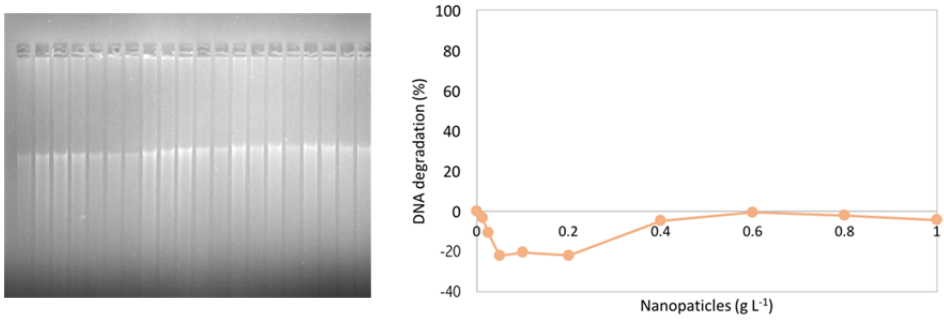

Figure 5.5. Schematic representation of the processing of the electrophoretic results and DNA damage for the nanobiocatalyst for different concentrations (12.5-1000 mg L^{-1}) at pH 7

5.4. **Conclusions**

The study demonstrated that it is possible to use the silica-coated superparamagnetic nanoparticles as support of different enzymes, such as GAO and AAO, and used as precursor for enzyme cascade reactions to produce added value bio-based products (DFF and FFCA) with high efficiency rates. One of the main results of this study is that the nanobiocatalyst is magnetically recoverable and can be reused in repeated HMF biotransformation cycles. The easy recovery of the nanobiocatalyst from the reaction media is a significant advantage from an operational perspective. Moreover, the nanobiocatalyst does not present effect on DNA damage, suggesting that it is a safe nanosystem to be use in different applications. Further research should focus on the development of an enzymatic magnetic reactor to demonstrate the scalability of the process.

5.5. References

Wrigstedt, P., Keskiväli, J., Perea-Buceta, J. E., & Repo, T. 2017. One-pot transformation of carbohydrates into valuable furan derivatives via 5-Hydroxymethylfurfural. Chem Cat Chem, 9(22), 4244-4255.

Cherubini, F. 2010. The biorefinery concept: Using biomass instead of oil for producing energy and chemicals. Energy Conversion Management, 51: 1412-142

Ito,N., S.E.V. Phillips,, K.D.S. Yadav,, P.F. Knowles (1994) Crystal structure of a free radical enzyme, Galactose Oxidase. J. Mol. Biol. 238(5) 704–814.

Parikka, K, A.-S. Leppänen,, L. Pitkänen,, M. Reunanen,, S. Willför, M. Tenkanen, J. .2010. Oxidation of Polysaccharides by Galactose Oxidase Agric. Food Chem. 58(1): 262–71.

Pickl, M., Fuchs, M., Glueck, S. M., & Faber, K., 2015. The substrate tolerance of alcohol oxidases. Applied Microbiology and Biotechnology, 99(16): 6617–6642.

Karich, A.; Kleeberg, S.B.; Ullrich, R.; Hofrichter, M., 2018. Enzymatic preparation of 2,5-Furandicarboxylic acid (FDCA)—A Substitute of Terephthalic Acid—By the Joined Action of Three Fungal Enzymes. Microorganisms 6, 5.

Královec, Havelek,R. Kročová,E., Kučírková, L., Hauschke, M., Bartáček,J., Palarčík, J., Sedlák,M. 2019. Silica-coated iron oxide nanoparticles-induced cytotoxicity, genotoxicity and its underlying mechanism in human HK-2 renal proximal tubule epithelial cells. Mutation Research/Genetic Toxicology and Environmental Mutagenesis, 844: 35-45.

Laurent, S., Saei, A.A., Behzadi, S., Panahifar, A., Mahmoudi, M., 2014. Superparamagnetic iron oxide nanoparticles for delivery of therapeutic agents: opportunities and challenges. Expert Opin. Drug Deliv. 11, 1449–70.

Fernández-Bertólez, N., Costa,C., Brandão, F., Kiliç, G., Duarte,J., Teixeira, J., Pásaro, E., Valdiglesias, C., Laffon,B. 2018. Toxicological assessment of silica-coated iron oxide nanoparticles in human astrocytes, Food and Chemical Toxicology, 118:13-23.

Chapter 6

Development of an enzymatic reactor with internal magnetic separation for biotechnological applications

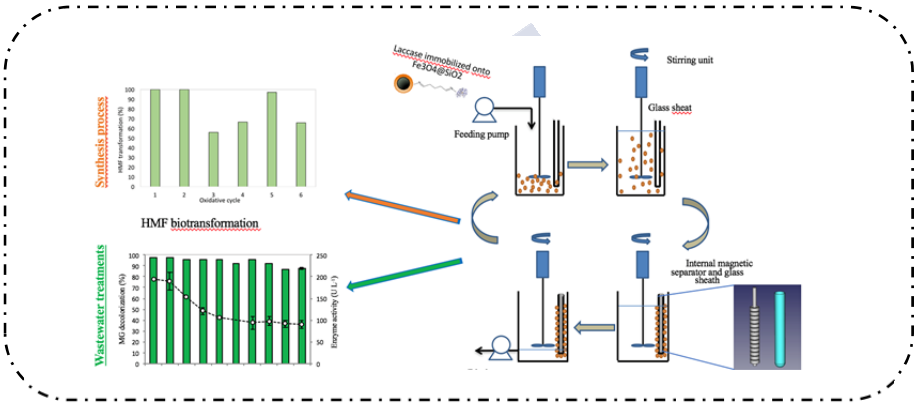

A new sequential batch reactor (SBR) coupled to an internal magnetic separator was developed. The separator consists of a set of axially magnetized permanent toroidal magnets, distributed along a non-magnetic steel rod, uniformly spaced with alternate polarity, which provide an external magnetic field of up to 1.2 T. The feasibility of magnetic separation was assessed for the retention of the nanobiocatalyst based on laccase immobilized on silica-coated mNPs. The proof of concept was evaluated for the enzymatic decolorization of the MG dye and the transformation of HMF, with complete recovery of the nanobiocatalyst (99%) and high biotransformation efficiency of both compounds. The characterization of the reaction products of MG by laccase was conducted HPLC-DAD-ESI-MS. Moreover, the biotransformation products showed less microtoxicity than the parent compound and increased biodegradability. Beyond laboratory scale experiments, the reactor proposed here was scaled-up to a volume of 100 L and the environmental performance and cost analysis were estimated.

USC
UNIVERSIDADE
DE SANTIAGO
DE COMPOSTELA

OUTLINE

CHAPTER 6

6.1. Introduction

In Chapters 3 to 5 different enzymes were immobilized onto silica-coated magnetic nanoparticles and were successfully used as nanobiocatalysts for different biotransformation reactions such as CEC removal. One of the main advantages of using mNPs is that they can facilitate the recovery of the biocatalyst from the reaction medium by applying a magnetic field. The efficient magnetic separation of the enzyme would imply very low mechanical stress on the nanoparticle compared to centrifugation or filtration (Kalkan *et al.* 2012).

Despite the huge number of papers dealing with mNPs for a wide range of applications: biosensors, electronics, biomedical sciences, chemical industries and other use (Lee *et al.* 2006, Kaushik *et al.* 2006, Mahdavi *et al.* 2013), the number of magnetic reactor alternatives is very limited so far. Crossing the line towards a more effective application of mNPs means to develop a reactor configuration that ensure the separation of the nanoparticles when the reaction medium needs to be withdrawn, while being environmentally friendly and cost effective. Wang *et al.* (2012) applied a magnetically stabilized fluidized bed reactor (MSFB) with laccase immobilized on mNPs for the removal of phenols present in coking wastewater. The MSFB reactor consisted of a glass column and four copper wire coils connected to a power supply, operated with temperature control by means of a water jacket. Ardao *et al*. (2013) designed a stirred tank reactor with a magnet placed in the outlet stream of the reactor to facilitate the separation of the magnetic biocatalyst. A system of valves allowed the flow to be reversed at regular intervals to return the enzyme back to the reactor. One of the challenges of this configuration is to avoid the aggregation of the nanoparticles caused by magnetic retention. Another type of reactor corresponds to a dynamic magnetic trap reactor configuration based on two sets of electromagnets (Duan *et al*. 2014). Not only the requirement of energy, but also the remarkable increase in temperature were the major drawbacks associated with its operation. Taking into account the potentiality of oxidative enzymes as biocatalysts, from biotransformation of pollutants to enzymatic synthesis (Chebil *et al.* 2015, Majeau *et al.* 2010, Muñiz-Mouro *et al*. 2017), the primary objective of this study was to develop a novel enzyme sequential batch reactor (SBR) based on *Tv* laccase and *AAO* immobilized onto silica-coated mNPs (Fe_3O_4@SiO_2) for the biotransformation of a dye: methyl green (MG) dye and a multifunctional molecule: 5-Hydroxymethylfurfural (HMF). The selection of both

types of substrates for enzymatic oxidation is justified by the fact that they represent two different fields of application. On the one hand, MG is a synthetic colorant used to dye wool, leather, silk or as an antiseptic and can pose acute toxicity to fish (Kusvuran *et al.* 2011). In this context, the enzymatic system may represent an alternative to advanced oxidation treatment. Secondly, HMF was chosen as model compound for biotransformation on high value-added chemicals. Therefore, the enzymatic system can be considered in this case as a synthesis alternative due to the transformation process of the compound.

The SBR consisted in a tank coupled with an internal magnet module consisting of a non-magnetic rod with aligned permanent magnets in an alternating polarity, covered by a glass sheath. This reactor configuration does not require energy consumption for magnetic separation. The modelling of the magnetic field aims to demonstrate the performance of the magnetic separation system in comparison with the conventional layout of passive magnets. In the pursuit of a real scale development, the design of a pilot-scale reactor (100 L) will provide inventory data to conduct its environmental assessment and cost analysis.

6.2. Materials and methods

6.2.1. Chemicals, enzymes and nanoparticles

3-aminopropyl-triethoxy-silane (APTES) (≥98%), 2-2′-azinobis-3-ethylbenzothiazoline-6-sulfonate (ABTS) (≥98%), glutaraldehyde (25%) commercial laccase from *Trametes versicolor* (activity≥ 0.5 U mg^{-1}) were purchased from Sigma-Aldrich. Silica-coated mNPS were prepared and characterized as in Chapter 3.

6.2.2. Decolorization of MG by laccase immobilized onto silica-coated MNPs

Laccase was immobilized onto silica-coated mNPs by sorption-assisted surface conjugation, based on the aminofunctionalization of the mNPs and glutaraldehyde cross-linking with laccase (Moldes-Diz *et al.* 2018). Prior to testing in the magnetic reactor, an initial objective was to assess the capacity of the immobilized laccase for the decolorization of the dye. For this purpose, an initial activity of 1000 U L^{-1} was tested to decolorize MG (20 mg L^{-1}) in 10-mL flasks at variable pH between 3 and 7, using McIlvaine buffer (80 mM citric acid, 40 mM Na_2HPO_4), sodium acetate and phosphate buffer solutions (100 mM). Samples were withdrawn periodically

and analyzed to assess the decrease in absorbance at 630 nm. In parallel, controls lacking laccase but with functionalized silica-coated mNPs were also carried out with the objective of verifying that the decolorization was due exclusively to enzymatic catalysis. In order to determine the effect of pH on the nanobiocatalyst activity and the biotransformation rates of MG, the point of zero charge (pHpzc) of nanobiocatalyst was determined in a Zetasizer Nano ZS from pH 2 to 12.

6.2.3. Development and modelling of the magnetic sequential batch reactor (SBR)

The configuration of the magnetic sequential batch reactor (SBR) included the following elements: peristaltic pumps with adjustable flow rate, a stirred glass reactor of 5 L and a pneumatic cylinder with air for the periodic movement of the magnetic bar inside the reactor. The reactor cover, made of methacrylate, is closed by means of methacrylate flanges that ensure the tightness of the assembly, with ports for the inlet and outlet streams, connection of the stirring rod, hole for the glass tube and a plug/stopper for manual/automatic loading of the magnetic nanoparticles. The operation of the reactor is controlled by its corresponding PLC control with an adjustable timing for sequential operation (Figure 6.1).

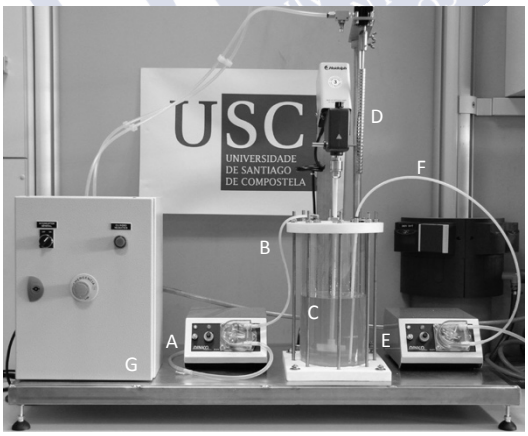

Figure 6.1. Configuration of the sequential batch reactor (SBR) laboratory (5 L) reactor comprising: A) peristaltic feeding pump; B) inlet flow; C) stirring unit; D) internal magnetic separator and pneumatic cylinder; E) peristaltic discharge pump; F) outlet flow and G) programmable logic controller (PLC)

The internal magnetic separator was constructed using commercially available permanent toroidal magnets with axial magnetization (14 NdFeB magnets of 6x15x6 mm, Superparamagnet, Germany) inserted in a non-magnetic steel rod, with poles arranged with alternate polarity. A magnet array model was developed to quantify the magnetic field under alternating polarity. The operation of the reactor was carried out in 4 different phases (Figure 6.2): i) loading of the nanobiocatalyst and feeding of the reaction medium (72 mL min^{-1}); ii) reaction stage; iii) separation of the nanobiocatalyst after reaction (2 min); iv) discharge of the effluent (72 mL min^{-1}). The retention of the silica-coated mNPs in the reactor was monitored by measuring Fe^{2+} concentration in the effluent of the different cycles by flame atomic absorption spectroscopy (FAAS).

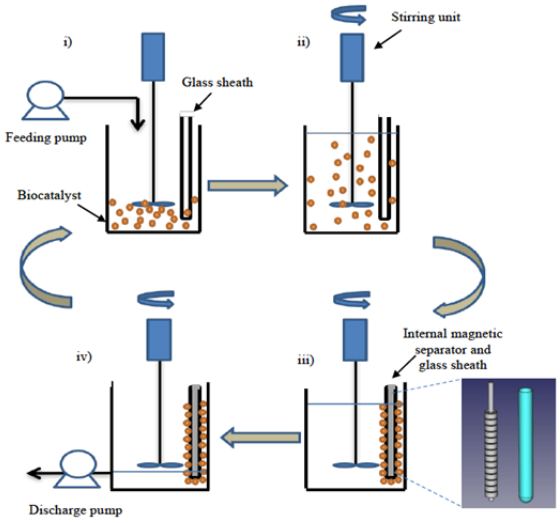

Figure 6.2. Cycles of the sequential batch reactor (SBR) coupled to an internal magnetic separator

The simulation of the magnetic field was performed using COMSOL Multiphysics ® version 5.3 with AC/DC Module, using the model referred as magnetic fields, no currents (mfnc). The grid was limited to one cylinder with the following dimensions: 100 x 85 mm (diameter x length). As a boundary condition, a zero-magnetic potential for the cylinder surface was considered. Neodymium

magnets were simulated using the following physical data: relative magnetic permeability (μ_T) of 1.05 and remnant field (B_T) of 1.3 T.

6.2.4. Biotransformation of MG and HMF in the magnetic SBR by laccase immobilized onto silica-coated magnetic nanoparticles

The influent containing MG (20 mg L^{-1} in 100 mM phosphate buffer, pH 6) was fed to the magnetic reactor with immobilized laccase added in a single initial pulse of 200 U L^{-1}. The reactor was operated in cycles of 6 h and at the beginning of each cycle, laccase activity was measured. In parallel, a control experiment with functionalized magnetic nanoparticles lacking laccase was also performed. The effluent was freeze-dried to evaluate the effect of the different biotransformation products (BP) at concentrations between 0.5-5 g L^{-1} on laccase activity after 24 h. The percentage of dye decolorization was calculated from the decrease in the characteristic absorbance of MG (630 nm).

Regarding the biotransformation of HMF, the influent (2 mM in 100 mM phosphate buffer, pH 6) was transformed in consecutive cycles with 1000 U L^{-1} of AAO. The oxidation products from HMF were determined by High-Performance Liquid Chromatography (HPLC). The analysis was performed on a Jasco XLC HPLC (Jasco Analitica) equipped with a 3110 MD diode array detector (detection at 280 nm) and an Aminex HPX-87H column maintained at 60°C. Gradient elution (flow rate of 0.6 mL min^{-1}), with 5 mM of H_2SO_4.

6.2.5. Envisioning the biotransformation of MG present in a textile effluent

To evaluate the influence of the composition of a secondary effluent on enzymatic stability and the rate of MG biotransformation, experiments were carried out with the secondary effluent of a WWTP with an initial TOC and COD of 6.97 mg L^{-1} and 15.36 mg L^{-1}, respectively. The secondary effluent was spiked with the dye (20 mg L^{-1}), simulating the composition expected in a real textile effluent. The reactor operated for 6 cycles with immobilized laccase added in a single initial pulse of 100 U L^{-1}. The percentage of dye decolorization was calculated from the decrease in the characteristic absorbance of MG (630 nm). Moreover, the monitoring of the total organic carbon (TOC) concentration using a Shimadzu TOC-L equipment made it possible to determine the degree of dye removal due to enzymatic treatment.

6.2.6. Identification of laccase-catalyzed reaction products from MG decolorization

The identification of MG oxidation products by laccase was conducted in a batch experiment. Each reactor (20 mL) contained 20 mg L^{-1} of MG in an ammonium acetate buffer (pH 6) with an initial laccase activity of 1000 U L^{-1}. Samples were periodically withdrawn and analysed by High Performance Liquid Chromatography (HPLC) with a diode array detector (DAD) coupled to Mass Spectrometry (MS) using the Electrospray Ionization Source (ESI) (HPLC-DAD-ESI-MS) to follow the appearance of the different metabolites obtained from the transformation of the parent compound. The analysis of MG intermediates was performed according to the methodology developed and described by Mai et al (2008). Two different kinds of solvents were prepared in this study. Solvent A was 25mM aqueous ammonium acetate buffer (pH 6) while solvent B was methanol instead of ammonium acetate. LC was caried out on an Zorbax® Eclipse XDB-C18 column (250 mm x 4.6 mm i.d., dp=5µm). The flow rate of the mobile phase was set at 1.0 mL min^{-1}. A linear gradient was set as follows: t=0, A=95, B=5; t=20, A=50, B=50; t=60, A=10,B=90; t=65, A=95, B=5. Mass spectrometric detection was performed on a G6410B triple quadrupole mass spectrometer (Agilent, USA) equipped with an ESI. The ESI source was operated with heated nebulizer probe at 350°C. ESI was carried out with nitrogen as sheath (240 kPa, 10 L min^{-1}) with the preliminary nebulization and to initiate the ionization process. Capillary voltage was optimized for the maximum response during perfusion of the MG standard (4500 V).

6.2.7. Toxicity and biodegradability assays

In order to investigate the potential toxicity of the transformation products obtained after enzyme treatment, a Microtox® test based on the luminescent marine bacterium *Vibrium fischeri* was performed using a Microtox® model 500 Analyzer according to the protocol defined in the Standard Methods, 1999. The results were expressed as half of the maximum effective concentration at 15 min ($EC_{50,\ 15min}$), which corresponds to the concentration of the pollutant that causes a 50% reduction in the light output of *Vibrium fischeri* after 15 min incubation.

Aerobic biodegradability was determined by monitoring oxygen consumption by aerobic sewage sludge in duplicate assays of treated and untreated effluents for 5 days. The concentration of total and volatile solids in aerobic sludge samples was quantified according to Standard Methods (1999), at values ranging from 3.1 to 3.4 g L^{-1} and 2.1 to 2.4 g L^{-1}, respectively. After sampling, the sludge was washed with phosphate buffer (200 mM, pH 7) and stored at 4°C. Oxygen consumption was measured with an automated OxiTop device (WTW) according to the Standard Methods (1999). The technique was based on the reduction of pressure inside the closed flasks containing the inoculated sample, being proportional to oxygen consumption.

Anaerobic biodegradability was determined by monitoring methane production in triplicate assays of treated and untreated effluent for 17 days in 100 mL bottles. Anaerobic sewage sludge was used as inoculum, and the biomass concentration was fixed at 2 g L^{-1} of volatile suspended solids (VSS). Biogas production was monitored using a pressure transducer (Centrepoint Electronics), and its composition was analyzed by Gas Chromatography (HP, 5890 Series II), using helium as carrier gas.

6.2.8. Environmental performance and cost analysis

The design of the reactor was adapted to a scale of 100 L with a daily flow of 400-600 L d^{-1} for a hydraulic retention time of 4-6 h, consisting on the elements described in Section 2.4 coupled with four magnetic bars inside the reactor to retain the nanobiocatalyst.

Environmental performance

The environmental performance of the enzymatic treatment was analyzed according to the Life Cycle Analysis (LCA) methodology and compared with a more widespread advanced oxidation process, such as ozonization. LCA has proven to be a versatile methodology for quantitatively assessing the environmental impacts of products and services (Baumann *et al.* 2004). To apply the LCA methodology, inventory data from laboratory and pilot plant experiments was collected. Background data (electricity and chemical production) were obtained from the Ecoinvent® database (Doka, 2003, Althaus *et al.* 2007, Dones *et al.* 2007). To ensure the validity of the comparison, the functional unit of the study was defined as the

color removal (90%) from an effluent containing 20 mg L^{-1} of the dye MG for a treatment volume of 1 m^3. The environmental assessment was conducted using ReCiPe Midpoint characterization factors (Goedkoop *et al*. 2018) and the following impact categories were considered in the analysis: climate change (CC), ozone layer depletion (OD), terrestrial acidification (OT), freshwater eutrophication (EF), marine eutrophication (MEs), human toxicity (HT), photochemical oxidant formation (POF), freshwater ecotoxicity (FET), marine ecotoxicity (MET) and fossil depletion (FD). SimaPro 8.02 (PréConsutants, 2018) was the software used for the computational implementation of life cycle inventory data and the calculation of environmental profiles.

Cost analysis

The estimation of capital costs included the reactor vessel, the magnetic separation unit, pumps and PLC control, with a depreciation period of 10 years. The operational costs included the production of the nanoparticles and enzyme, processes that differed significantly in terms of production scheme, chemical and energy requirements, performance and availability. Consequently, different supports (silica-coated magnetic nanoparticles and magnetized silica nanoparticles) and enzymes (Laccase and Manganese Peroxidase) were considered. For the electricity cost, a tariff of 0.114 € kWh^{-1} was considered (Eurostat, 2018)

6.3. Results and discussion

6.3.1. Characterization of the magnetic reactor and modelling of the magnetic field

Figure 6.3 shows a simulation of axial slices of the magnet arrays (limited to 4 for better clarity) of both configurations, alternate and series polarity, showing magnetic fields in the range of 50 mT to 1.2 T. In the case of series arrangement, the magnetic field reaches high values but only at the interspaces between the individual magnets and at the top and bottom of the bar.

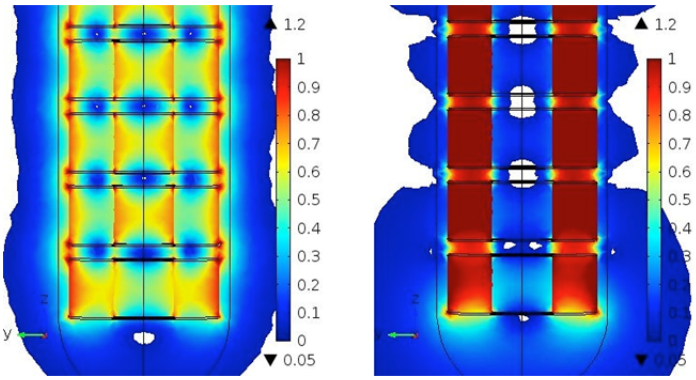

Figure 6.3. Modelling of magnetic fields (T) produced by both configurations of magnets array: alternate and series polarity.

The magnetic field goes from the north pole of one magnet to the south pole of the adjacent magnet and there is no effect on the outer volume bounded by the glass sheath. For the alternate configuration, when placing face-to-face poles of the same polarity, the magnetic field lines must extend to find the opposite pole, and consequently, the high gradient area (that defines the intensity of the magnetic field) is remarkably superior. It was found that for the alternate one, the magnetic field at 8.5 mm from the axis (corresponding to the outer face of the sheath) has a maximum of about 400 mT, whereas at 11 mm it is below 100 mT. The resulting gradient is approximately 120 T mm^{-1}. According to the magnetic force equation:

$$F = (m \cdot \nabla) B \qquad \text{(eq. 1)}$$

where the magnetic force depends on the magnetic moment (m) and magnetic field (B), the mobility of individual particles of approximately 100 nm would not exceed a few mm s^{-1}. However, due to agglomeration, the resulting magnetic moment would increase more rapidly than the decrease in mobility, allowing the separation and accumulation in the outside of the sheath (Mandel *et al.* 2012). In order to demonstrate the retention capacity of the nanobiocatalyst by the magnetic separation system, the concentration of ferrous ions in the effluent was monitored and it was found that the recovery of the magnetic nanoparticles after 2 min was greater than 99%, which was repeatedly maintained throughout the operation (10 cycles).

Recent research has also used magnetic enzyme reactors, such as Wang *et al.* (2012) who applied a magnetically stabilized fluidized bed reactor for phenol degradation in coking wastewater or Duan *et al.* (2014) who used a reactor with a system of electromagnets and a microcontroller. These reactors require an energy source for the operation of the electromagnet, with the drawbacks of power consumption and temperature increase. In contrast, the use of an internal magnetic separation unit is an alternative to these configurations, with a higher magnetic field on the outside of the sheath, which leads to an efficient recovery of the nanobiocatalyst without associated energy consumption.

6.3.2. Decolorization of MG by laccase immobilized onto silica-coated magnetic nanoparticles

As presented in the description of the operational sequence of the enzymatic magnetic reactor, it is mandatory to establish the reaction time required for the biotransformation of the target compound, in this case, to accomplish extensive decolorization of the dye. Moreover, other basic variables such as pH and enzyme activity must be selected prior to reactor operation and will be application-specific.

The influence of pH on MG decolorization (20 mg L^{-1}) and enzyme stability was investigated in batch experiments in a range of 3-7 for free and immobilized enzymes (Table 6.1). An improvement in MG transformation was observed when pH was increased from acidic to neutral conditions. However, MG decolorization was also found in the control with silica-coated mNPs lacking laccase at pH 3 and 7. After 6 h of incubation, 40% and 80% of MG were decolorized at pH 3 and 7, respectively. The coloured cation of triphenylmethyl dyes in basic and acidic medium becomes a carbinol (non-resonant) base (Mohammed *et al.* 2010). Hassan *et al.* (2011) found that after 4 h of MG incubation at pH 4.5 and 9.6, the concentration decreased by about 10% and 30% respectively. Moreover, a higher MG decolorization was achieved by free laccase for the entire pH range (Table 6.1). The lower oxidation of the immobilized laccase to phenolic compounds was also observed by other authors. Arca-Ramos *et al.* (2016) found that this lower oxidation capacity was related to the aggregation of the nanobiocatalyst, which could reduce the accessibility of the substrate.

Table 6.1. MG biotransformation and enzyme stability at variable pH by free laccase and laccase immobilized onto mNP for 24 h

	Biotransformation rate ($\mu M\ h^{-1}$)		Control decolorization (%)[a]		Residual activity (%)[b]	
pH	**Free**	**Immobilized**	**Free**	**Immobilized**	**Free**	**Immobilized**
3	2.27	1.96	42.0	35.0	0.67	66.2
5	5.08	2.83	6.0	4.0	53.9	83.8
6	4.67	4.46	8.0	5.0	78.1	89.5
7	5.89	3.50	93.0	85.0	99.5	99.8

The stability of the nanobiocatalyst and consequently its potential for aggregation is associated with attractive and repulsive forces determined by the zeta potential. Figure 6.4 shows the zeta potential profile of the nanobiocatalyst for a pH range between 2 and 12. Thus, the point of zero charge (pHzc) is around pH 5.3. Above this pH, the nanobiocatalyst is negatively charged, which is consistent with previous results where higher biotransformation rates were observed from pH 5-7 (Table 6.1), since the dye is positively charged and there are no repulsive forces between the dye and the nanobiocatalyst. However, the zeta potential values are less than -30 mV (Figure 6.4), which indicates that the nanobiocatalyst is not completely stable and may present some aggregation and therefore the accessibility of the substrate is reduced in this case.

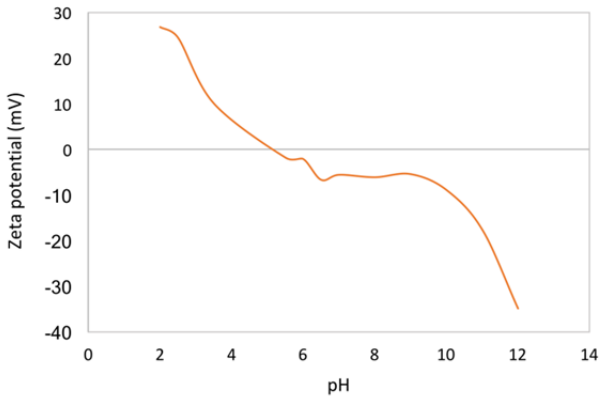

Figure 6.4. Zeta potential curve obtained for laccase immobilized onto Fe_3O_4@SiO_2 suspended in distilled water environment.

Enzymatic stability, similar to biotransformation, was significantly improved in a pH range of 3 to 7. However, a slight difference was observed between the free and immobilized enzyme in acidic conditions. After 24 h, the free enzyme retained only 0.7% of its initial activity at pH 3 while the immobilized enzyme maintained 66.2% of its activity at the beginning of the experiment (Table 6.1). Therefore, in subsequent experiments, pH 6 was selected as the optimal for MG decolorization.

6.3.3. Sequential batch reactor for the biotransformation of methyl green and HMF by laccase immobilized onto magnetic nanoparticles

The designed reactor was used to assess the ability of immobilized laccase to biotransform MG and HMF in repeated 6-h cycles. Immobilized laccase reached a percentage of MG decolorization higher than 95% in the first cycle, decreasing slightly to 87% after the tenth cycle which implies that 90 U L^{-1} is sufficient to achieve high decolourization values (Figure 6.5).

Kunamneni *et al.* (2008) studied the decolorization of MG by laccase immobilized on epoxy-activated carriers, but decolorization was 67% lower. The slight decay on biotransformation after 10 cycles may be due to the accumulation of biotransformation products that influence the oxidation capacity of the nanobiocatalyst.

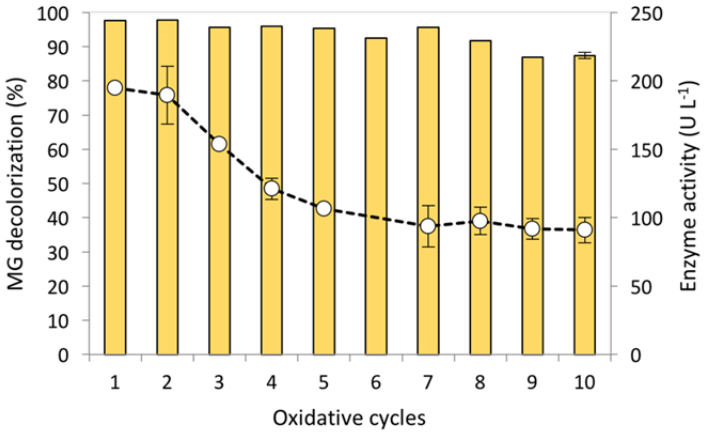

Figure 6.5. MG decolorization (%, yellow bars) and enzyme activity (○) in subsequent cycles of enzymatic treatment with laccase immobilized onto mNP.

Different concentrations of biotransformation products between 0.5-5 g L^{-1} were tested with 200 U L^{-1} of immobilized enzyme at acetate buffer pH 5 after incubation for 24 h. The results show that higher values of biotransformation products led to a decline in enzyme activity (Figure 6.6).

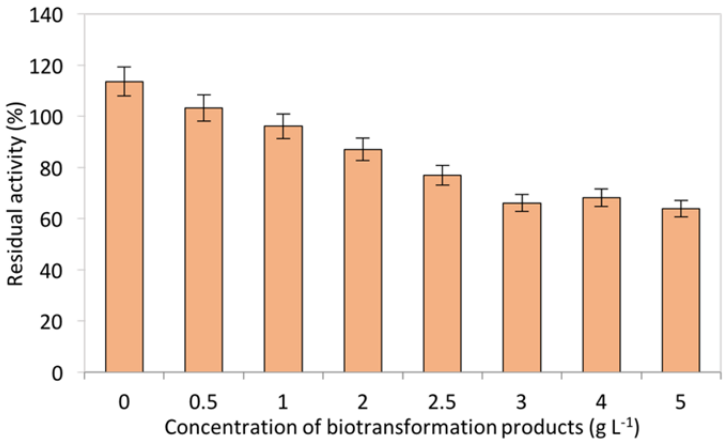

Figure 6.6. Biotransformation products effect on enzyme activity at different concentrations

The reactor was also operated for the biotransformation of HMF. Immobilized laccase achieved the complete transformation of HMF (2 mM) into FFCA the two first cycles and it was almost 60% in the all other cycles (Figure 6.7). On the other hand, after the second cycle, activity dropped 20% but remained constant thereafter.

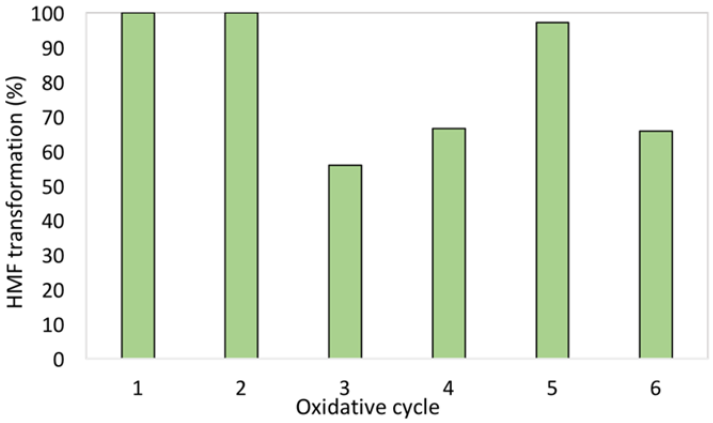

Figure 6.6. Biotransformation rates of HMF to FFCA

6.3.4. Envisioning the biotransformation of MG present in a textile effluent

The capacity of the nanobiocatalyst to biotransform MG present in a textile effluent was evaluated. The immobilized laccase reached a percentage of MG decolorization higher than 95% (Figure 6.8), and was maintained after 6 cycles (Figure 6.9). The immobilized laccase retained 95% of its initial activity after consecutive batches of MG decolorization with magnetic separation. Although the decolorization of MG was almost complete after 6 h, the removal of TOC was determined to be 38%. These findings imply that mineralization by enzymatic treatment is not successful and that biotransformation products of MG can be obtained.

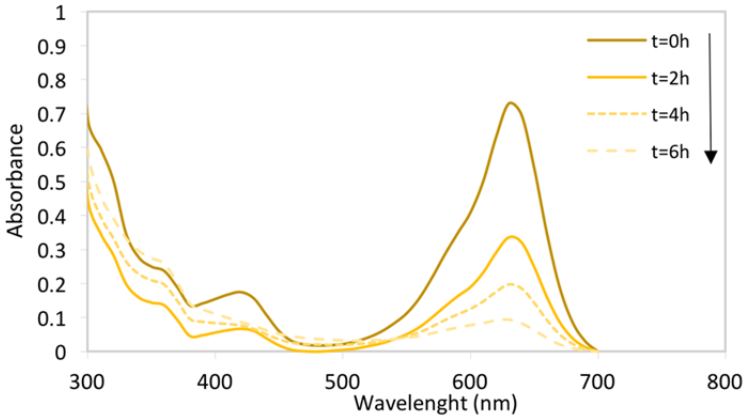

Figure 6.8. UV spectra of MG at various enzymatic treatment times ($[MG]_0$=20 mg L^{-1} in secondary effluent from a WWTP)

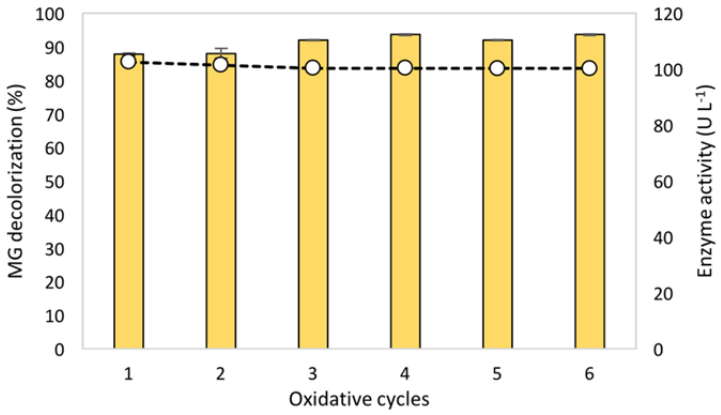

Figure 6.9. MG decolorization (%, grey bars) and enzyme activity (○) in subsequent cycles of enzymatic treatment with laccase immobilized onto mNP in a secondary effluent from a WWTP.

6.3.5. Evaluation of MG biotransformation products

With the goal of characterizing the reaction products of MG, an additional study was conducted using an HPLC-DAD-ESI-MS. The time course evolution of the

initial dye concentration and the transformation products were followed (Figure 6.10). The dye and its related intermediates are marked as A-G species in the total ion chromatogram at the beginning of the reaction, after 4 h and after 24 h of enzymatic treatment. Besides, the transformation products were also followed for 28 days. Seven components with a retention time shorter than 35 min were identified (Table 6.2) and a biotransformation mechanism was proposed (Figure 6.11). Other unidentified products with retention times higher than 40 min accumulated over time. The molecular ion peaks appeared in the acidic forms of the intermediates. The results of the HPLC-ESI mass spectra are summarized in Table 3.

Table 6.2. Molecular ions peaks from HPLC-ESI mass spectra

Peaks	Molecular formula	Retention time (min)	$[M+H^+]$	ESI-MS spectrum ions [m/z]	Absorption maximum (nm)
A,MG	$C_{27}H_{37}N_3O$	28.75	418.0	372;269	259.5
B	$C_{26}H_{34}N_3O$	33.91	404.0	358;254.8	254.8
C	$C_{25}H_{32}N_3O$	22.96	390.0	345;254.8	251.4
D	$C_{24}H_{29}N_3O$	18.34	376.0	432	246.8
E	$C_{23}H_{27}N_3O$	20.38	362.0	351.8;322.8;212.8	242.8
F	$C_{19}H_{25}N_2O$	16.54	297.0	310.8;281.8;267.8	372.4
G	$C_{18}H_{23}N_2O$	9.51	283.0	268;253.8;147.8	362.5

The substrate MG was detected as the carbinol base (A), as confirmed by mass spectral analysis (m/z= 418) and absorption spectra (λ_{max}=259.5 nm) (Mai *et al.* 2008, Chen *et al.* 2007). The cationic molecules of the MG dye become the colorless carbinol base, which is a tertiary alcohol [4-(*N*-ethyl-*N,N*-dimethylamino)][4´-(*N´,N´*-dimethylamino)][4´´-(*N´´,N´´* dimethylamino)] tripehyl methanol, by hydroxide anion. The intensity of A decreased over the reaction time and disappeared after 6 h of enzymatic treatment (data not shown), similar to what was observed for MG by spectrophotometry in section 6.3.4. Compound A was then attacked by the enzyme, producing demethylated intermediates in a stepwise process. Compound B, m/z= 404, resulted from the mono-N-demethylation of A, and reached its maximum concentration after 2 h. Other N-demethylated intermediates were observed: C (m/z=390) after 4 h and D (m/z= 376) and E

(m/z=362) after 24 h (Table 6.3). On the other hand, the attack to the central carbon portion of A produced compound F (m/z=297), which corresponds to 4-(*N*-ethyl-*N,N*-dimethylamino)-4´-(*N´,N´* dimethylamino) benzophenone with a higher concentration after 15 days, and its demethylated compound G (m/z=283) after 28 days of enzymatic transformation (Table 6.3). These intermediates have also been identified during photodegradation of MG by TiO_2 and ZnO (Mai *et al.* 2008, Chen *et al.* 2007).

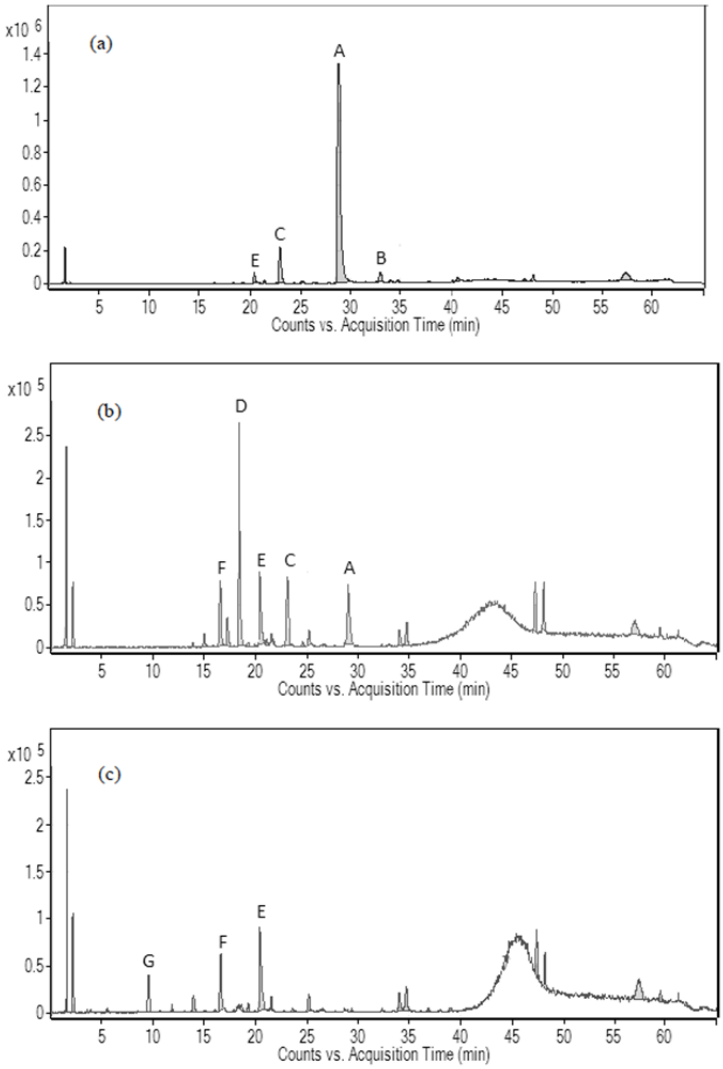

Figure 6.10. Total ion chromatogram of the biotransformation products, recorded at 0 h (a), 4 h (b) and 24 h (c).

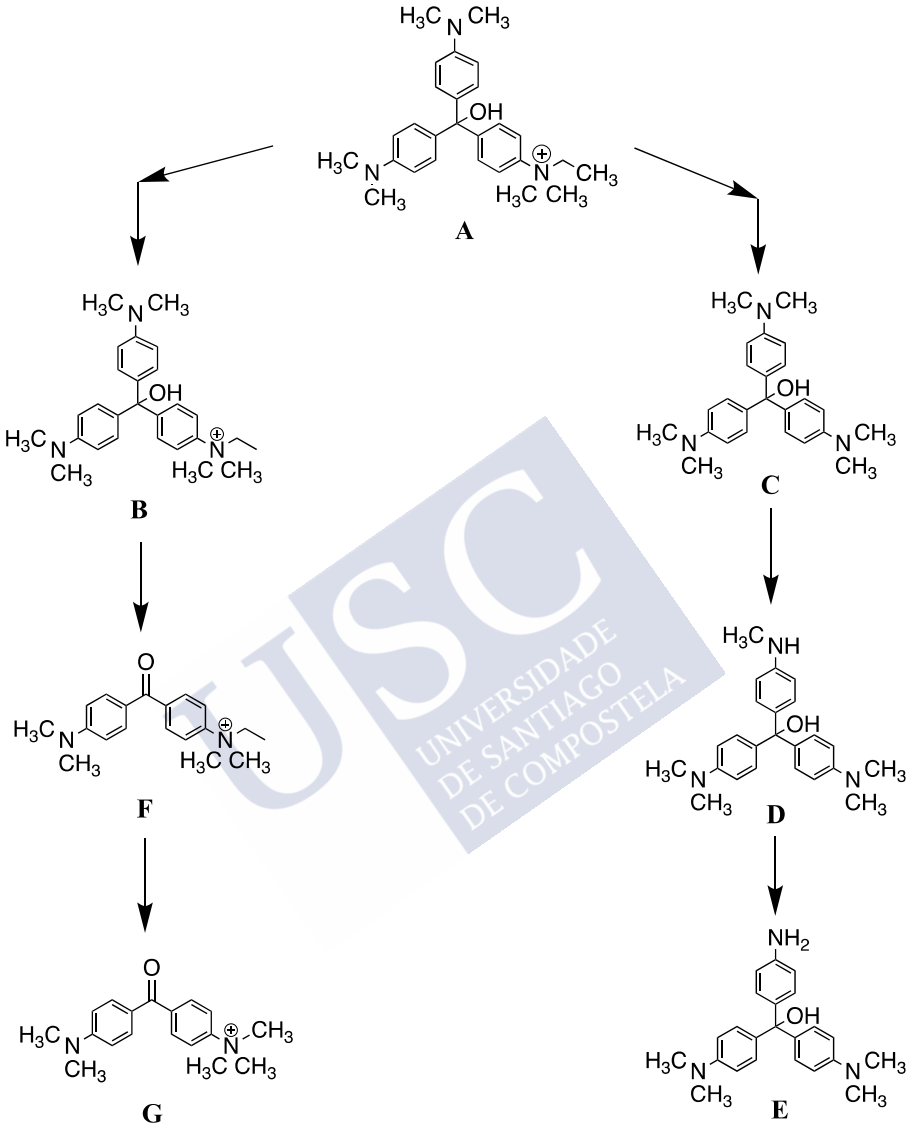

Figure 6.11. Proposed pathway of MG by the enzymatic treatment

Table 6.3. Area distribution of MG biotransformation products

	Peaks Area						
Time	**A**	**B**	**C**	**D**	**E**	**F**	**G**
0	27037619	405569	2438520	-	-	-	-
2 h	10814996	6872707	2986889	-	-	-	-
4 h	1253914	272119	3268634	22063	901657	68025	-
8h	-	-	-	50141	1173370	90165	23928
1 day	-	-	-	138962	3185730	246805	$2{\cdot}10^6$
2 days	-	-	-	122304	316424	186460	$2{\cdot}10^6$
8 days	-	-	-	199010	88750	260637	$5{\cdot}10^6$
15 days	-	-	-	415598	-	475234	$6{\cdot}10^6$
28 days	-	-	-	460591	-	451844	$5{\cdot}10^6$

6.3.6. Toxicity and biodegradability of the biotransformation products

Detoxification of dyes by free or immobilized laccases is an important target to consider, since, as previously reported, dye transformation products may lead to more toxic metabolites (Champagne *et al.* 2010). The toxicity of the laccase-catalyzed transformation products from MG was evaluated by the Microtox assay. Control and 24-h treated samples showed $EC_{50\%}$ (15 min) values of 7 and 12%, respectively. The low $EC_{50\%,15min}$ value of MG reflects the high toxicity of the dye to Microtox® test bacteria (Gabarrel *et al.* 2012, Gasser *et al.* 2014). After laccase treatment, toxicity decreased, suggesting the generation of biotransformation products less toxic than the parent substrate.

Aerobic biodegradability of the treated effluent was evaluated by measuring the cumulative oxygen consumption over 5 days (Figure 6.12). Untreated MG resulted in low oxygen consumption values, confirming the recalcitrant character of this dye. Moreover, laccase treatment increased effluent biodegradability with values of oxygen consumption significantly higher than those found for the control.

Anaerobic biodegradability enhanced considerably after enzymatic transformation (Figure 6.13). In this sense, after 100 h of anaerobic treatment, the methane accumulated for laccase catalysed transformation products of MG was 87.5% higher than the control.

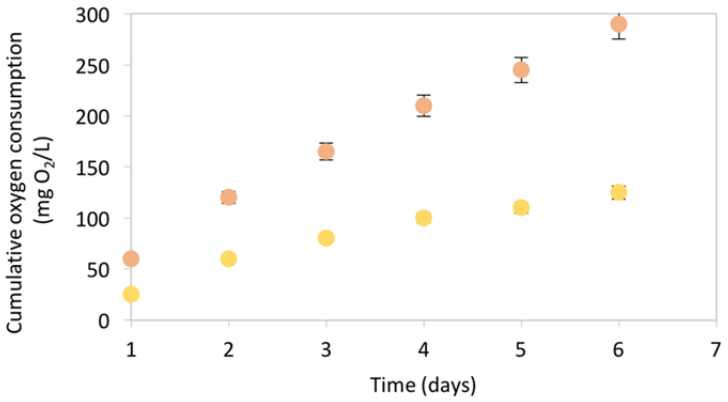

Figure 6.12. Cumulative oxygen consumption during aerobic biotransformation experiments with samples taken after 24 h of laccase-catalyzed transformation of MG (●) and corresponding controls lacking enzyme (●).

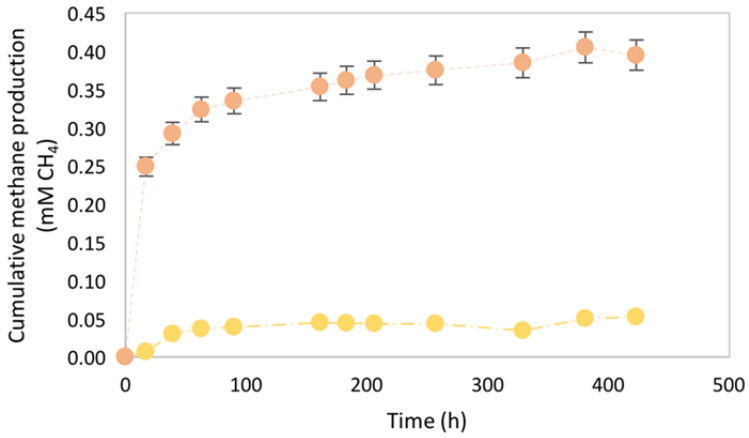

Figure 6.13. Cumulative methane production during anaerobic biotransformation experiments with samples taken after 24 h of laccase-catalyzed transformation of MG (●) and corresponding controls lacking enzyme (●).

The superior biodegradability of the enzymatic treatment effluent suggests the generation of more biodegradable products and would therefore favour the applicability of laccase-catalysed removal system as an environmentally-friendly technology for the removal of synthetic dyes from aquatic environments.

6.3.7. Environmental performance and cost analysis

The magnetic reactor was scaled-up to a volume of 100 L, which can be used as a demonstration example to be applied in different enzymatic processes. Regarding wastewater treatment, this magnetic reaction is not foreseen as an alternative for the treatment of primary streams, but as an advanced oxidation alternative in concentrated streams to treat reject water from membrane separation systems. Thus, wastewater with high concentrations of recalcitrant contaminants such as dyes, pharmaceuticals or endocrine disrupting chemicals. For this type of compounds, there are previous works that demonstrate the high potential of laccase and other oxidative enzymes for the degradation of these compounds in short periods of time (4-6 h). However, the real application requires systems that enable the recovery of the enzyme and prevent its inactivation.

Environmental performance

The development of new processes must meet sustainability criteria. According to the methodology applied in the comparative evaluation of the enzymatic treatment and the ozonization process, the latter taken as a representative example of an advanced oxidation system implemented at the commercial level, the enzymatic treatment system has less environmental impact in all the categories evaluated (Figure 6.14).

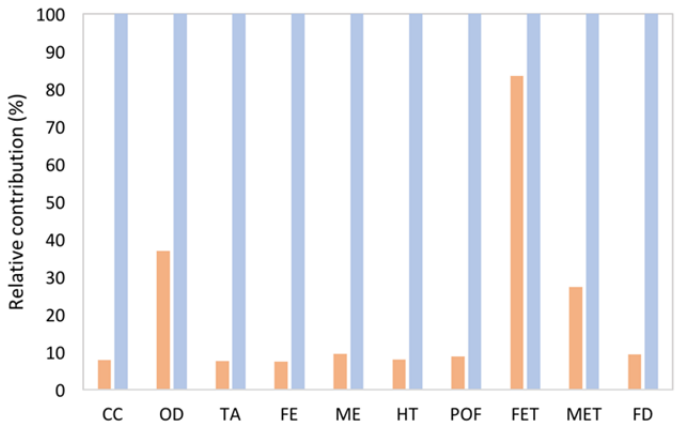

Figure 6.14. Comparative environmental profiles (%) for enzymatic treatment (orange bars) and ozonization process (blue bars) to each impact category.

The enzymatic treatment represents 83% of the ozonation score in FET, almost half of the ozonation in OD and less than 10% of those for ozonation in CC, TA, FE, ME, HT, POF and FD. Gabarrell *et al.* (2012) found similar results in the comparison between enzymatic treatment and granular activated carbon (GAC). As in this case, GAC had a greater environmental impact than the enzymatic treatment with values in six categories.

Cost analysis

Table 6.4. Operational cost associated pilot plant application of 100-L

	Cost estimation	**References**
Capital costs		
PLC		
Investment	7,158 €	Adepro, (2018)
Capital cost	0.003 € m^{-3}	
Reactor		
Volume	100 L	
Investment	19,225.27 €	Adepro, (2018)
Capital cost	0.008 € m^{-3}	
Separation unit		
Investment	586 €	Adepro, (2018)
Capital cost	0.0003 € m^{-3}	
Total capital costs	**0.0113 € m^{-3}**	
Operational costs		
Energy consumption		
Pumps	0.072 kWh (0.4 h)	Dinko, (2018)
	0.009 € m^{-3}	Eurostat, (2018)
Pneumatic system	0.18 kWh (0.08 h)	Namerah, (2018)
	0.09 € m^{-3}	Eurostat, (2018)
Nanobiocatalyst		
Enzyme	0.06-1.48 € m^{-3}	Gasser *et al.* (2014); Lopez *et al.* (2011) ; Osma *et al.* (2011)
Support material	0.036-2.08 € m^{-3}	Feijoo et al. (2017)
Chemicals	0.037 € m^{-3}	Moldes-Diz et al. (2018); Hommes et al. (2012)
Energy consumption	0.003 € m^{-3}	Estimated from consumption data
Total operational costs	**0.239- 3.69 € m^{-3}**	
Total costs	**0.25-3.7 € m^{-3}**	

The scale-up of the reactor made it possible to estimate the capital and operation costs associated with a pilot-scale application (Table 6.4). According to the estimation provided by the equipment manufacturer (ADEPRO Ingeniería, Spain), the total capital investment, including cost of the equipment, instrumentation, freight, taxes, direct and indirect installation costs, should be about 26,969.27 €. However, it is necessary to add operating costs to the initial investment, including annual costs related to the use of enzymes (3,285-81,030 €), nanoparticles (1.88-457,189.87 €), chemicals (2,041.29 €) etc. The values of capital and operational costs are referred to the flow of wastewater (in m^3 per year). Considering a useful lifetime of the reactor of 10 years, the capital costs account for a minor contribution: 0.011 € m^{-3} whereas the operational costs vary depending on the support and enzyme from 0.239 € m^{-3} to 3.69 € m^{-3}. The costs of other processes such as ozonation, powder-activated carbon or laccase immobilized on silica nanoparticles were estimated to be 0.078, 0.114 and 0.130 € m^{-3}, respectively (Gasser *et al.* 2014) The estimated costs for the treatment with the magnetic nanobiocatalyst are slightly higher, but the cost could be reduced if more cost-effective production of the biocatalyst was possible. In fact, the main factors with a remarkable cost are the chemicals and energy required. For instance, 70% of total costs of silica-coated mNPs comes from cyclohexane, Igepal CO-520 and IPA (0.67 € m^{-3}, 0.26 € $m^{-3}$and 0.56 € m^{-3}, respectively). Once the costs have been estimated, the scale-up of the novel magnetic enzymatic treatment technology to a pilot scale demonstrated potential technical and economic feasibility.

6.4. Conclusions

In the present work, we have developed an innovative, simple and efficient system for biotransformation processes based on the use of laccase immobilized in magnetic nanoparticles. The reactor configuration described in this paper offers a novel magnetic separation system with proved technical feasibility and low energy consumption. The internal separation unit, composed of a set of toroidal magnets aligned in alternate polarity, provided a magnetic field that guaranteed the almost complete recovery of the nanobiocatalyst (99%). The magnetic SBR was successfully operated for 10 cycles of MG decolorization and 6 cycles of HMF biotransformation. The scale-up of the reactor and the estimation of capital and operational costs demonstrate the potential of this system for other biotransformation reactions, provided that the biocatalyst can be immobilized onto a magnetic support.

6.5. References

Adepro Ingeniería S.L. Pilot plant design and budget. http://www.adeproingenieria.com/ (Accessed on April 2018)

Althaus, H-J., M. Chudacoff, R. Hischier, N. Jungbluth, M. Osses, A. Primas, Life Cycle Inventories of Chemicals, Ecoinvent Report No. 8 v.2.0 EMPA, Swiss Center for Life Cycle Inventories, Düberndorf, Switzerland, 2007.

Arca-Ramos, A., E.M. Ammann, C.A. Gasser, P. Nastold, G. Eibes, G. Feijoo, J.M. Lema, M.T. Moreira, P.F.-X. Corvini, Assessing the use of nanoimmobilized laccases to remove micropollutants from wastewater, Environ Sci Pollut Res Int. 23 (2016) 3217–3228.

Ardao, I.D., P. Demarche, R. Nair, S.N. Agathos, Micropollutants clean-up by bioinspired entrapped laccases in a continuous reactor with magnetic retention, Proceedings of the 2nd European Symposium of Water Technology and Management. (2013) 141-146.

Baumann, H., A.-M. Tillman, The Hitch Hiker's Guide to LCA: An Orientation in Life Cycle Assessment Methodology and Applications, Ed: 1, Studentlitteratur AB, Lund, 2004.

Champagne, P.P., J.A. Ramsay, Dye decolorization and detoxification by laccase immobilized on porous glass beads, Bioresource Technology. 101 (2010) 2230–2235.

Chebil, L., G.B. Rhouma, L.C.-G. and M. Ghoul, Enzymatic Polymerization of Rutin and Esculin and Evaluation of the Antioxidant Capacity of Polyrutin and Polyesculin, Biotechnology. (2015).

Chen, C-C-. C.-S. Lu, Mechanistic Studies of the Photocatalytic Degradation of Methyl Green: An Investigation of Products of the Decomposition Processes, Environ. Sci. Technol. 41 (2007) 4389–4396.

Dinko. Peristaltic pumps. http://www.dinko.es/es/bombas-perist%C3%A1lticas-caudal-variable_8652 (Accessed on April 2018)

Doka, G. Life Cycle Inventories of waste treatment services; Ecoinvent Report No. 13; Swiss Center for Life Cycle Inventories, Düberndorf, Switzerland, 2003.

Dones, R. C. Bauer, R. Bolliger, B. Burger, E.M. Faist, R. Frischknecht, T. Heck, N. Jungbluth, A. Röder, M. Tuchschmid, Life Cycle Inventories of Energy Systems: Results for Current Systems in Switzerland and other UCTE Countries, Ecoinvent Report No. 5, Swiss Center for Life Cycle Inventories, Düberndorf, Switzerland, 2007.

Duan, X., S.C. Corgié, D.J. Aneshansley, P. Wang, L.P. Walker, E.P. Giannelis, Hierarchical hybrid peroxidase catalysts for remediation of phenol wastewater, Chemphyschem. 15 (2014) 974–980.

Feijoo, S., S. González-García, Y. Moldes-Diz, C. Vazquez-Vazquez, G. Feijoo, M.T. Moreira, Comparative life cycle assessment of different synthesis routes of magnetic nanoparticles, Journal of Cleaner Production. C (2017) 528–538.

Gabarrell, X., M. Font, T. Vicent, G. Caminal, M. Sarrà, P. Blánquez, A comparative life cycle assessment of two treatment technologies for the Grey Lanaset G textile dye: biodegradation by Trametes versicolor and granular activated carbon adsorption, Int J Life Cycle Assess. 17 (2012) 613–624.

Gasser, C.A., L. Yu, J. Svojitka, T. Wintgens, E.M. Ammann, P. Shahgaldian, P.F.-X. Corvini, G. Hommes, Advanced enzymatic elimination of phenolic contaminants in wastewater: a nano approach at field scale, Appl. Microbiol. Biotechnol. 98 (2014) 3305–3316.

Goedkoop, M., R. Heijungs, M. Huijbregts, A life cycle impact assesment method which comprises harmonised category indicators at the midpoint and the endpoint level. https://www.leidenuniv.nl/cml/ssp/publications recipe_characterisation.pdf (Accessed on July 2018)

González-García, S., G. Feijoo, C. Heathcote, A. Kandelbauer, M.T. Moreira, Environmental assessment of green hardboard production coupled with a laccase activated system, Journal of Cleaner Production. 19 (2011) 445–453.

Hassan, M.A., L.M.. Fayoumi, M.M. Jamal, Kinetic study of the discoloration of triphenylmethane dyes in function of pH, salt effect., J. Univ. Technol. Metall. 46 (2011) 395–400.

Kaushik, A, R. Khan, P.R. Solanki, P. Pandey, J. Alam, S. Ahmad, B.D. Malhotra, Iron oxide nanoparticles-chitosan composite based glucose biosensor, Biosens Bioelectron. 24 (2008) 676–683.

Kunamneni, A. (2008), Decolorization of synthetic dyes by laccase immobilized on epoxy-activated carriers. Process Biochem, 43: 232-240

Kusvuran, E., O. Gulnaz, A. Samil, O. Yildirim, Decolorization of malachite green, decolorization kinetics and stoichiometry of ozone-malachite green and removal of antibacterial activity with ozonation processes, J. Hazard. Mater. 186 (2011) 133–143.

Lee, H E. Lee, D.K. Kim, N.K. Jang, Y.Y. Jeong, S. Jon, Antibiofouling polymer-coated superparamagnetic iron oxide nanoparticles as potential magnetic resonance contrast agents for in vivo cancer imaging, J. Am. Chem. Soc. 128 (2006) 7383–7389.

López, C., M.T. Moreira, G. Feijoo, J.M. Lema, Economic comparison of enzymatic reactors and advanced oxidation processes applied to the degradation of phenol as a model compound. Biocatalysis and biotransformation. 29 (2011) 344-353.

Mahdavi, M., M.B. Ahmad, M.J. Haron, F. Namvar, B. Nadi, M.Z.A. Rahman, J. Amin, Synthesis, Surface Modification and Characterisation of Biocompatible Magnetic Iron Oxide Nanoparticles for Biomedical Applications, Molecules. 18 (2013) 7533–7548.

Mai, F.D., C.C. Chen, J.L. Chen, S.C. Liu, Photodegradation of methyl green using visible irradiation in ZnO suspensions: Determination of the reaction pathway and identification of intermediates by a high-performance liquid chromatography–photodiode array-electrospray ionization-mass spectrometry method, Journal of Chromatography A. 1189 (2008) 355–365.

Majeau, J.A., S.K. Brar, R.D. Tyagi, Laccases for removal of recalcitrant and emerging pollutants, Bioresource Technology. 101 (2010) 2331–2350.

Mandel, K., F. Hutter, The magnetic nanoparticle separation problem, Nano Today. 7 (2012) 485–487.

Mohammed, Y., J.F. Iyun, S.O. Idris, Kinetic approach to the mechanism of the redox reaction of malachite green and permanganate ion in aqueous acidic medium, AJPAC. 3 (2010) 269–274.

Moldes-Diz Y., Gamallo M., Eibes G., Vargas-Osorio Z., Vazquez-Vazquez C., Feijoo G., Lema J. M., Moreira M. T., Development of a Superparamagnetic Laccase Nanobiocatalyst for the Enzymatic Biotransformation of Xenobiotics, Journal of Environmental Engineering. 144 (2018) 04018007.

Muñiz-Mouro, A., I.M. Oliveira, B. Gullón, T.A. Lú-Chau, M.T. Moreira, J.M. Lema, G. Eibes, Comprehensive investigation of the enzymatic oligomerization of esculin by laccase in ethanol : water mixtures, RSC Adv. 7 (2017) 38424–38433.

Namerah. Air compressors. http://www.namerah.com/service/ screwcompressor-22kw/ (Accessed on April 2018)

PRé Consutants. 2018. https://www.pre-sustainability.com (Accessed on July 2018).

Eurostat. Electricity price statistics, http://ec.europa.eu/eurostat/statistics-explained/index.php/Electricity_price (Accessed on July 2018).

Osma, J.F., J.L. Toca-Herrera, S. Rodríguez-Couto, Cost analysis in laccase production. J Environ Manage, 92 (2011) 2907-2912.

Standard Methods For the Examination of Water and Wastewater, 20th Revised edition, American Water Works Association,US, Washington, 1999.

Wang, F., Y. Hu, C. Guo, W. Huang, C.-Z. Liu, Enhanced phenol degradation in coking wastewater by immobilized laccase on magnetic mesoporous silica nanoparticles in a magnetically stabilized fluidized bed, Bioresource Technology. 110 (2012) 120–124.

Chapter 7

Comparative life cycle assessment of different synthesis routes of magnetic nanoparticles

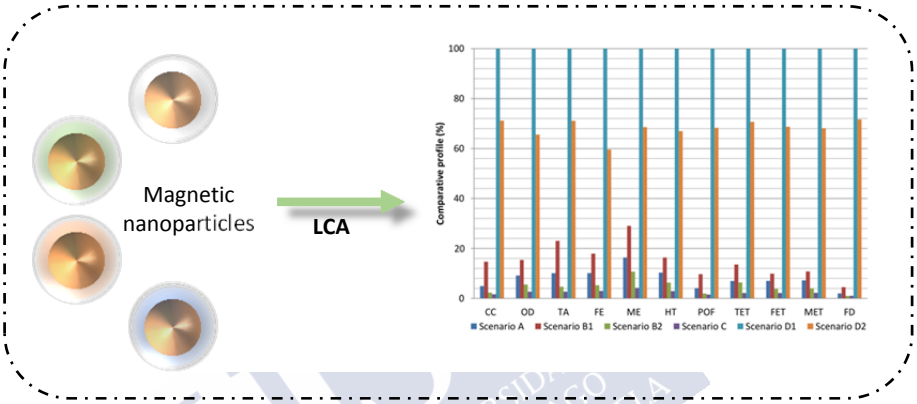

The environmental evaluation of different synthesis routes of mNPs used as supports for immobilization of enzymes was considered by using Life cycle assessment (LCA) perspective in the manufacturing stage of the mNPs production, especially for silica-coated superparamagnetic nanoparticles. Among the different environmental impacts and indicators, the values of Carbon Footprint vary between 26.5 kg CO_2 eq and 1.61 kg eq per gram of mNP. However, the diverse types of nanoparticles perform differently as support for immobilization of laccase, an oxidative enzyme with high oxidation potential. Accordingly, the balance between the environmental impacts associated to mNP production and the efficiency of enzyme immobilization was reached for polyethylemine-coated mNPs, which provided satisfactory levels in both indicators. Despite the great interest in the production of nanoparticles, there are a number of issues encountered in the application of LCA methodology to nanoproducts: lack of comparable reports and data availability, both imply uncertainties associated with the estimation of environmental impacts of NPs.

USC
UNIVERSIDADE
DE SANTIAGO
DE COMPOSTELA

OUTLINE

7.1. Introduction

In Chapter 2 different nanoparticles were used for the immobilization of different enzymes with the aim to achieve high enzyme loadings. Once the nanobiocatalysts were formulated, they were used for different applications, ranging from the oxidation of pollutants (Chapters 3-4) to production of value added bio-based products (Chapter 5). However, due to the early stages of development of nanoscience, new materials are being synthesized on small scales and no impacts of nanotechnology in environment are available in terms of environmental indicators associated to their production.

Given the early stages of development of nanoscience, new materials are being synthesized on small scales (hundreds of milligrams or less) for testing specific physical properties. As a result, the examination of any unintended properties of the material or concerns about efficiencies of the production process is often deferred. In view of that possibility, we need to address the impacts of nanotechnology from a prospective perspective, not only from the technological complexity of a production system but also from the potential health and environmental risks associated. The assessment of the environmental impacts of nanoscale materials before they are accepted as mature technologies presents an opportunity to minimize presumed negative consequences from the very beginning of the concept design stage and ultimately lead to the implementation of green chemistry processes.

The methodology that can be applied for the holistic assessment of nanotechnologies can be based on a life cycle perspective (Grieger *et al*., 2012). The application of Life Cycle Assessment (LCA) to nanotechnology would include all aspects of activities during the life of a product, such as extraction of raw materials and resources, production processes, use of products, recovery, recycling of some fractions and final disposal at the end-of-life stage. However, there are inherent difficulties when striving a comprehensive analysis of nanomaterials. The major obstacles include the uncertainty arising from the immature nature of the technology, the availability of extensive information on processes subjected to patent protection and the lack of characterization factors for LCA impact assessment (Tsuzuki, 2013). Although these drawbacks can be a major obstacle to

overcome, the development of new nanomaterials can be carried out with sustainability in mind.

The available LCA studies on ENMs are focused on nanomaterials such as CdTe, carbon nanofibres and nanotubes, nanoclay, nanoscale Pt-group metals, Nanocrystaline-Si, Ag, titanium and titanium oxide. Hischier and Walser (2012) and Gavankar *et al*. (2012) reviewed all studies applying LCA to ENMs, whilst Upadhyayula *et al*. (2012) specifically focused on carbon nanotubes (CNTs) and carbon nanofibres (CNFs). The main outcomes from these studies report that energy and chemicals use during ENM synthesis contributes a dominant share of total life cycle environmental impacts (Walser *et al*., 2011; Eckelman *et al*., 2012). However, the LCIs cannot be classified as comprehensive as they often lack ENM specific data related to the outputs of the processes (Hischier and Walser, 2012).

In this chapter, we aim to examine how the application of LCA principles to nanoscience can be helpful in the decision-making process to guide technological progress within this emerging field. Different approaches of mNPs synthesis were evaluated; from the production of oleic-acid stabilized magnetite to production schemes where the coating of a shell on the preformed nanoparticles is developed: polyacrylic acid, polyethylenimine and silica-coated magnetic nanoparticles. Moreover, an additional criterion for selection would also identify the performance of the different mNPs for the immobilization of the target enzyme.

7.2. Materials and methods

7.2.1. Goal and scope definition

The aim of this study is to assess the environmental profiles of different mNPs production routes. To do so, the comparative analysis is based on primary data from the production scenarios of mNPs developed by the NanoMag group at the University of Santiago de Compostela. **Figure 7.1** displays the production sequences under environmental evaluation. The detailed description of the four scenarios is reported below.

The LCA functional unit must be selected carefully to allow comparisons between the production systems. Therefore, all the environmental results will be reported and discussed per gram of mNP.

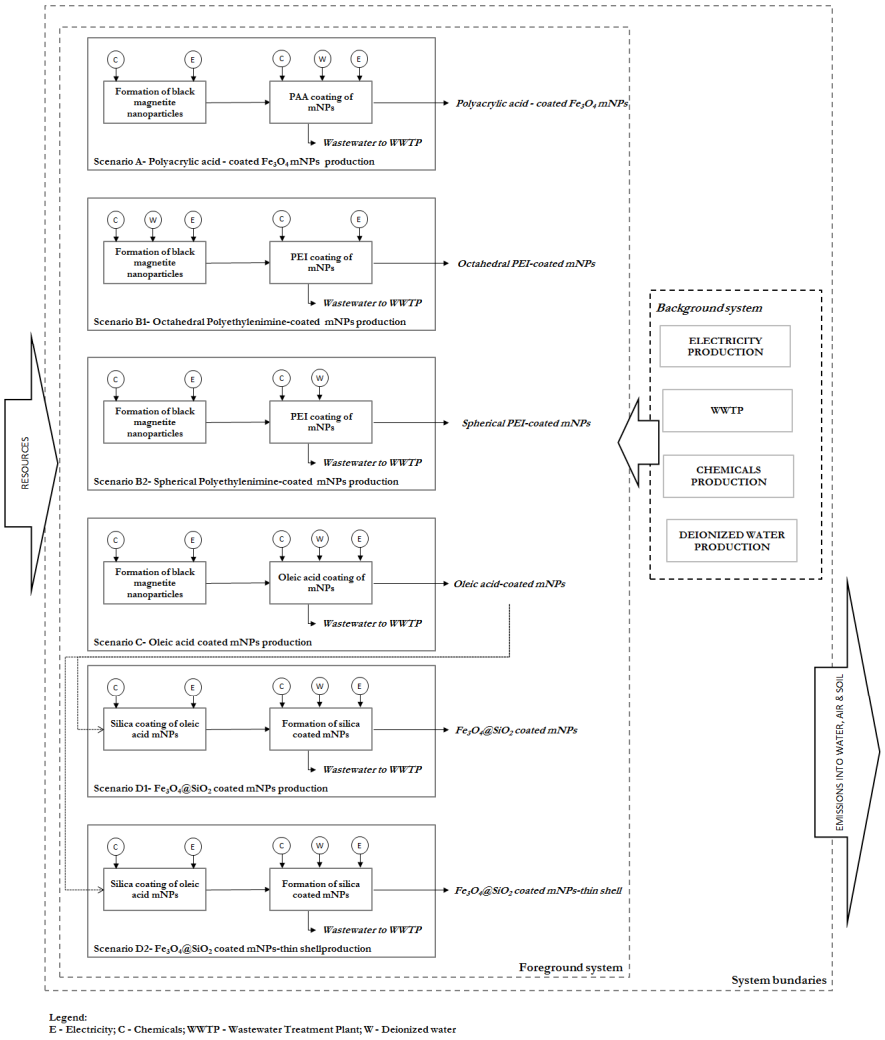

Figure 7.1. Block Flow Diagrams depicting the different production routes of mNPs

7.2.2. Description of the mNPs production scenarios

Preparation of Polyacrylic acid-coated magnetic nanoparticles (Scenario A)

Polyacrylic acid-coated Fe_3O_4 nanoparticles have been prepared by co-precipitation of Fe^{2+} and Fe^{3+} salts, following the Massart method (1981). In a typical synthesis, 24.3 g of $FeCl_3.6H_2O$ and 16.7 g of $FeSO_4.7H_2O$ (molar ratio Fe^{3+}/Fe^{2+} of 1.5) are placed in a 500-mL round-bottom flask and dissolved in 200 mL of 0.01 M HCl solution with mechanical stirring. Temperature is increased to 60°C and 60 mL of ammonia solution (28%) is added to the mixture, observing the immediate formation of black magnetite nanoparticles. Secondly, 3.9 g of polyacrylic acid is added 30 s after the addition of the ammonia solution and the reaction is allowed to continue for 1 h. After cooling down to room temperature, pH is acidified to 4 by the addition of HCl (9% wt). Finally, the magnetic nanoparticles are magnetically separated and washed four times with deionized water and finally re-dispersed in water.

Preparation of Polyethylenimine-coated mNPs (Scenario B): Octahedral PEI-coated mNPs (Scenario B1) and Spherical PEI-coated mNPs (Scenario B2)

Polyethylenimine (PEI) is a branched polymer with a high-density amine group, $(CH_2CH_2NH)_n$. Due to the different pKa values of the primary, secondary and tertiary amino groups, PEI has the ability to capture protons at different pH conditions, which is known as the 'proton sponge' mechanism. PEI molecules bounded to particles by electrostatic interaction and the negative charges on the surface of the particles were converted to positive charges. Due to its unique properties, PEI appears to be one of the most appropriate molecules for the surface modification of mNPs for biological applications.

The production process of the polyethylenimine (PEI)-coated mNPs by oxidative precipitation is carried out following the method described by Goon *et al*. (2010). Nitrogen gas is bubbled in deionized water in order to remove dissolved oxygen. Solutions of $FeSO_4 \cdot 7H_2O$, NaOH and KNO_3 prepared in deionized and des-oxygenated water are mixed and after 5 min, temperature is increased up to 90℃ to complete the reaction after 2 h. Next, the magnetic nanoparticles are magnetically separated and washed three times with deionized water and immediately re-dispersed in water. Finally, 10 mL of PEI solution (20 $g \cdot L^{-1}$) is added

to the magnetite nanoparticles obtained previously. The magnetic nanoparticles are magnetically shaken (500 rpm, 1 h) and dried for 12 h at 75°C in order to improve the polymer absorption on the nanoparticles.

The production process of spherical PEI-coated mNPs started with the formation of the black magnetite nanoparticles obtained as aforementioned in Scenario A (Massart, 1981). PEI (2 g) was added to the magnetite nanoparticles. After the reaction and cooling down to room temperature, pH was acidified to 4 with HCl. Then, the magnetic nanoparticles were magnetically separated and washed four times with deionized water and finally re-dispersed in water.

Preparation of oleic-acid mNPs (Scenario C)

Oleic acid is a surfactant used to stabilize the mNPs synthesized by the traditional co-precipitation method. Oleic acid forms a waterproof shell around the mNPs. The procedure to produce oleic-acid-coated Fe_3O_4 mNPs starts with the incubation of black magnetite nanoparticles (as indicated in Scenario A) with oleic acid. The reaction is allowed to continue for 1 h before being heated on a hot plate until flocculation occurred. The mNPs are washed twice with deionized water to remove residual concentration of the surfactant molecules and finally re-dispersed in cyclohexane.

Preparation of Fe_3O_4@SiO_2 coated mNPs (Scenario D)

The Fe_3O_4@SiO_2 coated mNPs were prepared through a water-in-cyclohexane reverse micro-emulsion starting from the oleic-acid mNPs previously obtained in Scenario C (Fang *et al*., 2011; Han *et al*., 2008). The reverse micro-emulsion method considered to coat magnetic nanoparticles with silica requires neither the use of silane coupling agents as surface primers nor a polymer stabilizer.

Fe_3O_4@SiO_2 coated mNPs (Scenario D1)

In a typical synthesis, polyoxyethylene(5)nonylphenyl ether (Igepal CO-520) and cyclohexane are mechanically stirred for 15 min before the addition of oleic-acid magnetite nanoparticles (2.5% wt in cyclohexane). Finally, ammonium hydroxide solution and tetraethyl orthosilicate (TEOS) are added consecutively under stirring to form a transparent red solution of reverse micro-emulsion until complete reaction after 18 h. The core-shell nanoparticles are precipitated with isopropanol (IPA) to disrupt the reverse microemulsion and washed four times with

IPA and deionized water. Finally, they are subjected to several cycles of centrifugation (9000 rpm, 120 min) and washed with deionized water until no foam is observed. Then, the core-shell nanoparticles were re-dispersed in deionized water to a concentration ca. 0.5% wt (determined by thermogravimetric analysis).

Fe_3O_4@SiO_2 coated mNPs (silica thin shell) (Scenario D2)

The production of magnetic nanoparticles with a thin silica-coating were produced following the procedure previously mentioned in Scenario D1. In this case, the concentration of cyclohexane added was 0.5% wt and the core-shell nanoparticles were re-dispersed in deionized water to a concentration ca. 0.75% wt (determined by thermogravimetric analysis).

7.2.3. Inventory data

A reliable environmental assessment requires the collection of high value Life Cycle Inventory (LCI) data. In this study, inventory data for the foreground systems (direct inputs and outputs for each scenario) such as electricity requirements (estimated with power and operational data from the different units: reactors, dryers, heaters) as well as use of chemicals and water were average data from lab-scale experiments. Concerning the background system, the inventory data corresponding to several inputs (production of electricity, chemicals and water) as well as the wastewater treatment process were taken from Ecoinvent database® v3 (Dones *et al*., 2007; Althaus *et al*., 2007; Doka, 2007). A summary of the primary data is displayed in Tables 7.1 to 7.7 for the different scenarios. It is important to remark that regarding electricity production, the process defined in the database has been updated managing data for the average electricity generation and import/export data from Spain in 2014 (Red Eléctrica de España, 2014).

Table 7.1. Size distribution of the different magnetic nanoparticles

Magnetic nanoparticles	Size (nm)
Fe_3O_4@PAA	10.1
Octahedral Fe_3O_4@PEI	50-100
Spherical Fe_3O_4@PEI	10
Fe_3O_4@OA	8-10
Fe_3O_4@SiO_2	21.5
Fe_3O_4@SiO_2 (thin layer)	17

Table 7.2. Global inventory of the production of PAA-coated Fe_3O_4 mNPs (Scenario A)

Inventory	Amount	Unit
Inputs from Technosphere		
Formation of magnetite nanoparticles		
$FeCl_3 \cdot 6H_2O$ (99% wt)	24.3	g
$FeSO_4 \cdot 7H_2O$ (99% wt)	16.7	g
NH_4OH (28% wt)	60	mL
HCl (37% wt)	98.5	mg
Electricity for agitation	441	kJ
Electricity for heating (60°C)	1134	kJ
PAA coating of mNPs		
Polyacrylic acid	3.9	g
Electricity for heating (200°C)	648	kJ
Electricity for ultrasonic bath	192	kJ
Deionized water	0.50	L
Outputs to Technosphere		
Polyacrylic acid - coated Fe_3O_4mNPs	5	g
Emissions to treatment facility		
Wastewater	0.4	L

Table 7.3. Global inventory of the production of Octahedral PEI-coated mNPs (Scenario B1)

Inventory	Amount	Unit
Inputs from Technosphere		
Formation of magnetite nanoparticles		
$FeSO_4 \cdot 7H_2O$ (99% wt)	14	g
NaOH	8	g
KNO_3	40	g
Electricity from agitation	588	kJ
Electricity from heating (90°C)	1296	kJ
Electricity from ultrasonic bath	96	kJ
Deionized water	0.5	L
PEI coating mNPs		
Polyethylenimine (PEI)	4	g
Electricity	4125	kJ
Outputs to Technosphere		
PEI coated nanoparticles	6.4	g
Emissions to treatment facility		
Wastewater	0.35	L

Table 7.4. Global inventory of the production of Spherical PEI-coated mNPs (Scenario B2)

Inventory	Amount	Unit
Inputs from Technosphere		
Formation of magnetite nanoparticles		
$FeCl_3 \cdot 6H_2O$ (99% wt)	12.2	g
$FeSO_4 \cdot 7H_2O$ (99% wt)	8.4	g
HCl (37% wt)	98.5	mg
NH_4OH (28% wt)	30.0	mL
Electricity for agitation	441	kJ
Electricity for heating (60°C)	1134	kJ
PEI coating mNPs		
Polyethylenimine (PEI)	2	g
HCl (9% wt)	35	mL
Deionized water	0.5	L
Outputs to Technosphere		
PEI coated nanoparticles	7-7.5	g
Emissions to treatment facility		
Wastewater	0.5	L

Table 7.5. Global inventory of the production of Oleic acid coated mNPs (Scenario C)

Inventory	Amount	Unit
Inputs from Technosphere		
Formation of magnetite nanoparticles		
$FeCl_3 \cdot 6H_2O$ (99% wt)	24.3	g
$FeSO_4 \cdot 7H_2O$ (99% wt)	16.3	g
HCl (37% wt)	197	mg
NH_4OH (28% wt)	60	mL
Electricity for agitation	441	kJ
Electricity for heating (60°C)	1134	kJ
Oleic acid coating mNPs		
Oleic acid	4.0	g
Electricity for heating (200°C)	648	kJ
Deionized water	0.5	L
Cyclohexane	120	mL
Outputs to Technosphere		
Oleic acid coated nanoparticles	22.5	g
Emissions to treatment facility		
Wastewater	0.4	L

Table 7.6. Global inventory of the production of Fe_3O_4@SiO_2 coated mNPs (Scenario D1)

Inventory	Amount	Unit
Inputs from Technosphere		
Silica coating of oleic acid mNPs		
Oleic acid coated nanoparticles	1	g
Igepal CO-520	150	g
Cyclohexane	1.8	kg
NH_4OH (28% wt)	21	mL
TEOS	24	mL
Electricity for agitation	189	kJ
Electricity for mechanical agitation	4032	kJ
Formation of silica coated mNPs		
IPA	7.1	kg
Deionized water	0.5	L
Electricity for agitation	210	kJ
Electricity for ultrasonic bath	192	kJ
Outputs to Technosphere		
Fe_3O_4@SiO_2 coated nanoparticles	7.5	g
Emissions to treatment facility		
Wastewater	0.7	L

Table 7.7. Global inventory of the production of Fe_3O_4@SiO_2 coated mNPs-thin shell (Scenario D2)

Inventory	Amount	Unit
Inputs from Technosphere		
Silica coating of oleic acid mNPs		
Oleic acid coated nanoparticles	1	g
Igepal CO-520	150	g
Cyclohexane	360	g
NH_4OH (28% wt)	21	mL
TEOS	24	mL
Electricity for agitation	189	kJ
Electricity for mechanical agitation	4032	kJ
Formation of silica coated mNPs		
IPA	7.1	kg
Deionized water	0.5	L
Electricity for agitation	210	kJ
Electricity for ultrasonic bath	192	kJ

Table 7.7 (cont.). Global inventory of the production of Fe_3O_4@SiO_2 coated mNPs-thin shell (Scenario D2)

Outputs to Technosphere		
Fe_3O_4@SiO_2 coated nanoparticles	7.5	g
Emissions to treatment facility		
Wastewater	0.7	L

7.2.4. Impact assessment methodology

Among the steps defined within the Life Cycle Impact Assessment of the LCA methodology (ISO 14040, 2006), only classification and characterization were undertaken. The mNPs production scenarios under assessment involve emissions to the environment and consumption of resources throughout the global systems. The environmental impacts of these emissions and resources consumption can be computed in terms of different impact categories. In this study, the environmental assessment was conducted using characterization factors from ReCipe Midpoint methodology (Goedkopp *et al*., 2008) and the following impact categories have considered in the analysis: climate change (CC), ozone depletion (OD), terrestrial acidification (TA), freshwater eutrophication (FE), marine eutrophication (ME), human toxicity (HT), photochemical oxidant formation (POF), terrestrial ecotoxicity (TET), freshwater ecotoxicity (FET), marine ecotoxicity (MET) and fossil depletion (FD). Moreover, special attention will be paid on the carbon footprint profiles corresponding to the different production routes considering the results obtained in CC. To do so, SimaPro 7.3.3 has been the software used for the computational implementation of the life cycle inventory data (PRé Consultants, 2017).

7.3. Environmental results

The aim of this study is to analyze from an environmental perspective the environmental profiles associated with four different mNPs production schemes in order to identify the one with the best environmental perspective. The performance of the different types of mNPs as support for immobilization of enzymes was also investigated as additional criteria and a balance between the environmental impacts associated to mNP production and the efficiency of enzyme immobilization must determine which one is the most suitable support for the intended use of laccase immobilization.

The different production routes rendered into viable magnetic nanoparticles, whose superparamagnetic characteristics were evidenced under a magnetic field. Characterization of the nanoparticles was also performed following the standard procedures of transmission electron microscopy to determine shape, size, and uniformity of the particles under optimum conditions. The magnetite nanoparticles were predominantly spherical with variable size as depicted in Table 7.1. Once that the different routes provided different types of mNPs, these processes were environmental assessed according to stages and processes depicted in Figure 7.1.

Considering that detailed inventory data directly from industrial production are unavailable, the evaluation of the environmental impacts associated to NPs production was based on data from laboratory-scale and process modeling. The characterization results for the different production schemes are shown in Table 7.8.

The worst profile obtained corresponded with Scenario D1 performing the production of Fe_3O_4@SiO_2 coated mNPs. Although all scenarios include one production stage in common, that is, the reaction leading to the formation of magnetite nanoparticles, remarkable differences were identified on the basis of the requirements of chemicals for the formulation of the final NPs.

Differences are also evidenced in the second stage of production, focused on the coating of the previously formed NPs. This stage also requires magnetic separation, washing and re-dispersion, as can be seen in A, B1, B2 and C. However, in Scenaria D1 and D2, the production of Fe_3O_4@SiO_2 coated mNPs and Fe_3O_4@SiO_2 coated mNPs-thin shell is based on the use of oleic acid coated mNPs (from Scenario C) as main raw material and they require isopropanol for formation of the silica coated nanoparticles. Thus, activities such as precipitation, centrifugation, washing and re-dispersion are also included in this stage.

Table 7.8. Environmental impacts in the production of nanoparticles per functional unit

		Scenario			
Impact category	Unit	A	B1	B2	C
CC	kg CO_2 eq	$7.94 \cdot 10^{-2}$	$2.37 \cdot 10^{-1}$	$3.74 \cdot 10^{-2}$	$2.65 \cdot 10^{-2}$
OD	kg CFC-11 eq	$7.45 \cdot 10^{-9}$	$1.25 \cdot 10^{-8}$	$4.49 \cdot 10^{-9}$	$2.19 \cdot 10^{-9}$
TA	kg SO_2 eq	$6.32 \cdot 10^{-4}$	$1.45 \cdot 10^{-3}$	$2.94 \cdot 10^{-4}$	$1.70 \cdot 10^{-4}$
FE	kg P eq	$3.83 \cdot 10^{-5}$	$6.76 \cdot 10^{-5}$	$1.99 \cdot 10^{-5}$	$1.13 \cdot 10^{-5}$
ME	kg N eq	$3.52 \cdot 10^{-5}$	$6.23 \cdot 10^{-5}$	$2.30 \cdot 10^{-5}$	$9.00 \cdot 10^{-6}$
HT	kg 1,4-DB eq	$3.85 \cdot 10^{-2}$	$6.11 \cdot 10^{-2}$	$2.34 \cdot 10^{-2}$	$1.09 \cdot 10^{-2}$
POF	kg NMVOC	$3.09 \cdot 10^{-4}$	$7.31 \cdot 10^{-4}$	$1.45 \cdot 10^{-4}$	$1.16 \cdot 10^{-4}$
TET	kg 1,4-DB eq	$3.56 \cdot 10^{-6}$	$6.94 \cdot 10^{-6}$	$3.26 \cdot 10^{-6}$	$1.09 \cdot 10^{-6}$
FET	kg 1,4-DB eq	$9.36 \cdot 10^{-4}$	$1.32 \cdot 10^{-3}$	$5.11 \cdot 10^{-4}$	$2.90 \cdot 10^{-4}$
MET	kg 1,4-DB eq	$9.08 \cdot 10^{-4}$	$1.35 \cdot 10^{-3}$	$5.03 \cdot 10^{-4}$	$2.80 \cdot 10^{-4}$
FD	kg oil eq	$2.25 \cdot 10^{-2}$	$5.03 \cdot 10^{-2}$	$1.08 \cdot 10^{-2}$	$1.15 \cdot 10^{-2}$

Table 7.8 (cont.) Environmental impacts in the production of nanoparticles per functional unit

		Scenario	
Impact category	Unit	D1	D2
CC	kg CO_2 eq	1.61	1.15
OD	kg CFC-11 eq	$8.13 \cdot 10^{-8}$	$5.33 \cdot 10^{-8}$
TA	kg SO_2 eq	$6.29 \cdot 10^{-3}$	$4.47 \cdot 10^{-3}$
FE	kg P eq	$3.78 \cdot 10^{-4}$	$2.25 \cdot 10^{-4}$
ME	kg N eq	$2.15 \cdot 10^{-4}$	$1.47 \cdot 10^{-4}$
HT	kg 1,4-DB eq	$3.73 \cdot 10^{-1}$	$2.50 \cdot 10^{-1}$
POF	kg NMVOC	$7.53 \cdot 10^{-3}$	$5.14 \cdot 10^{-3}$
TET	kg 1,4-DB eq	$5.11 \cdot 10^{-5}$	$3.61 \cdot 10^{-5}$
FET	kg 1,4-DB eq	$1.34 \cdot 10^{-2}$	$9.20 \cdot 10^{-3}$
MET	kg 1,4-DB eq	$1.26 \cdot 10^{-2}$	$8.56 \cdot 10^{-3}$
FD	kg oil eq	1.12	$8.06 \cdot 10^{-1}$

The effect of these production differences is reflected not only on the environmental results but also on the mNPs production yields. According to the inventory data displayed in Tables 7.2-7.7, a large range of production values is obtained from 5 g of mNPs in scenario A to 22.5 g of mNPs in Scenario C. Global results show that, across synthesis routes, impacts associated with the consumption of energy are dominant but also chemicals used in the formulations and for re-dispersion are relevant.

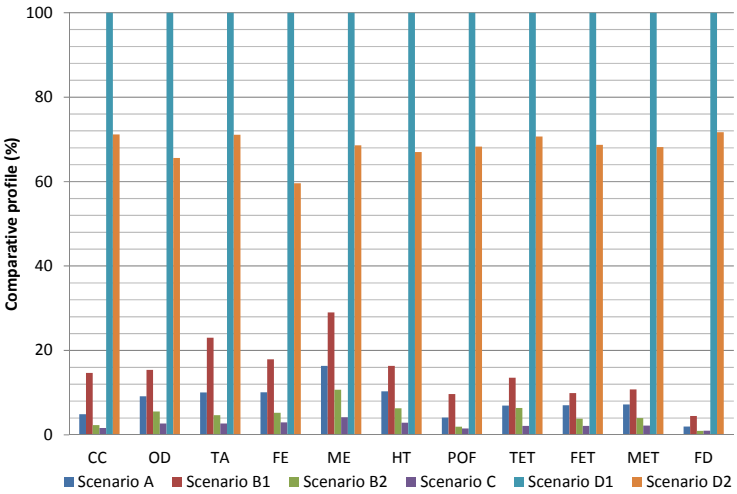

Figure 7.2. Comparative environmental profiles of the different mNPs production routes

In line with Figure 7.2 and Table 7.8, the production of 1 g of oleic acid coated mNPs (Scenario C) should report the best profile regardless the impact category with reduction of 97-99% with regard to the worst option (Scenario D1 in all categories). According to these global comparative results, it is unquestionable that increasing the complexity of the mNPs production route as it is performed in Scenarios D1 and D2, would have to be discussed from an environmental perspective due to the highest environmental burdens obtained per g of mNPs. Moreover, and although it will be analyzed in more detail below, Scenario D2 does not achieve the highest level of laccase immobilization despite the worse environmental profile. In order to identify the main responsible input of these negative results, the different production routes will be separately assessed.

Scenario A: Polyacrylic acid - coated Fe_3O_4 mNPs

The production of Polyacrylic acid-coated Fe_3O_4 mNPs involves two stages carried out in the pilot plant (formation of magnetite NPs and PAA coating) as well as the treatment of the wastewater. Figure 7.3 displays the contributions to the global environmental profile from the different stages involved.

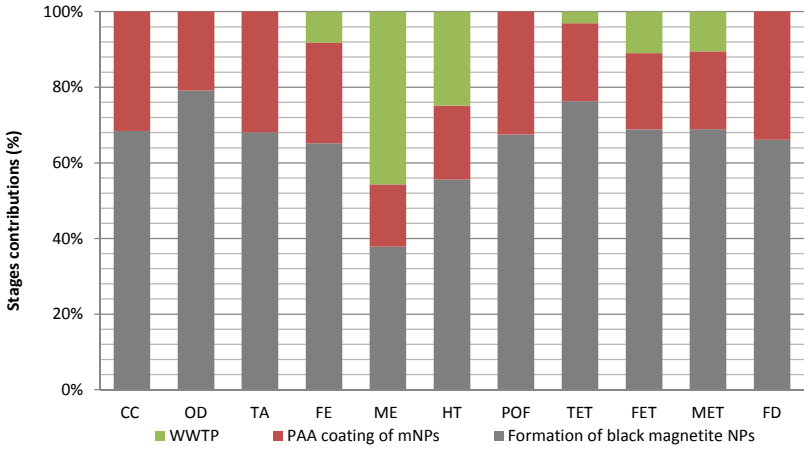

Figure 7.3. Contributions to the environmental impacts for the stages in Scenario A.

According to Figure 7.3, the formation of magnetite NPs is the most important environmental stage and it reports contributions ranging from 38% to 79% depending on the category. The large contribution from this subsystem can be expected since in this step, 65% of total electricity requirements take place as well as the largest consumption of chemicals. Contributions from the coating stage are specifically remarkable in categories such as CC, TA, POF and FD. All these categories are inherently related and highly dependent on electricity requirements, which represent contributing ratios ranging from 80% to 97% depending on the category. The treatment of the wastewater produced in the synthesis is only outstanding in two categories: ME and HT (46% and 25% of total contributions). If the environmental burdens derived from the formation of magnetite NPs are assessed in more detail, Figure 7.4 displays the ratios from the responsible processes of these results.

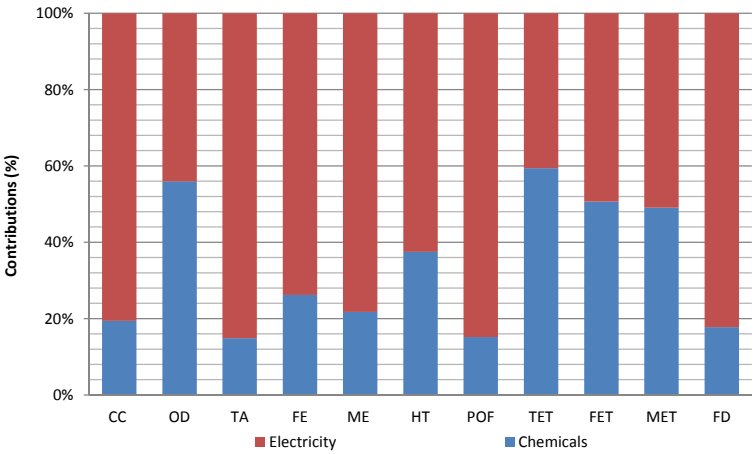

Figure 7.4. Environmental impacts associated to the formation of magnetite NPs

According to Figure 4, electricity requirements in this stage can be considered as the environmental *hotspot*. Production of electricity contributes to more than 63% of total life cycle impacts (except OD, TET, FET and MET) and heating at 60°C is the most important contributor. Within the contributions from the chemical requirements, special attention should be paid to the ammonia solution since the use of this chemical is responsible of ratios ranging from 28% to 66% of impacts derived from chemicals.

Scenario B1

This scenario is focused on the production of PEI-coated mNPs under an oxidative precipitation scheme. Once again, two production stages are carried out in the pilot plant: formation of magnetite NPs and PEI coating. In addition, the wastewater stream has to be treated in a further stage. The ratios to the global environmental profile from steps involved in the production systems are displayed in Figure 7.5. In this scenario, the two steps performed within the pilot plant are responsible of 82 to 100% of the environmental impacts. Thus, contributions from the WWTP are minor. However, and in contrast to Scenario A, the largest electricity requirement takes place in the coating stage: 68% of total electricity consumption, due to the drying step at 75°C. Contribution from electricity consumption to PEI coating of mNPs step represents ~98% (on average) of the total impacts. Regarding the formation of magnetite NPs, the environmental profile derived from this

subsystem is assigned to chemicals and electricity requirements. Thus, the contribution from deionized water requirements is negligible as it is displayed in Figure 7.6, regardless the impact category.

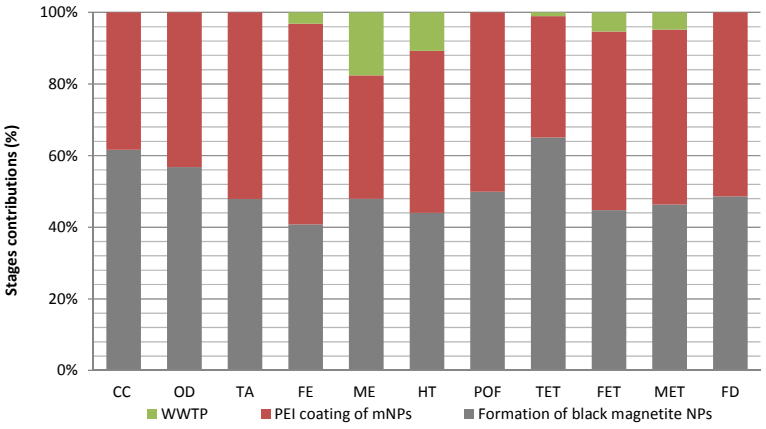

Figure 7.5. Contributions to the environmental impacts for the stages in Scenario B1.

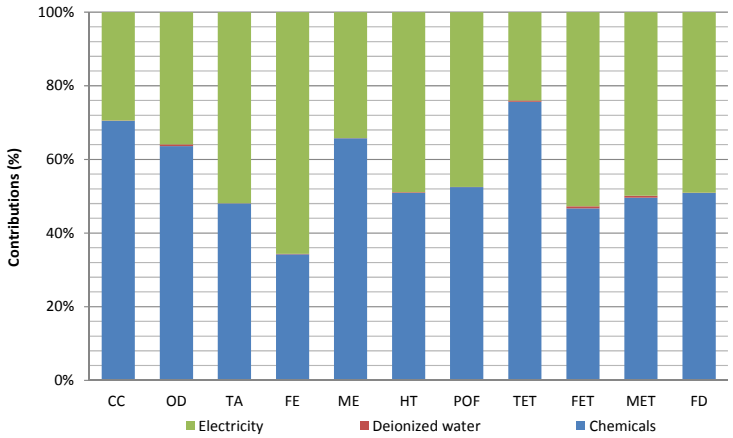

Figure 7.6. Environmental impact distribution for the formation of magnetite NPs stage

As displayed in Figure 7.6, the required chemicals are also an environmental *hotspot* and special attention should be paid to the consumption of potassium nitrate since the impacts derived from this chemical add up to 76-97% of the

burdens. Thus, further improvement activities should be focused on searching alternative chemicals with better environmental profile or even, on reducing its use. Electricity is also remarkable in this stage, being outstanding the heating process at 90°C. In global, the environmental *hotspots* in this scenario are the large electricity requirements (specifically in the drying process) as well as the consumption of potassium nitrate.

Scenario B2

This scenario is focused on the production of spherical PEI-coated mNPS. Some differences were identified in the production system regarding Octahedral PEI-coated mNPs (Scenario B1). The main differences are linked to the chemicals used in the formation of magnetite nanoparticles step since ammonium hydroxide is used instead of potassium nitrate as well as in the PEI coating mNPs step, where no heating is required in contrast to Scenario B1. Figure 7.7 displays the contributions to the global environmental profile from the involving stages.

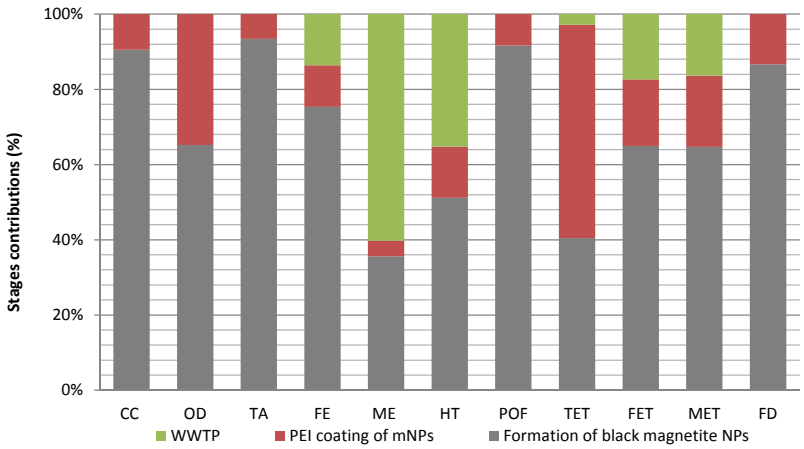

Figure 7.7. Contributions to the environmental impacts for the stages in Scenario B2.

According to Figure 7.7, undoubtedly the production of magnetite NPs is the environmental critical stage since in all the categories assessed, except in terms of

ME and TET, contributing ratios higher than 50% are achieved. Beyond the analysis of this critical step, Figure 7.8 displays the ratios from the responsible processes of these environmental results.

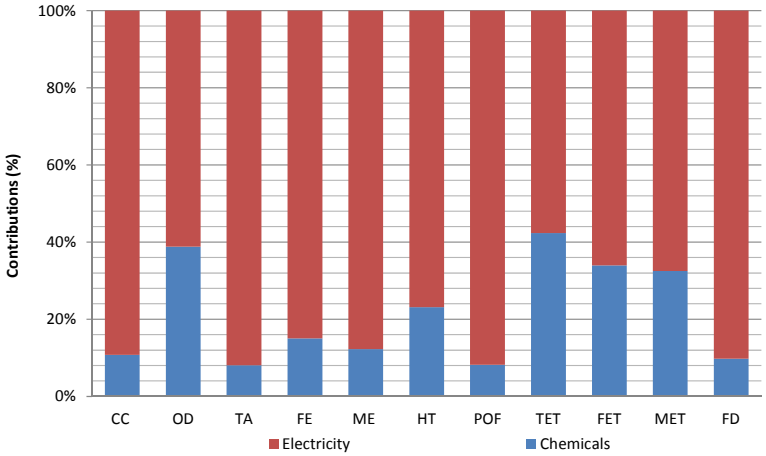

Figure 7.8. Environmental impact distribution regarding processes involved in the formation of magnetite NPs stage

According to Figure 7.8, the electricity requirements can be once again considered as environmental *hotspot*. This factor contributes to 61-92% of total impacts derived from this stage (depending on the category), being the heating process (at 60°C) the most important contributor. Regarding spherical PEI coating of mNPs stage, 100% of impacts are linked to the chemicals required since deionized water consumption reports negligible contributions. Within these chemicals, 82-97% of the environmental burdens derive from HCl consumption.

Scenario C

In this route, oleic acid coated mNPs are produced considering oleic acid as a surfactant used to stabilize the mNPs synthesized by the traditional co-precipitation method as previously reported. Two production stages are carried out in the pilot plant, all of them common to the other scenarios although under specific conditions: formation of magnetite NPs and oleic acid coating of mNPs. In addition, the wastewater stream is treated in a further stage. Figure 7.9 displays the contributions to the global environmental profile from the involving stages.

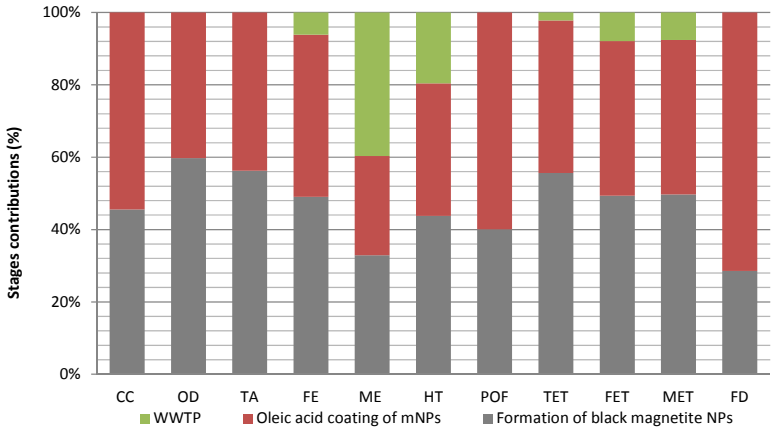

Figure 7.9. Contributions to the environmental impacts from the stages in Scenario C.

According to Figure 7.9, similar contributing ratios can be identified from the stages performed at the pilot plant being contribution from the WWTP only remarkable in terms of ME and HT. Both stages require chemicals and electricity, although electricity requirements are higher in the first stage than the second one (71% vs 29%). Beyond the analysis of the stage of reaction for the formation of magnetite NPs, Figure 7.10 displays the ratios from the responsible processes of these environmental results.

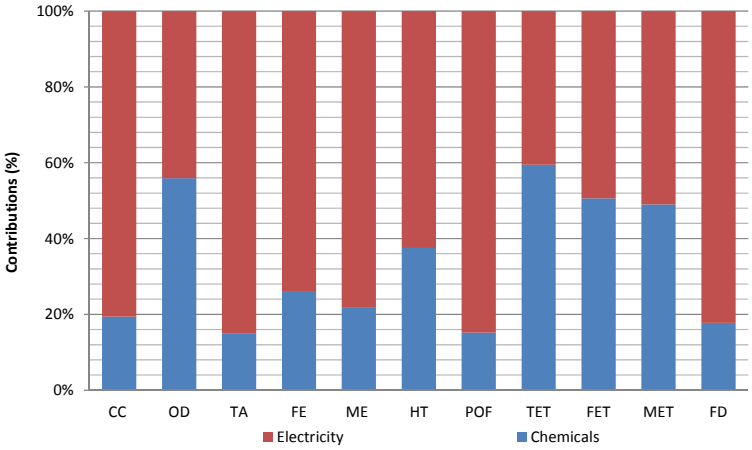

Figure 7.10. Environmental impact distribution regarding processes involved in the formation of magnetite NPs step.

According to Figure 7.10, the production of electricity requirements is once again considered as environmental *hotspot* with remarkable contributions in almost all the categories (41-85%). Once again, the heating activity (in this case at 60°C) is the main responsible of these results. Within the contributions from the chemical requirements, special attention should be paid to the ammonium hydroxide since reports impart ratios of environmental impacts in this stage.

Regarding the second step, oleic acid coating of mNPs, Figure 7.11 displays the contributions from processes involved and according to it, the consumption of chemicals is the environmental *hotspot*, being the cyclohexane required in the re-dispersion the responsible of more than 97% of impacts from chemicals.

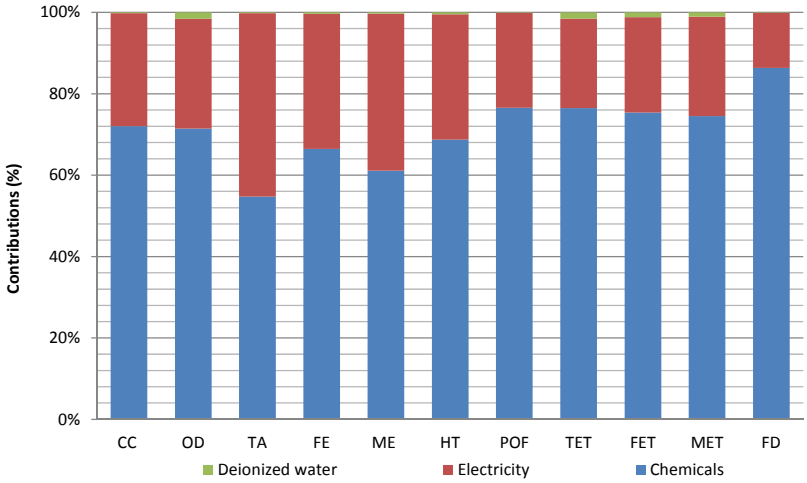

Figure 7.11. Environmental impact distribution of the processes involved in the formation of magnetite NPs step.

Scenario D1

This scenario aims to produce Fe_3O_4@SiO_2 coated mNPs considering oleic-acid mNPs as raw material. The production scheme is completed with four addition steps: silica coating of oleic acid mNPs and formation of silica coated mNPs. As difference to previous routes, oleic acid coated mNPs are the core-shell NP, previously re-dispersed with cyclohexane. Next, the core-shell NPs are precipitated with IPA and re-dispersed in deionized water. Figure 7.12 displays the environmental profile per impact categories in terms of contributions from steps or activities involved in the production system.

According to the results displayed in Figure 7.12, the silica coating stage of oleic acid mNPs is unquestionably an environmental *hotspot* since this stage is responsible for more than 50% of contributions to almost all the different impact categories (except in terms of CC, FET, MET and FD). In this step, the oleic-acid mNPs are mixed in a reactor with chemicals (Igepal CO-520, cyclohexane, TEOS and NH_4OH) in order to produce the core-shell mNPs.

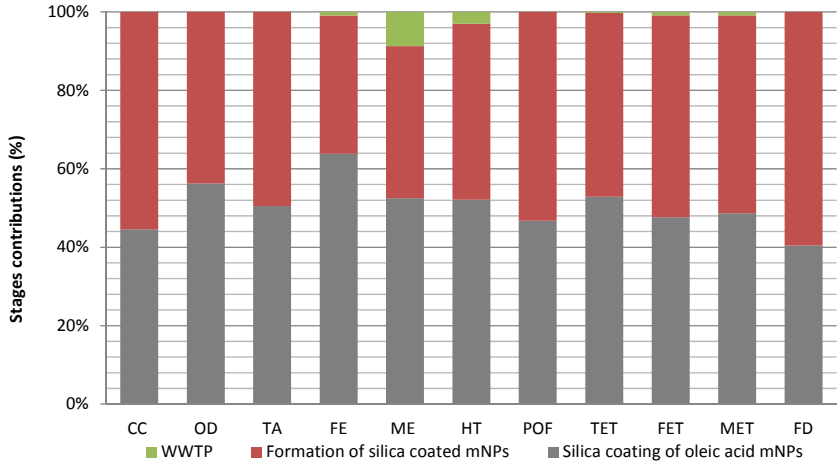

Figure 7.12. Contributions to the environmental impacts from the stages of Scenario D1.

Figure 7.13 displays the distribution of environmental burdens from the reactor step between the main factors involved: chemicals, oleic acid-coated mNPs and electricity consumptions. contributions from chemicals are higher than 75%. The cyclohexane required in the formulation is the environmental critical chemical since it is responsible for more than 86% of burdens derived from chemicals contributions regardless the impact category. However, in the majority of impact categories assessed, contributions from electricity are higher than 50%.

Regarding electricity, it is consumed in this step in the agitation activities, being remarkable the mechanical agitation required to obtain the transparent red solution of reverse micro-emulsion until complete reaction (97% of total electrical requirements). Regarding chemicals, the cyclohexane required in the formulation is the environmental critical chemical since it is responsible for more than 85% of burdens derived from chemicals contributions regardless the impact category.

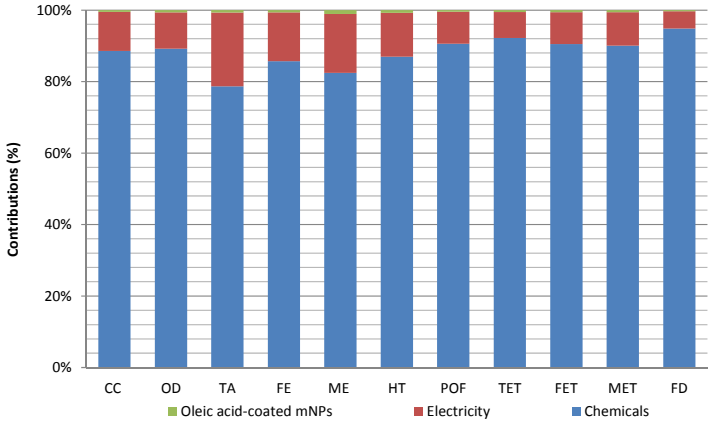

Figure 7.13. Environmental impacts distribution of the silica coating process of oleic acid-mNPs

Regarding the stage related to the formation of the silica coated mNPs, contributions range from 35% to 60% depending on the category. In this step, the core-shell mNPs are precipitated with isopropanol in order to break the reverse micro-emulsion prepared in the previous stage, and finally, washed and re-dispersed with deionized water. Taking a look into the derived environmental profile, the contributing actors are presented in Figure 7.14.

Figure 7.14. Environmental impacts distribution of the formation of the silica coated mNPs

According to the profile reported in Figure 7.14, the consumption of isopropanol can be considered as an environmental *hotspot*. Thus, special attention

should be paid on the requirements of isopropanol and cyclohexane in this type of mNP production system in order to improve its environmental profile.

Scenario D2

This scenario aims to produce Fe_3O_4@SiO_2 coated mNPs also considering oleic-acid mNPs as raw material but with a lower consumption of cyclohexane in order to produce mNPs with a thin silica-coating. The main remarkable difference regarding Scenario D1 is the lowest requirement of cyclohexane that is five times lower than in Scenario D1. Since cyclohexane is an environmental *hotspot* as previously indicated, environmental improvements of around 28-40% are expected for this type of mNPs since the same amount of mNPs is produced per batch (see Table 7.8 and Figure 7.2). Figure 7.15 displays the environmental profile per impact categories in terms of contributions from steps or activities involved in the production system.

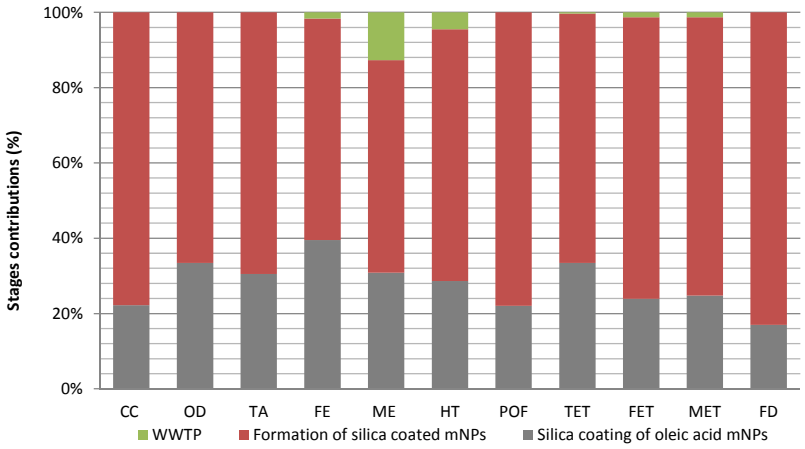

Figure 7.15. Contributions to the environmental impacts from the stages of Scenario D2.

In this scenario and as different to Scenario D1, both stages carried out with the pilot plant considerable change their behavior in the environmental profile. Thus, the effect from the silica coating of oleic acid mNPs step is not as remarkable as in Scenario D1, being the formation of silica coated mNPs the environmental

critical stage. The reduction on cyclohexane requirements is the main responsible of the environmental improvements. Assessing in more detail the contributions from this step (silica coating of oleic acid mNPs), Figure 7.16 displays the contributing ratios and as difference to Scenario D1, the environmental *hotspot* is related with chemicals requirements and cyclohexane consumption is also the most important chemical from an environmental perspective with contributing ratios of 54% to 75% (depending on the category) of impacts derived from chemicals. However, the electricity consumption is only responsible for less than of 40% of impacts derived from this stage.

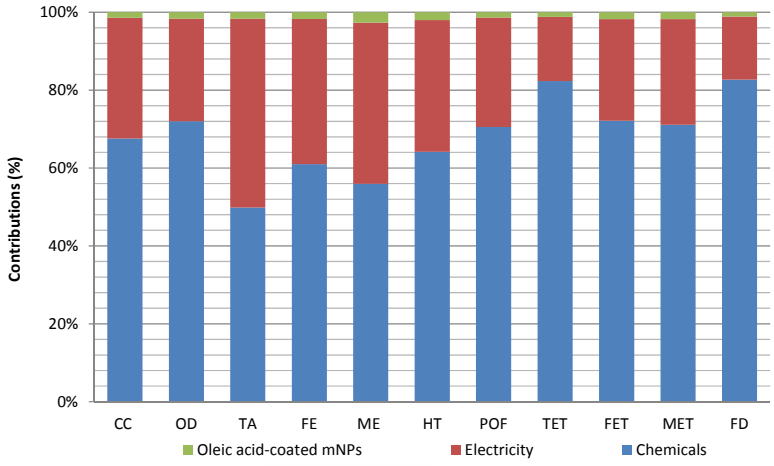

Figure 7.16. Environmental impacts distribution of the process of silica coated-mNPs

Since no differences have been identified in the second step (formation of the silica coated mNPs) between Scenario D1 and Scenario D2, the same behavior and profile (Figure 7.14) is expected.

Environmental analysis per unit immobilization yield

As previously indicated, the environmental profiles for the different mNPs production routes are displayed considering as functional unit one gram of mNPs. Nevertheless, and although these mNPs can be used for enzyme immobilization

(the main purpose), they do not present the same immobilization yields and in line with experimental assays, they are totally different (Table 7.9).

Table 7.9. Enzyme load per mg of mNP and per batch of production.

Scenario	Enzyme load ($U\ mg^{-1}$mNPs)	Enzyme batch (U batch mNPs)
A	0.107	535
B1	0.811	5190
B2	1.54	11165
C	0.2	4500
D1	2.66	19950
D2	1.14	8550

According to it, Scenario D1 (Fe_3O_4@SiO_2 coated mNPs) should be preferred in terms of units of enzyme immobilized per batch and Scenario A (Polyacrylic acid-coated Fe_3O_4 mNPs) should be the worst option. If the production routes are assessed from an environmental perspective, the consideration of the unit of laccase immobilized as functional unit entirely change the environmental profiles as reported in Figure 7.17. This alternative functional unit considers both the mNPs production yield and the enzyme unit immobilization yield.

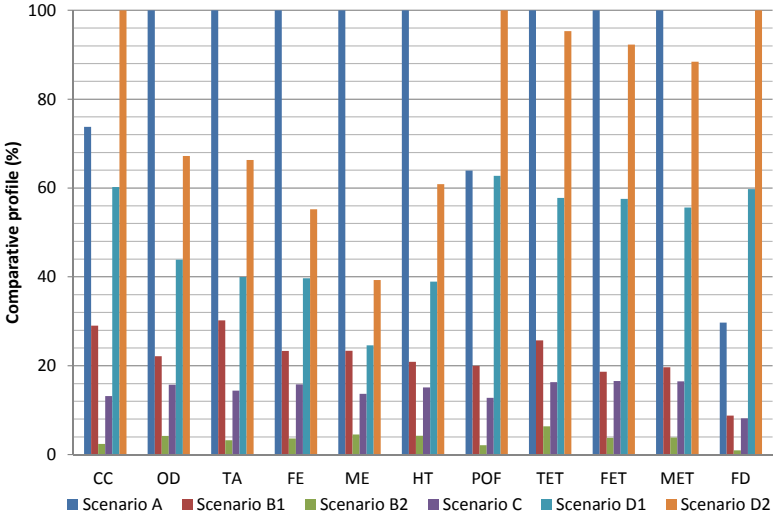

Figure 7.17. Comparative environmental profiles for the different scenarios considering 1 U of enzyme immobilized.

Taking into account the environmental profiles displayed in Figure 7.17, Scenario A and Scenario D2 should be the worst options regardless the impact category considered for assessment (as different to the results reported per gram of mNP, where Scenario D1 is undoubtedly the undesirable route). However, Scenario B2 (Spherical PEI-coated mNPs) should be preferred since reductions of around ~97% could be obtained with respect to Scenario A and Scenario D2 (depending on the category). Thus, Spherical PEI-coated mNPs could be considered as the best option not only from technical but also from environmental perspective. Paying special attention to carbon footprint, that is, to greenhouse gases (GHG) emissions, the sequence of preference of mNPs production routes to be chosen entirely changes when the results are reported per unit of laccase immobilized and gram of mNP produced.

In terms of Carbon Footprint, the preferred sequence should be the following (Table 7.10):

Scenario C < Scenario B2 < Scenario A < Scenario B1 < Scenario D2 < Scenario D1

Table 7.10. Carbon Footprint results per gram of mNP for the different production routes.

Production route	Carbon Footprint
Scenario C	26.5 g CO_2 eq/g mNP
Scenario B2	37.4 g CO_2 eq/g mNP
Scenario A	79.4 g CO_2 eq/g mNP
Scenario B1	237 g CO_2 eq/g mNP
Scenario D2	1.15 kg CO_2 eq/g mNP
Scenario D1	1.61 kg CO_2 eq/g mNP

When expressed in terms of units of laccase immobilized, the sequence would be (Table 7.11):

Scenario B2 < Scenario C < Scenario B1 < Scenario D1 < Scenario A < Scenario D2

Table 7.11. Carbon Footprint results per unit of Laccase immobilized (U) for the different production routes.

Production route	Carbon Footprint
Scenario B2	24.3 mg CO_2 eq/U
Scenario C	0.13 g CO_2 eq/U
Scenario B1	0.29 g CO_2 eq/U
Scenario D1	0.61 g CO_2 eq/U
Scenario A	0.74 g CO_2 eq/U
Scenario D2	1.01 g CO_2 eq/U

According to these results, differences on the selection of the best production sequence are clear as well as on the magnitude of the environmental burden. Regarding contributing processes, there is a clear factor of contributions to carbon footprint regardless the scenario under assessment: the large electricity requirements. However, it should be highlighted that the production systems have been assessed at pilot scale and optimizations should be required at large scale. Moreover, special attention should be paid on the functional unit selected to report the environmental results since it could clearly affect decision making strategies.

7.4. **Conclusions**

This work provides the first detailed life cycle inventory and environmental assessment for the different alternatives of magnetic nanoparticles production. As well as highlighting again the importance of energy and chemicals use, the conducted assessment demonstrates the validity of the assumptions for the LCI. Thus, changes in the analyzed key parameters result in limited variations of the obtained environmental profile with respect to the baseline scenario.

Spherical PEI-coated mNPs are the most reliable option over the other supports due to the highest amount of laccase units immobilized per production batch. In addition, the environmental impacts associated to its production support its selection as the most suitable synthesis route.

7.5. References

Althaus H.J., Chudacoff M., Hischier R., Jungbluth N., Osses M., Primas A. 2007. Life Cycle Inventories of Chemicals. Ecoinvent report No.8 v2.0 EMPA, Swiss Centre for Life Cycle Inventories, Düberdorf.

Arroyo M. 1998. Inmovilización de enzimas. Fundamentos, métodos y aplicaciones. Ars Pharmaceutica; 39(2):23-39

Ayyad O., Muñoz-Rojas D., Oro-Sole J., Gomez-Romero P, 2010. From silver nanoparticles to nanostructures through matrix chemistry. Journal of Nanoparticle Research; 12: 337-345

Barreto J.A., O´Malley W., Kubell M., Graham B., Stephan H., Spiccia L. 2011 Nanomaterials: Applications in cancer imaging ant therapy. Advanced Materials; 23(12): 18-40

Babic A., Lindner A.B., Vulic M., Stewart E.J., Radman M. 2008 Direct Visualization of Horizontal Gene Transfer. Science; 319: 1533-1536

Brady D., Jordaan J. 2009. Advances in enzyme immobilisation. Biotechnology letters; 31: 1639

Bruce P.G., Scrosati B., Tarascon J-M. 2008. Nanomaterials for rechargeable lithium batteries. Agewandte Chemie International Edition; 47(16): 2930-2946

Chang L. H., Sasirekha N., Chen Y.W., Wang W.J. 2006. Preferential oxidation of CO in H-2 stream over Au/MnO2-CeO2 catalysts. Industrial Engineering Chemical Research; 45: 4927-4935

Colvin V. L. 2003. The potential environmental impact of engineered nanomaterials. Nature Biotechnology; 21(10): 1166-1170

Courrol L.C., Silva F. Gomes L. 2007. A simple method to synthesize silver nanoparticles by photo-reduction. Colloids and Surfaces A: Physicochemical and Engineering Aspects; 305: 54-57

Das S., Mitra S., Khurana S.M.P., Debnath N. 2013. Nanomaterials for biomedical applications. Frontiers in Life Science; 7(3): 90-98

Deng Y-H., Wang C-C., Hu J-H., Yang W-L-.,Fu Y-S. 2005. Investigation of formation of silica-coated magnetite nanoparticles via sol-gel approach. Colloids and Surfaces A: Physicochemical and Engineering Aspects; 262: 87-93

Doka G. 2003 Life Cycle inventories of Waste Treatment Services. Ecoinvent report No. 13, Swiss Centre for Life Cycle Inventories, Dübendorf.

Dones R., Bauer C., Bolliger R., Burger B., Faist E.M., Frischknecht R., Heck T., Jungbluth N., Röder A., Tuchschmid M. 2007. Life Cycle Inventories of Energy Systems: Results for Current Systems in Switzerland and other UCTE countries. Ecoinvent report No. 5, Swiss Centre for Life Cycle Inventories, Dümbendorf.

Eckelman M., Mosher M., Gonzalez A., Sherman J. Comparative Life Cycle 2012. Assessment of Disposable and Reusable Laryngeal Mask Airways. Anesthesia & Analgesia; 114(5): 1067-1072

Fang Y., Loc W.S., Lu W., Fang J. 2011. Synthesis of In2O3@SiO2 core–shell nanoparticles with enhanced deeper energy level emissions of In2O3. Langmuir; 27(23): 14091-14095.

Gavankar S., Suh S. 2012. Life cycle assessment at nanoscale: review and recommendations. The international Journal of Life Cycle Assessment; 17(3):295-303

Goedkoop M.J., Heijungs R., Huijbregts M., Schryver A.D., Strujis J., Zelm R. 2008. A life cycle impact assessment method which comprises harmonised category indicators at the midpoint and the endpoint level. First edition (revised). Report I: Characterisation ReCiPe.

Goon I., Zhang C., Lim M., Gooding J.J., Amal R. 2010. Controlled fabrication of Polyethylenimine-functionalized magnetic nanoparticles for the sequestration and quantification of free Cu2+. Langmuir; 26(14): 12247-1225

Grieger K.D., Laurent A., Miseljic M., Christensen F., Baun A., Olsen S.I. 2012. Analysis of current research addressing complementary use of life-cycle assessment and risk assessment for engineered nanomaterials: have lessons been learned from previous experience with chemicals? Journal of Nanoparticle Research; 14:958

Grillo R., Rosa A.H, Fraceto L.F. 2015. Engineered nanoparticles and organic matter: A review of the state-of-the-art. Chemosphere; 119: 608-619

Gupta A.K., Gupta M. 2005. Synthesis and surface engineering of iron oxide nanoparticles for biomedical applications. Biomaterials; 26(18):3995-4021

Han Y., Jiang, J., Lee S.S, Ying J.Y. 2008. Reverse microemulsion-mediated synthesis of silica-coated gold and silver nanoparticles. Langmuir; 24(11): 5842-5848.

Hischier R., Walser T. 2012. Life cycle assessment of engineered nanomaterials: State of the art and strategies to overcome existing gaps. Science of Total Environment; 425:271-282

ISO 14040:2006. 2006. Environmental management. Life cycle assessment-Principles and framework. Geneve, Switzerland

Kalishwaralal K., BarathManiKanth S., Pandian S.R.K., Deepak V., Gurunathan S. 2010. Silver nano-A trove for retinal therapies. Journal of Controlled Released; 145: 76-9

Kulkarni, SA, Sawadh, PS; Palei, PK. 2014. Synthesis and Characterization of Superparamagnetic Fe3O4@SiO2 Nanoparticles. Journal of the Korean Chemical Society, 58: 100-104.

Laurent S., Forge D., Port M., Roch A., Robic C., Est L.V., Muller R.N. 2008. Magnetic Iron Oxide Nanoparticles: Synthesis, Stabilization, Vectorization, Physicochemical Characterizations, and Biological Applications. Chemical Reviews; 108(6):2064-2110

Li Y., Gao W., Ci L., Wang C., Ajayan P.M. 2010. Catalytic performance of Pt nanoparticles om reduced graphene oxide for methanol electro-oxidation. Carbon; 48: 1124-1130

Li Q., Mahebdra S., Lyon D.Y., Brunet L., Liga M.V., Li D., Alvarez P. J.J. 2008. Antimicrobial nanomaterials for water disinfection and microbial control: Potential applications and implications. Water Research; 42: 4591-4602

López-Quintela M.A., Tojo C., Blanco M.C., García-Río L., Leis J.R. 2004. Microemulsion dynamics and reactions in microemulsions. Current Opinion in Colloid & Interface Science; 9:264-278

Massart R. 1981. Preparation of aqueous magnetic liquids in alkaline and acidic media. IEEE Transactions on Magnetics; 17(2): 1247-1248

Michalet X., Pinaud F.F., Bentolilla L.A., Trsay J.M., Doose S., Li J.J., Sundaresan G., Wu A.M., Gambhir S., Weiss S. 2005. Quantum dots for live cells, in vivo imaging and diagnostics. Science; 307 (5709): 538-544

Nersisyian H. H., Lee J.H., Lee S. I., Won C.W. 2003a. The role of the reaction medium in the self-propagating high temperature synthesis of nanosized tantalum powder. Combustion and Flame; 135: 539-545

Nersisyian H. H., Lee J. H., Son H.T., Won C.W., Maeng D.Y. 2003b. A new and effective chemical reduction method for preparation of nanosized silver powder and colloid dispersion. Materials Research Bulleting; 38: 949-956

Nersisyian H. H., Lee J. H., Won C.W. 2003c. Combustion of TiO2-Mg and TiO2-Mg-C systems in the presence of NaCl to synthesize nanocrystaline Ti and TiC powders. Materials Research Bulleting; 38: 1135-1146

Nowack B., Krug H.F., Height M. 2011; 120 Years of nanosilver history: implications for policy makers. Environmental Science and Technology ;45(4): 1177-1183

PRé Consultants, 2017. http://www.pre.nl (Accesed in June 2017)

Qu X., Alvarez P.J.J., Li Q. 2013. Applications of nanotechnology in water and wastewater treatment. Water Research; 47: 3391-3946

Red Eléctrica de España. Avance del informe del Sistema Eléctrico Español 2014 at: http://www.ree.es/sites/default/files/downloadable/avance_informe_sistema_electrico_ 2014.pdf, (Accessed June 2017)

Salamanca-Buentebello F., Persad D.L. Court E.B., Martin D.K., Daar A.S.,Singer P.A. 2005 Nanotechnology and the Developing World. PLoS Med; 2(5): e97

Sathishkumar M., Sneha K., Yun Y.S. 2010. Immobilization of silver nanoparticles synthesized using Curcuma longa tuber powder and extract on cotton cloth for bactericidal activity. Bioresource Technologies; 101: 7958-7965

Tsuzuki, T., 2013. Nanotechnology Commercialisation. Pan Stanford Publishing. Singapore.

Upadhyayula V.K.K., Meyer D.E., Curran M.A., Gonzalez M.A. 2012. Life cycle assessment as a tool to enhance the environmental performance of carbon nanotubes products: a review. Journal of Cleaner Production; 26:37-47

Walser T., Demou E., Lang D.J., Hellweg S. 2011. Prospective Environmental Life Cycle Assessment of Nanosilver T-Shirts. Environmental Science & Technology; 45(10): 4570-4578

Xie Y., Ye R., Liu H. 2006. Synthesis of silver nanoparticles in reverse micelles stabilized by natural biosurfactants. Colloids and Surfaces A: Physicochemical and Engineering Aspects; 279(1): 175-178

Zeiri L., Bronk B.V., Shabtai Y., Czégé J., Efrima S. 2002. Silver metal induced surface enhanced Raman of bacteria. Colloids and Surfaces A: Physicochemical and Engineering Aspects; 208(1):357-362.

USC
UNIVERSIDADE
DE SANTIAGO
DE COMPOSTELA

General conclusions

USC
UNIVERSIDADE
DE SANTIAGO
DE COMPOSTELA

This doctoral thesis aims to contribute to the development of a new technology that explores the oxidative potential of oxidoreductases for the treatment of pollutants in wastewater and in parallel, considers its application in the field of biotechnology through the oxidative potential of enzymes as biocatalysts for the synthesis of products.

The work developed in this thesis addressed the development of a biocatalyst suitable for the enzymatic treatment of recalcitrant pollutants, more specifically emerging contaminants, such as endocrine disrupting chemicals or active pharmaceutical compounds, thanks to the oxidative action of the enzyme laccase. These types of contaminants may be present in urban and industrial wastewater, but existing treatment plants do not ensure their transformation into products with less contaminating potential. On the other hand, the transformation of compounds into valuable products for plastic building blocks such as DFF or FFCA emerges as a biotechnological process of interest based on research oriented to the area of bioplastics. From the proofs of concept, it is important to consider the design and development of a new enzymatic magnetic reactor for an application closer to the definite scale-up of the process.

The following conclusions are drawn from these two main topics of this thesis:

Development of a biocatalyst for the enzymatic treatment of contaminants and the transformation of compounds into valuable building blocks:

1. Immobilization of two laccases, three oxidases and one peroxygenase. These enzymes were immobilized by different methods of self-immobilization such as cross-linked aggregates (CLEAs), non-covalent bonding on commercial supports and superparamagnetic nanoparticles that lead to the highest enzymatic immobilization yields by covalent magnetic nanoconjugates of silica-coated magnetic nanoparticles in all cases, formed by the covalent attachment of enzyme between the aldehyde groups of the enzymes.
2. The process of immobilization of the laccase *Trametes versicolor (Tv)* immobilized onto silica-coated magnetic nanoparticles (smNP) was optimized obtaining high enzyme loads. The resulting nanobiocatalyst exhibited higher stability than free laccases in WWTP effluents, in addition to tolerating a higher

pH range and even maintaining higher levels of activity in the presence of inhibiting agents. On the other hand, the biotransformation of BPA, Phenol, E1, E2, EE2 and MG was possible with transformation rates comparable to those of the free enzyme.

3. *Tv*-smNP conjugates was reusable in different transformation cycles of BPA, MG and E2 in wastewater matrices of secondary effluents with constant transformation rates after 10 cycles. In addition, the enzyme stability was minimally affected, which ensures that the enzyme can be used longer, without the need to add fresh enzyme after each stage of batch treatment.

4. The transformation products of BPA, MG and E2 were analysed after enzymatic treatment to determine potential toxicity. No toxicity was detected in BPA and E2 and a decrease in toxicity was detected in MG transformation products.

5. Laccase Pycnoporus sanguineus (Pyc) produced by agroindustrial wastes was immobilized in smNP with high enzymatic loads and the conjugate exhibits greater stability than free laccase at acid pH and in the presence of inhibiting agents. The reuse of the nanobiocatalyst has been tested in 6 cycles of transformation of BPA and MG with high rates of biotransformation.

6. The potential toxicity of the nanobiocatalyst (Pyc-smNP) and the resulting enzymatic treatment medium of BPA and MG was evaluated and no toxicity was detected.

7. Galactose oxidase (GAO) and Aryl alcohol oxidase (AAO) were successfully immobilized in smNP. The nanobiocatalyst biotransforms 5-HMF into DFF and FFCA with high transformation rates even better than those of the free enzyme. AAO-smNP was tested in 6 5-HMF transformation cycles with high biotransformation rates and enzymatic stability.

8. The genotoxicity of the nanobiocatalyst (AAO-smNP) was studied and no DNA damage was found when applying the nanobiocatalyst suggesting that it is a safe nanosystem to be used in different applications.

9. The environmental evaluation of the different nanomaterials used as supports was carried out and spherical PEI-coated mNPs were the most reliable option over the other supports as far as the environmental perspective is concerned.

Development of a new enzymatic magnetic reactor for environmental and biotechnological applications:

1. A sequential batch reactor (SBR) coupled to an internal magnetic separator was developed. The separator consists of a set of axially magnetized permanet toroidal magnets, distributed along a non-magnetic steel rod, uniformly spaced with alternate polarity, which provide an external magnetic field of up to 1.2
2. The feasibility of magnetic separation for the retention of the nanobiocatalyst based on enzyme immobilized on smMP was assessed. The reactor was tested for enzymatic decolorization of MG dye and the transformation of HMF, with complete recovery of the nanobiocatalyst and high biotransformation efficiency of both compounds.
3. The toxicity of the medium after treatment in the SBR was assessed and the biotransformation product of MG showed less microtoxicity that the parent compound and higher biodegradability.
4. The reactor was scaled-up to a volume of 100 L and the environmental performance and cost analysis were estimated, suggesting the potential of this system for other biotransformation reactions.

USC
UNIVERSIDADE
DE SANTIAGO
DE COMPOSTELA

List of publications

USC
UNIVERSIDADE
DE SANTIAGO
DE COMPOSTELA

CONFERENCES PROCEEDINGS

Y. Moldes-Diz, F.Manteiga, G. Feijoo, M.T. Moreira, Sustainable producton of plastic builing blocks by enzymatic biocatalysis, 13th International Chemical and Biological Engineering Conference (Oral, 2018)

F. Manteiga, Y.Moldes-Diz, C. Vázquez-Vázquez, G. Feijoo, M.T. Moreira, Immobilized galactose oxidase as a firs stage in enzyme cascade synthesis, Jornadas Españolas de Biocatálisis (Oral, 2018)

Y.Moldes-Diz, M.Gamallo, G. Eibes, G.Feijoo, J.M. Lema, M.T.Moreira, *Green robust nanobiocatalyst for phenol transformation*, 10th World Congress of Chemical Engineering (Poster, 2018)

M.Gamallo, Y.Moldes-Diz, G. Eibes, G.Feijoo, J.M. Lema, M.T.Moreira, *Heterogeneous Fenton catalytic removal of Reactive Blue 19 based on potentiality of magnetite nanoparticles*, 10th World Congress of Chemical Engineering (Poster,2018)

Y.Moldes-Diz, J.C. Martinez-Patiño, M.Gamallo, G.Eibes, J.M. Lema, G.Feijoo, M.T. Moreira, *Production of Ganoderma lucidum laccase and its applicability as biocatalysts for dye decolorization,* Congreso Nacional de Biotecnología (Biotec2017) (Oral,2017)

Y.Moldes-Diz, I.Safarik, M.Gamallo, G.Eibes, J.M. Lema, G.Feijoo, M.T.Moreira, *Preparation of a nanobiocatalyst based on silica nanoparticles with magnetic surface modification and its application for enzymatic catalysis*, Congreso Nacional de Biotecnología (Biotec2017) (Oral,2017)

Y.Moldes-Diz, G.Eibes, J.M.Lema, G.Feijoo, M.T. Moreira, *Development and application of an enzymatic reactor with magnetic nanoparticles for the removal of emerging pollutants,* The 13th IWA Leading Edge Conference on Water and Wastewater Technologies (Oral,2016)

Y.Moldes-Diz, S.Azerrad, M.Gamallo, G.Eibes, J.M. Lema, G.Feijoo, M.T. Moreira, *Potentiality of laccase immobilized onto magnetic nanoparticles for estrogens transformation*, 10th International Society for Environmental Biotechnology (Poster, 2016)

JOURNAL PUBLICATIONS

Y.Moldes-Diz, G.Eibes, C.Vázquez-Vázquez, J.Mira, A.Fondado, G.Feijoo, J.M. Lema, M.T. Moreira, *A novel enzyme reactor based on superparmagnetic nanoparticles for biotechnological applications,* Journal of Environmental Chemical Engineering, 6, 5950-5960.

Y.Moldes-Diz, M.Gamallo, G.Eibes, Z.Vargas-Osorio, C.Vázquez-Vázquez, G.Feijoo, J.M. Lema, M.T. Moreira, *Development of a superparamagnetic laccase nanobiocatalyst for the enzymatic biotransformation of xenobiotics*, Journal of Environmental Engineering, DOI:10.1061/(ASCE)EE.1943-780.0001333

M.T. Moreira, Y.Moldes-Diz, S.Feijoo, G.Eibes, J.M. Lema, G.Feijoo, *Formulation of laccase nanobiocatalysts based on ionic and covalent interactions for the enhanced oxidation of phenolic compounds*, Applied Sciences, 851. DOI:10.339

S. Feijoo,, S. González-García, Y. Moldes-Diz, C. Vazquez-Vazquez, G. Feijoo, M.T. Moreira, Comparative life cycle assessment of different synthesis routes of magnetic nanoparticles, Journal of Cleaner Production. C (2017) 528–538.

M.Gamallo, Y.Moldes-Diz, G.Eibes, G.Feijoo, J.M.Lema, M.T. Moreira, *Sequential reactors for the removal of endocrine disrupting chemicals by laccase immobilized onto fumed silica microparticles*, Biocatalysis and Biotransformation, DOI:10.1080/10242422.2017.1316489

BOOK CHAPTERS

S.Feijoo, S. González-García, Y.Moldes-Diz, C. Vázquez-Vázquez, G.Feijoo, M.T. Moreira, *The environmental impact of magnetic nanoparticles under the perspective of carboon footprint*, Chapter 3 in Environmental Carbon Footprints, Ed. by Subramanian Senthilkannan Muthu, Elsevier. ISBN:978-0-12-812849-7

M.Gamallo, Y.Moldes-Diz, R.Taboada-Puig, J.M. Lema, G.Feijoo, M.T. Moreira, *Textil wastewater treatment by advanced oxidation processes: a comparison study*, Chapter 6 in Life Cycle Assesment of wastewater treatment, Ed. by Mu. Naushad, CRC Press.

PATENTS

Y. Moldes-Diz, G.Eibes, A. Arca-Ramos, C.Vázquez-Vázquez, A.Fondado, J.Mira,J.M.Lema, G.Feijoo, M.T. Moreira, *Procedimiento y sistema para la eliminación de microcontaminantes mediante un reactor con enzima inmovilizada en nanopartículas m ´magnéticas y unidad de separación interna,* National patent (OEPM) publish at 11/0572016. Publish number: 2559111

Y.Moldes-Diz, G.Eibes, A. Arca-Ramos, C.Vázquez-Vázquez, A.Fondado, J.Mira, J.M.Lema, G.Feijoo, M.T. Moreira, *Procedimiento y sistema para reacciones de síntesis química en un reactor con enzima inmovilizada en nanopartículas magnéticas y unidad de separación interna,* National patent (OEPM) publish at 11/05/2016. Publish number: 2558582

USC
UNIVERSIDADE
DE SANTIAGO
DE COMPOSTELA

ACKNOWLEDGEMENTS/AGRADECIMIENTOS

En primer lugar, quería agradecer al Departamento de Ingeniería Química de la Universidade de Santiago de Compostela (USC) por haberme dado la oportunidad de llevar a cabo mi tesis doctoral. Además, me gustaría dar las gracias al Ministerio de Economía y Competitividad de España por la financiación aportada a través de los proyectos ENTIRE y MODENA, y a través de la ayuda para contratos predoctorales para la formación de doctores 2014.

Comentar también que esta tesis no habría podido ser llevado a cabo sin la gran ayuda, paciencia y apoyo de mis directores de tesis los Profesores Maite Moreira y Sindo Feijoo, los cuales han confiado en mí desde los inicios. Sindo siempre atento, optimista y enérgico y Maite, nada que decir que ella no sepa, gracias por estar siempre disponible para resolver mis dudas inmediatas y además de por el aporte científico, por ese apoyo incondicional ante cualquier circunstancia durante esta carrera de fondo. Muchas gracias también a todo el grupo de Nanomag, que han sido una parte esencial en esta tesis, además de gran ayuda a la hora elaborar los artículos científicos. I´d also thank to Pedro Alvarez, Ivo Safarik and María Manuela Pintado for giving me the unforgettable opportunity of carrying out different research stays at their departments.

También tengo que agradecer a toda la gente del Biogroup por todo lo que he aprendido y todos los momentos que he vivido con ellos y en especial a toda la gente que ha pasado por el laboratorio de enzimas. Gracias al personal técnico y administrativo del Biogroup y especialmente a Mar y Mónica por todo el tiempo dedicado al análisis de cada muestra y por atender todas mis dudas y problemas.

Me gustaría agradecer a todos mis amigos que me han estado apoyando y animando durante estos años. Gracias Alba, por seguirme en todos los viajes, por tu apoyo incondicional y nuestras charlas y conversaciones en la distancia durante horas. A Coral, Mari, Paola y Fran por aguantarme en esta última etapa siempre con una sonrisa. Gracias también a Tobi, por nuestros paseos más que necesarios para desconectar, has sido como una balsa de aceite en muchos momentos.

No me puedo olvidar de posiblemente la parte más importante de esta tesis, gracias a mis tíos y a mis padres, que constituyen un pilar fundamental, por su preocupación, apoyo incondicional, consejos, por todos los valores que me inculcaron y por sus palabras de ánimo, indispensables para llegar hasta aquí.

USC
UNIVERSIDADE
DE SANTIAGO
DE COMPOSTELA